2011

Semi-Automated Dental Cast Analysis Software

Mathew Thomas
Wright State University

SEMI-AUTOMATED DENTAL CAST ANALYSIS SOFTWARE

A thesis submitted in partial fulfillment
of the requirements for the degree of
Master of Science in Engineering

By

MATHEW THOMAS
B.S., Wright State University, Ohio, 2008

2011

Wright State University

WRIGHT STATE UNIVERSITY

SCHOOL OF GRADUATE STUDIES

June 30, 2011

I HEREBY RECOMMEND THAT THE THESIS PREPARED UNDER MY SUPERVISION BY Mathew Thomas ENTITLED Semi-Automated Dental Cast Analysis Software BE ACCEPTED IN PARTIAL FUFILLMENT OF THE REQUIREMENTS FOR THE DEGREE OF Master of Science in Engineering.

Julie A. Skipper, Ph.D.
Thesis Director

Thomas N. Hangartner, Ph.D.
Chair, Biomedical,
Industrial and Human
Factors Engineering

Committee on Final Examination

Julie A. Skipper, Ph.D.

Richard J. Sherwood, Ph.D.

Thomas N. Hangartner, Ph.D.

Andrew Hsu, Ph.D.
Dean, School of Graduate Studies

ABSTRACT

Thomas, Mathew. M.S. Egr., Department of Biomedical, Industrial and Human Factors Engineering, Wright State University, 2011. Semi-Automated Dental Cast Analysis Software.

Dental casts have been used extensively to study almost all aspects of the human dentition. These aspects varied from the study of tooth form and morphology, inheritance and genetics, growth and development, occlusion, arch alignment and crowding to mathematical determination of dental arch form.

The aim of this project was to develop a tool to semi-automate the measurement of dental casts that would be precise, accurate and efficient. Measurements include tooth widths, arch lengths and widths, angle of rotation and crown area for each tooth.

The task was divided into two different parts: first, the development of semi-automatic software to analyze 2D dental cast images and implementation of the process in a Graphical User Interface (GUI). The automated sections of the software were to be ideally executed without any user intervention, but it was anticipated that not all of the images would be successfully analyzed. Some factors that affect the automatic analysis are the quality of the casts, variations in tooth shape and image quality. During the

analysis, it is possible that some automatically-determined tooth boundaries and arch fits are erroneous. The GUI thus gives an interface for the user to execute the program, view the results of the automated measurements and make any manual adjustments before saving the results of all analyses.

The project objectives were attained. Of a test set of 96 maxilla and mandible images, analysis was successful on all of the images with none or limited manual intervention.

To assess accuracy, the results obtained using the software were successfully compared to those using traditional manual techniques taken with calipers, protractors, scales, thread, etc. The percentage error for measurements obtained using calipers were less than 1%. The developed software tool provides results that are more accurate and precise than those from manual analyses. The automated analysis process is also more effective than manual image analysis in that not all measurements can be obtained manually; the program automatically generates an output file containing over 260 variables of interest. Intraoperator and interoperator error analysis was also performed. We showed that the mean percentage intraoperator errors for the mesio-distal distances were 3.46% for the maxilla and 3.48% for the mandible and those for the bucco-lingual distances were 3.29% for the maxilla and 2.97% for the mandible. The mean percentage interoperator errors for mesio-distal distances were 5.82% for the maxilla and 4.46% for the mandible, and those for the bucco-lingual distances were 3.32% for the maxilla and 3.81% for the mandible. The software is currently being used to analyze over 2600 images.

TABLE OF CONTENTS

LIST OF FIGURES

LIST OF TABLES

ACKNOWLEDGEMENT

I express my sincere gratitude toward Dr. Julie A. Skipper and Dr. Richard Sherwood, under whose direction I was able to successfully complete this project and through whose encouragement I was able to realize my research potential. They have always guided me with patience through the various research obstacles and have helped me gain a better understanding of the diverse image processing concepts. I would also like to thank Dr. Richard J. Sherwood for helping me understand the basic concepts of craniofacial dentition and interpreting my results.

I am grateful to Dr. Thomas N. Hangartner for being on my advising committee.

I am thankful to Ms. Kimberly Lever, Research Assistant, Department of Community Health, who has been using the graphical user interface tool created for this project and whose input has been very important in developing a more user-friendly tool.

This project was supported by grant number R01DE018497 from the National Institute of Dental and Craniofacial Research of the National Institutes of Health.

DEDICATION

To my parents, Mr. Thomas Mathew and Ms. Annie Thomas, and my sister Mrs. Achamma Kurlekar, for their understanding support and, most of all, love.

1. INTRODUCTION

This section describes the long-term goals of the project for the Lifespan Health Research Center, followed by a brief description of the responsibilities for this particular thesis project.

Variations in tooth size can result from genetic as well as environmental factors.[1] A few factors that contribute to this are race, sex, heredity, environment, secular changes, and bilateral asymmetry.[1] The areas taken by the teeth within the dental arches are mainly determined by the size of the teeth and the space availability within the tooth developing parts of the jaw discrepancies which can lead to dental crowding.[2] The degree and rate of tooth wear, crowding and rotation has long been of interest and concern in both dentistry and anthropology.[3] The Jiri dental project examines, in detail, the morphology of the dentition and jaws in a human population from the small village of Jiri, Nepal. Jirels are the inhabitants of the Jiri area of the Dolkha district in Nepal. They have a total population of around 6,590 people. The population has limited access to orthodontic procedures and, thus, provides a unique opportunity to study the morphological integration of this region.

Overall aim of the project:

The long-term goal of the Jiri Dental project is to investigate the genetic architecture of craniofacial variation in humans using variance components-based statistical genetic methods. First, simple measurements describing the morphology in the area of interest are made, which is the goal of this thesis project. These measurements are subjected to quantitative genetic analyses that allow us to identify 1) how the genes affect a trait; 2) the proportion by which two traits are controlled by the same gene or sets of genes; and 3) to begin to localize the chromosomal regions harboring genes that influence variation. This includes characterizing the magnitude of genetic influences on dental phenotypes, examining how those genetic influences operate over time, identifying and localizing specific genetic polymorphisms that contribute to variations in growth and development, and elucidating how genetic and environmental factors interact during growth and development.[4]

As more and more studies identifying a genetic role in craniofacial syndromes are reported, understanding the role of individual genes, interactions between genes, and interactions between genes and the environment becomes of critical importance.[4] The search for the genetics underlying disease states has provided inspiration for a wide variety of research.[4] Genetic disorders can be caused by the mutation of one or more genes.[4] It becomes important to understand the different ways in which genetic disorders can present themselves along with other factors that can result in a wide variety of phenotypic manifestations.[4] Interaction between genes and between genes and the environment are clearly important in determining the phenotypic manifestation as well. Variability among normal genes would be expected to produce variable phenotypes when acting in concert with a mutated gene. The range of the phenotypic expression is multiplied when a diverse environment is introduced.[4]

Specific aim of the thesis:

The aim of this project is to develop a tool to semi-automate the measurement of the Jiri dental casts that will be reliable, precise and time efficient. The following phenotypic datasets will be collected from dental casts produced from the impressions: 1) standard dental and dental arch metrics including mesiodistal length and buccolingual width of each tooth; 2) measures of arcade size and shape like arch widths and arch lengths; and 3) measure of rotation and crown area for each tooth to better evaluate tooth-jaw interactions.[4]

2. BACKGROUND

Dental casts have been used extensively to study almost all aspects of human dentition. These aspects vary from the study of tooth structure and morphology, inheritance and genetics, occlusion, growth and development, dental crowding and arch alignment to the mathematical determination of dental arch fit.[5] The abundance of information obtained from dental casts (Figure 2.1) plays a major role in diagnoses, genetics evaluation and orthodontic treatment.[6]

This section discusses the basis of the desired dentition parameters to be measured and describes the main factors influencing these parameters. A detailed look at some previously used methods for dental cast analysis is also provided.

2.1 The Measurements

2.1.1 Mesio-distal and Bucco-lingual Points

The mesio-distal crown diameter can be termed as the distance between two lines which are parallel to each other and tangential to the mesial and distal points of the tooth (Figure 2.2).[7] This is usually an axis that is parallel and perpendicular to the occlusal and mesio-distal plane respectively for that tooth.[7]

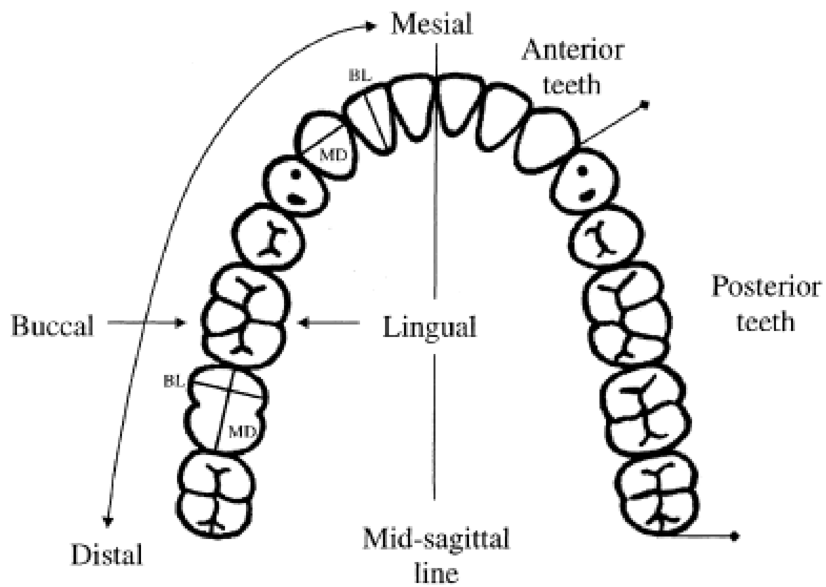

Figure 2.1: Diagrammatic representation of the dentition.[34] MD refers to mesio-distal length (Section 2.1.1) and BL refers to bucco-lingual width (Section 2.1.1).

The buccolingual diameter is the distance between two lines that are parallel and tangential to the lingual and buccal points respectively for each tooth (Figure 2.2).[7] The buccal point can be said to be on the convexity of the side for the incisors, canines and premolars and molars, the mesial most point of the buccal side is usually used for the measurement.[7]

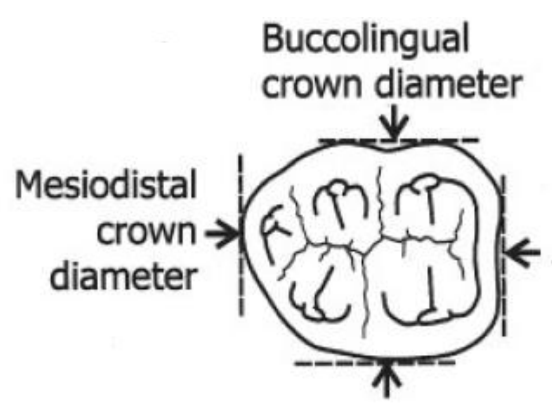

Figure 2.2: Mesio-distal and Bucco-lingual widths are calculated for each tooth.[31]

Anatomically, the mesiodistal diameter can be defined as the length of the tooth, and buccolingual diameter as the breadth. In actual practice, the mesiodistal diameter is usually the tooth width, and the buccolingual diameter is the thickness through the tooth.[8]

2.1.2 Arch Lengths and Arch Widths

Full arch length is a measure of the length, taken along the line generally connecting the mesial and distal tooth points, between the distal most points for the second molars at the left and right sides of the dentition. Half arch lengths for the left and right sides of the dentition are the distances between the distal most point for the second molar for that half and the mesial point of the central incisors for that half. Molar and canine arch lengths are a measure of the lengths between the distal points of the first molars and canines on either side.

Several arch width measurements are possible for each dentition, and the part of the teeth used for acquiring these measurements vary from study to study. Arch width measurements were made using the distal reference points for the canines and molars in this project (Figure 2.3). The main advantage of this approach is that if one tooth is missing, the mesial point of the previous tooth can be substituted since these two points will likely lie very close to one another. The user also has the option to exclude a tooth from the arch measurements. The program will also measure the distances between the lingual points for canines, pre-molars and molars.

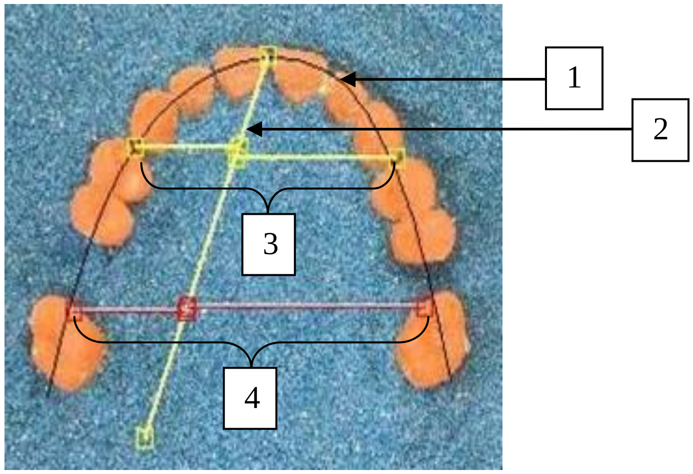

Figure 2.3. An example of some of the arch measurements where 1) is the arch fit, 2) is the midline for the dentition, 3) is the canine width and 4) is the molar width.

2.1.3 Angle of Rotation

There are different definitions for determining angle of rotation for a particular tooth. Some studies define it as the angle between the individual teeth and the arch (at any given point); others define it as the angle between the mesio-distal axis and the vertical axis line of reference.

2.2 Factors affecting the measurements

2.2.1 Attrition

Both interproximal and occlusal dental attritions result from a series of interactions between the teeth, their supporting structures and the masticatory apparatus. Attrition is the wear produced by contact between neighboring or opposing teeth.[9] The effects of dental attrition can result in dental crowding and cause reductions in the individual teeth measurements as well. The degree of attrition is determined by biological factors, such as the morphology of teeth and dental arches, the force and direction of masticatory movements and the hardness of the enamel and dentine.[9] The method by which the food is prepared increases dental attrition if any abrasive materials are added to the food. Interproximal attrition results in a reduction in the dental arch length because the mesio-distal crown diameters of the teeth are reduced.[9]

Several researchers have investigated dental attrition. Lysell's[9] results revealed that attrition increases regardless of gender as one gets older. The mandibular molars and incisors showed more attrition than the maxillary teeth and the incisors demonstrated the most attrition, and the extent of attrition decreases towards the distal end of the dentition. Lombardi[10] believed that the amount of grit in a diet causes most of the occlusal wear but was not the primary factor influencing interproximal wear. Wolpoff[11] determined that there is a high correlation between interproximal wear or malocclusion and the force required to chew the food. A diet consisting of hard foods would require applying more force, which results in the movement of teeth with respect to each other. This friction of neighboring teeth is the main cause of interproximal wear. Larsson et al.[12] showed that chewing hard food not only causes occlusal and interproximal attrition but makes the arch fit relatively shorter as a result of the mesial movements and attrition of the premolars and molars. The interproximal attrition results in a reduction in the rotation as well as crowding of the teeth.[8]

2.2.2 Dental Crowding

Dental crowding is the size disagreement between tooth and the jaw which results in a misalignment of the arch fit.[13] Crowding can be affected by environmental as well genetic factors and is extremely common, affecting most people with full dentition to some extent.[14] The size of each tooth and the space available for each tooth within the jaw are the primary factors that determine the positions in the dental arches that are taken up by the teeth.[15] Crowding could result from smaller jaws, bigger teeth, or from a combination of the two. Several explanations have been offered for the increase in dental crowding.[13] This includes modifications in food habits that lead in the reduction of chewing habits, lessen the stresses, lesser proximal wear and increases the tooth size. It is evident that a result of the interaction between dental arch and jaw is crowding.[13] In addition to crowding, modifications in the ordering of teeth sometimes happen, which are independent of this relation. Moorrees and Reed[16] proved that the dental crowding is largely dependent on how the teeth and the dental arch are related. Usually, societies with little crowding show higher degrees of occlusal and interproximal attrition.[3]

The inadequacy of arch length to accommodate full dentitions as a result of malocclusion is common. Since malocclusion can result from dental crowding, it is possible that selection pressures reduce dental arch length, thereby increasing the wear and tear of the tooth, especially the third molars, since they are the last teeth in the jaws to develop.[16]

2.2.3 Molar Agenesis

The more distal teeth in each dentition usually show more numerical variations than those nearer to the midline. Hence, there are more chances of the lateral incisors being absent than the central incisors and more possibilities of the distal molars (second and third molars) being absent than the first molars.[17] When at least one third molar is missing, the incidence of other missing teeth is raised thirteen-fold.[18] When third molar teeth are missing, the development of the posterior teeth is delayed, and the chances of reduced in sizes of the remaining teeth are increased.[18]

2.3 Factors Influencing Arch Measurements

2.3.1 Arch Length

Several studies have attempted to determine the changes in dental arches, particularly during the period of growth and adulthood. Arch dimensions undergo more changes during the growth and development period than during adulthood.[19]

It is believed that the primary form of the arch is obtained by the setup of the supporting bone, and once the teeth have erupted, by the circumoral musculature and intraoral functional forces.[20] A measure of the degree of discrepancy between the patient's arch form derived using coordinate points and an ideal arch fit would be a useful measure of malocclusion.[21]

2.3.2 Arch Width

The dental arch width depends on the width of the skeletal base structure and on the mesiodistal positions of the teeth within the bone. The width of the skeletal units like the tongue and other soft tissues can be influenced by genetic factors and modification factors such as the elasticity of the surrounding soft tissues.[22] Long duration of forces from lips, tongue and cheeks can also play a role in modifying positions of the tooth crowns, if the roots remain mediolaterally within the cortical bone.[22] Previous studies have used either the mesial, distal, buccal, lingual or centroid points of each tooth to obtain the width measurements.

2.4 Previously used measurement methods

2.4.1 Earlier Approaches

The earliest methods of measurement involved the use of a pair of wheel screw adjustable engineering dividers and a millimeter scale that could obtain readings in tenth of millimeters. The dividers were manually adjusted to measure the mesiodistal diameter using both casts and direct measurements inside the mouth, and the size was obtained from the millimeter scale by placing the divider points on the scale. Another more commonly used method involved the use of sliding calipers with a Vernier scale connected to the instrument. Both of these methods allow readings to the nearest 0.1 mm.[23] Hand held calipers are usually preferred because of how easy it is to use and transport, and several studies have confirmed the reasonable accuracy and repeatability of manual measurements made on dental casts.[24] The total mean difference between measurements made on two replicate casts by two different users was found to be 0.04 mm, which is considered a negligible difference.

Researchers have also used several other non-contact methods, including standardized photographs,[12] photocopies of casts,[25] occlusograms, laser holograms,[26] and prints and television images of the occlusal aspects of teeth. Schrimer and Wiltshire[27] as well as Champagne[28] compared measurements made on digitized casts obtained from a photocopier with those made manually on casts and concluded that calipers gave more accurate results than photocopies. Bhatia and Harrison[29] used a traveling microscope to determine the error between multiple trials of coordinate point selections and linear distance measurements on dental casts to prove the accuracy of the method.

2.4.2 Individual Measurement Methods

2.4.2.1 Angle of Rotation

Agha and Al-Saleem[30] conducted a study to measure canine rotations. This was accomplished by drawing horizontal lines from the mesial and distal points of the tooth to the midline (reference line) as shown in Figure 2.4a. The width of the canine is then defined as the angled distance between the horizontal mesial and distal lines. The angular measurement is made by drawing a continuation of the canine width line to meet the reference line, forming the angle to be measured (Figure 2.4b).

a: Reference line

b: Mesial distance

c: Distal distance

d: Canine width

e: Angle of rotation

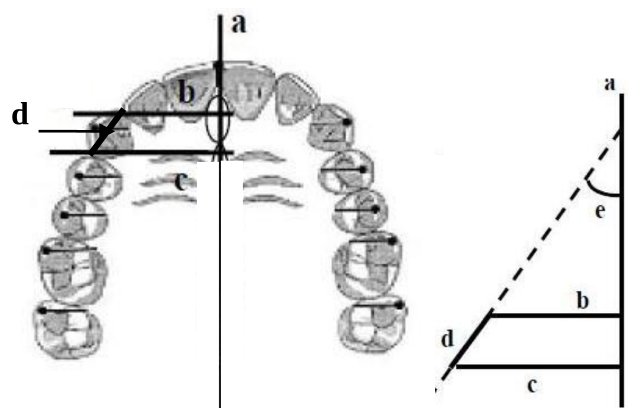

(a) (b)

Figure 2.4: a) Canine width is measured as the angled distance between the horizontal mesial and distal lines b and c.[30] b) Zoom of the section measuring the angle of rotation.[30]

Rougier[31] developed a method to measure the rotation of the first premolars using a standard arch form. The approach involves first drawing a dental arch by hand, and next, two lines were drawn where the first is the tangent to the dental arch in the mesio-distal direction on the particular tooth, and the second is a line through the bucco-lingual width (Figure 2.5). The angles are then determined between the perpendiculars to the first and second axis. If the bucco-lingual line is distal to the perpendicular line, the angle value is negative; if it points mesially, the angle is positive. This method is not easy to apply.

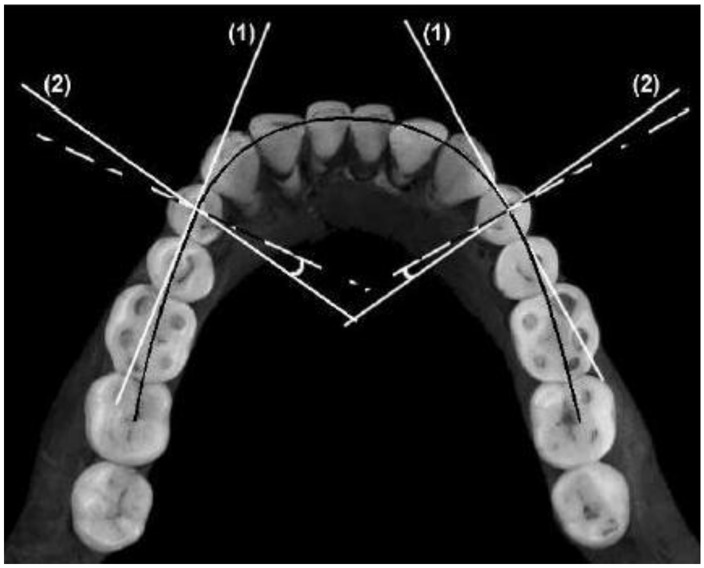

Figure 2.5: Representation of the rotation measurement of the premolar: the angle is measured between the perpendicular (dotted line) to axis (1) taken as the tangent to the dental arch on the premolar and axis (2) representing the long axis of the premolar crown.[31]

2.4.2.2 Arch Measurements

For determining arch fits, a review of the literature shows that several assumptions are made: 1) there must be an algebraic or geometric formula that explains the ideal arch form; 2) all ideal arches are the same shape and differ only in size; and 3) every ideal arch is considered to be symmetrical.[17] Many geometric forms and mathematical functions have been proposed as models of the human dental arch. However, it has become clear that models defined by one parameter alone cannot describe the dental arch form accurately.[32]

One of the primary attempts in order describe the dental arch form was the work of MacConail et al., who connected a catenary curve to the coordinate points.[33] A catenary curve is a freely hanging chain held at the ends. Conical sections like the parabola were also suggested by various researchers. BeGole[33] fitted cubic spline curves, whereas Lu[34] demonstrated application of polynomials. Mixed models using two functions, one each for the anterior and posterior dentition, have also been previously used.[20]

The established standards includes a description of the dental arch using geometric figures, like a catenary curve, a parabolic curve, an ellipse, a hyperbola, and a semi-circle connected to line segments.[35] However, the use of geometric shapes to describe an ideal dental arch was contraindicated when researchers found that the dental arch fit was not only represented and defined by shape, but involves several other factors, such as forces acting on the jaws and the position of the teeth [35]

Many studies have shown the accuracy of the fourth-order degree polynomial for the dental arch fit.[35] What one should recognize in the modeling of dental arches is that the dental arch fits determined to have similar mathematical forms and functions will not necessarily include the same pattern. Similarly, having the same order polynomials does not always mean it involves the same patterns. It will differ depending upon the different coefficients in the function.[22]

2.4.2.3 Tooth Widths

The mesiodistal width of a tooth is most commonly obtained as the widest distance between the surfaces of the crown, by holding a caliper to the mesial or lingual surfaces of each tooth (Figure 2.6). In cases of rotated teeth, the measurement is taken at the points between the approximate surfaces of the teeth where it is believed that normal contact with the neighboring teeth should occur.[15] Deviations from the perpendicular setup, like more severe tipping of a tooth could influence the accuracy.[13]

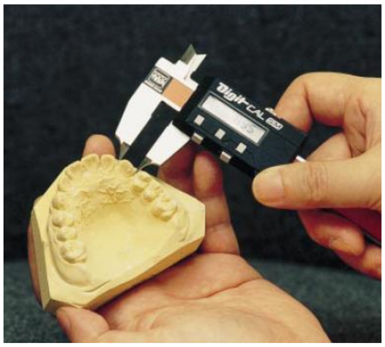

Figure 2.6. The caliper measuring the mesio-distal length for a canine tooth. The caliper is parallel to the occlusal surface.[64]

S. J. Rudge[36] calculated the intercanine width as the horizontal distance between the mid-point of the mesial and distal contact points of a canine to the equivalent mid-point on the opposite side of the arch. The intermolar width was calculated in a similar manner.

2.5 3D Measurements

Some earlier methods for three-dimensional measurements have been based on stereophotogrammetry,[37] the Optocom,[9] and the Reflex Metrograph[38] (H.F Ross, Ross Instruments Limited, Wiltshire, England). The Optocom is a microscope that is placed on a movable table, which uses precision pins and holes to hold the cast. The Reflexmetrograph consists of a semireflecting mirror with a moving light source fixed to a 3D slide system. Ryden and Martensson[10] investigated a three-dimensional holographic system for comparing dental cast holograms taken at different points of time, which was accurate and saved space, but did not prove to be practical in clinical practice due to cost and size of equipment.

2.6 Other Approaches

S.J. Rudge[36] devised a computer program to aid the direct analysis of study models using an electronic x-y reader (Figure 2.7). Coordinate points are marked using a pencil on the study model, which is then placed in an x-y reader to get the x- and y-coordinate values for each tooth. Using a stylus, the arch fit is drawn over the points. Absent teeth are designated by entering a specific code during the process.

The tooth width is calculated as

$$Tooth\,width \;=\; \sqrt{x^2 + \, y^2} \qquad [2.1]$$

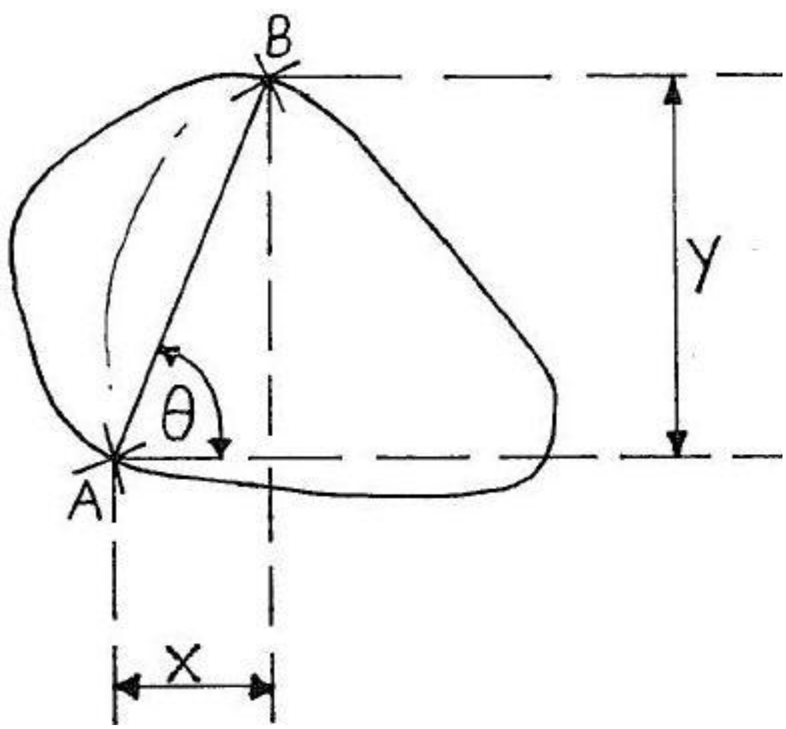

Figure 2.7: The measurements obtained using the S.J Rudge approach.[36] 'x' is the horizontal distance and 'y' is the vertical distance for the for the angled tooth width.

The rotation angle for each tooth is determined from the mesio-distal points and a vertical image axis, where

$$Tooth\ angle\ = arctan\left(\frac{y}{x}\right) \qquad [2.2]$$

The arch midline is computed as the linear least squares fit to the midpoints between equivalent pairs of teeth. To compute an arch fit, they used a Bonwill-Hawley-type[39] (Figure 2.8) arch, assumed to be the ideal arch form. In this approach, the sum of tooth widths for 6 anterior teeth defines the radius of a circle which is fitted tangentially inside the anterior part of the arch form.

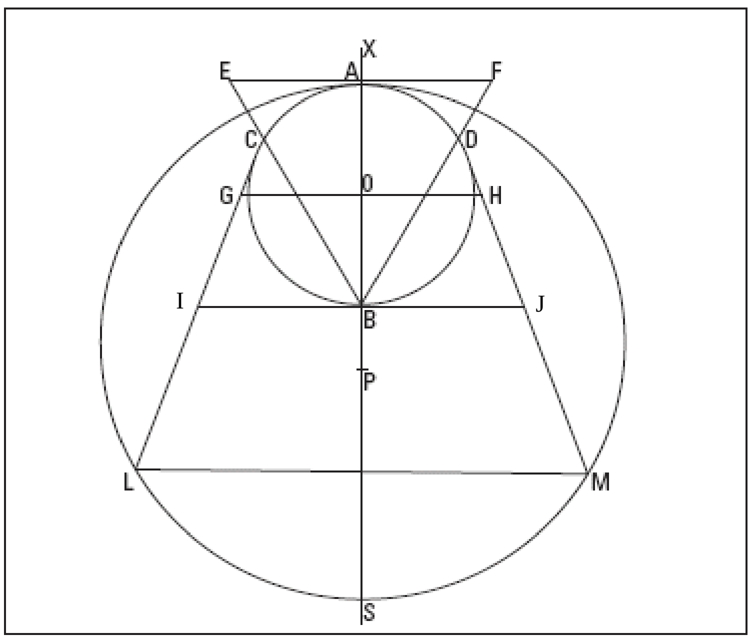

Figure 2.8: Bonwill-Hawley-type arch.[40] The sum of tooth widths for six anterior teeth defines the radius of a circle, which is fitted tangentially inside the anterior part of the arch form. Horizontal lines 'GH' and 'IJ' are drawn at the center and lower end of the circle, respectively. Using segment 'AB' as the diameter, a circle is drawn inside triangle 'BFE', in which the triangle 'BEF' approximately represents the area of the smaller circle that matches the arch fit.

Duguid[41] used a method employing a computer program to process information derived from the direct digitization of landmarks in plaster model dental casts. They obtained mesio-distal tooth widths, angles of rotation, arch widths and arch length. The mesio-distal widths for each tooth were found using the equation

$$\sqrt{[(x_2 - x_1)^2 + (y_2 - y_1)^2]} \qquad [2.3]$$

Angles were found from a mid-point at the center of the cast to a few points on either side of the arches (Figure 2.9). These lines were used as the radii at each tooth position, and a line was drawn through these points to give the shape of the arch curve. This curve is extended to the molars to give the required arch fit.

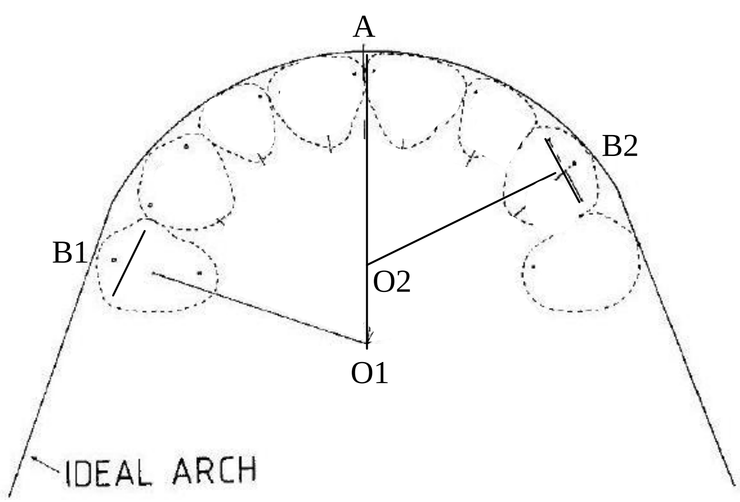

Figure 2.9. Ideal arch fitted to the anterior points on the casts. 'O1' and 'O2' are obtained as the points where the lines perpendicular to the mesio-distal points for the teeth intersect with the midline. The angles are determined between midlines 'AO1', 'AO2' and the line segments O1-B1, O2-B2 respectively.

Mok and Cooke[42] compared the use of sonic digitization using the DigiGraph Workstation (DigiGraph, Dolphin Imaging Systems, Valencia, California, USA) to the digital caliper. The DigiGraph Workstation permits the use of sonic digitization for registering linear distances and in order to obtain cephalometric values, mesio-distal tooth lengths and arch fit discrepancies as a one flow recording step. Sonic digitization technology is based upon an ultrasound technique and works by calculating the distance from the time taken for a sonic impulse to travel from a transmitter to a receiver. Their study compared the accuracy and reproducibility of mesio-distal widths and arch fit values obtained from casts as determined by the calipers and Digigraph Workstation. Compared with manual caliper readings, the tooth widths were over-estimated by 0.5 mm for the maxilla and 1.0 mm for the mandible using the sonic method. The sonic digitization was found to be less reliable than the digital caliper.[42]

2.7 Measurement Accuracy and Precision

The use of models is an accepted part of practical orthodontics and dental research. The cheaper mode of measurement of teeth on plaster study models involves the direct manual identification of specific landmarks anthropometrically.[43] This system, while reliable and accurate, is limited by the number of provided input parameters (e.g., coordinate points) as well as the interoperator and intraoperator reliabilities in correctly identifying the landmarks.[44] As the need for mathematically proven orthodontics is developing, the precision and reliability of several measurement methods used in research purposes must be evaluated.[45]

Virtual or digital models offer orthodontists an alternative to traditional plaster study models. Surface laser scanners are able to capture a complete digital image of the study model and transform it into a three-dimensional virtual model for further analysis. One advantage of this approach is that it avoids any contact with or distortion of the model surface. Previous studies have shown a 0.05 mm dimensional accuracy of laser-scanned digital models, which is considered highly accurate.[45, 46]

Quimby et al.[47] performed a study to determine the reproducibility and efficiency of the measurements made on models using the computer and found that the measurements made from computer models were as accurate and reliable as the measurements made from plaster models.[47]

Tomassetti et al.[48] compared four methods of conducting overall and anterior Bolton tooth-size analyses. The Bolton analysis was performed using Vernier calipers to study tooth-size discrepancies. The mean Vernier caliper results, obtained using this method, were compared with each of the following computerized methods: QuickCeph (QuickCeph Systems, Coronado, Calif), Hamilton Arch Tooth System (HATS) (GAC International, Central Islip, NY), and OrthoCad (CADENT Inc., Fairview, NJ). They found no significant error in any of the methods. The absolute difference of tooth measurement results from the different systems ranged from 0 mm to 5.6 mm (OrthoCAD versus Venier calipers), which gave an acceptable percentage error.[48] 0 mm here refers to the value for a missing tooth. They also found the range of measurement values were greater for OrthoCad than for other systems; a large difference in means indicates that this system is not suitable for research purposes and may have clinical limitations as well.

Whichever technique is used, the reliability of each system is affected by many factors. Sources of measurement error include the type of device or technique used, the skill of the operator/examiner, any impression and casting procedures and the condition of the tooth and related gingiva. Several factors may affect the accuracy and reproducibility of the measurements of the dental arch, like the size and space disagreements, the tilting of the teeth, rotations, and interproximal contacts of the teeth.[49]

3. MATERIALS AND METHODS

As stated earlier, the aim of the thesis is to develop software that can analyze 2D dental cast images. There are several steps in the 2D casting process. This chapter will focus first on the basic procedures of making the casts and acquiring their images, before describing the various measurement techniques.

3.1 Dental Casting

Standard whole mouth dental impression trays (Henry Schein, Melville, NY) are placed into the mouth of the individuals. Two different vinylpolysiloxane impression materials are used to get the final impression. The first is a fast set VP MIX PUTTY (Henry Schein, Melville, NY), consisting of a base and a catalyst, which are mixed into the impression tray. The individual bites into the tray, and this forms the initial base of the impression, over which the second impression material is poured and the individual is made to bite again to obtain the final impression. The second impression material is a regular body VP MIX HP (Henry Schein, Melville, NY). The latter material has the advantage of yielding a much higher-resolution impression, but it is much more expensive. To make the dental cast, an EPO-TEK 301 epoxy (Epoxy Technology Inc, Billerica, MA) is poured onto the final impression and allowed to set overnight. Since this epoxy has very low viscosity, the fast set VP MIX PUTTY is used to form a protective coating around regions of possible leakage.

3.2 Camera Setup and Image Acquisition

A Canon EOS 20-D (Canon U.S.A., Lake Success, NY) was used to acquire images of the dental casts. Once mounted at a height of 18.5 inches from the base, a level check is performed to ensure that the image axis is normal to the base. Light diffusers were used to scatter the multiple light sources and minimize strong shadows. By coupling the camera directly to the computer, images were acquired without disturbing the physical set-up of the camera. Settings such as ISO Speed, Format, Color Temperature, and Color Space, are displayed on the PC monitor and can be modified via the PC; our settings are documented in Table 3.1. Although this is a digital camera, the traditional ISO setting remains adjustable. ISO speed refers to film speed and is proportional to the film sensitivity to light; a higher ISO number refers to film with larger grain which requires less light to achieve the same image density as a slower film (lower ISO number). Unlike JPEG images, images saved in RAW format are minimally processed and contain all information needed to convert the data into an image that may be saved or printed in all available formats. Manipulations on RAW images yield fewer artifacts than those applied to .jpg images. Here, we initially save .raw files which are then converted to .tif format for subsequent processing in MATLAB.

Images of each cast are acquired and qualitatively checked for acceptability. .tif images of the upper and lower casts are stored in each patient's unique folder using the following naming convention: ABCDEFGHIJKLMNO, where 'A-F' is the 6 digit unique ID number for each individual, 'G-N' is the visit date (yyyy/dd/mm) and 'O' is either 'U' or

‘L’ for the maxilla or mandible, respectively. The naming convention of each individual patient folder contains the six digit ID number followed by the visit date.

Table 3.1: Camera settings used for acquisition of the dental cast images.

Setting	***Value***
ISO Speed	100
Format	RAW
Color Temp	5200 K
Color Space	sRGB
Distance from Base to Camera	18.5 in
Exposure Correction	+1
Exposure Time	4 sec
F-Stop	20

3.3 Experimental Setup for Acquiring the Cast Images

The colored dental cast (in our case, light reddish-brown) is placed in a shallow container containing sand of a contrasting color (in our case, blue). The sand has to be non-glossy, fine enough so that it can easily fill spaces between the teeth, and easy to clean off the cast. Mustard seeds were initially used for the Jiri Dental Study, but they were too large. Using small brushes, the sand particles are carefully arranged so that all teeth, and just the teeth, are visible. The sand is then leveled out as much as possible (Figure 3.1).

3.4 Steps for Cast Analysis

Semi-automated cast analysis is achieved via our custom MATLAB software. The primary analysis steps are now described.

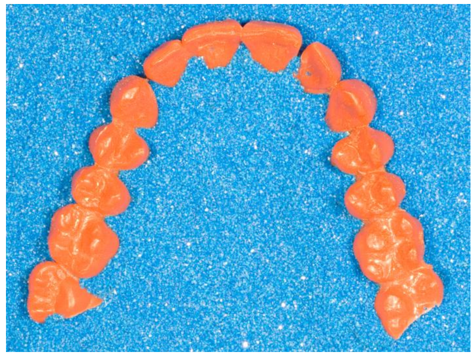

Figure 3.1: A cast image obtained after arranging and leveling out the sand in the tray.

3.4.1 Entering Patient Information

When the user selects the folder of interest, the subject ID number and the date of visit are obtained automatically from the folder name. Within the graphical user interface (GUI), the user then completes the data fields for age and type of dentition (permanent or deciduous), and records any missing teeth or notes teeth that are to be excluded from the arch fit measurements. Excluding a tooth from the arch fit is necessary when the user feels there is a displaced tooth that would compromise the utility of the subsequently calculated arch parameters.

3.4.2 Manual Selection of Coordinates Identifying Location of Each Tooth

The next step in the cast analysis is the manual selection of the location of each tooth's mesial-most, distal-most, buccal-most and lingual-most position in each image (maxilla and mandible). Knowing the number of pixels per unit length (e.g., pixels per centimeter), these coordinates are used to derive all image measurements. For permanent teeth, the 32 teeth yield a total of 128 points (64 points for each the maxilla and the mandible). For deciduous teeth, the 20 teeth yield a total of 80 points (40 points each for maxilla and mandible). The tooth numbering system used for permanent dentition is 1-16 and 17-32, where Tooth 1 is the left third molar of the maxilla (upper jaw), and the numbering continues to Tooth 16, which is the right upper third molar; Tooth 17 is the right third molar of the mandible (lower jaw), and the numbering continues to Tooth 32, which is the left lower third molar (Figure 3.2). Similarly, the tooth numbering system used for deciduous dentition is 1-10 and 11-20, where Tooth 1 is the left second molar of the maxilla, Tooth 10 is the upper right second molar, Tooth 11 is the right second molar of the mandible, and Tooth 20 is the lower left second molar. The coordinate point correspondence is maintained throughout the subsequent image processing operations (e.g., Tooth 1 yields coordinate points 1-4; Tooth 2 yields coordinate points 5-8, etc.); each missing tooth is denoted by changing its corresponding coordinate point values to zeros. For example, if Tooth 1 is missing, coordinate points 1-4 are set to zero. All coordinate point pixel indices (x, y pairs) are written into the data structure containing patient information, which is eventually output in Excel format. The Excel file is subsequently imported into the LHRC database and used to create the Excel-based analysis report.

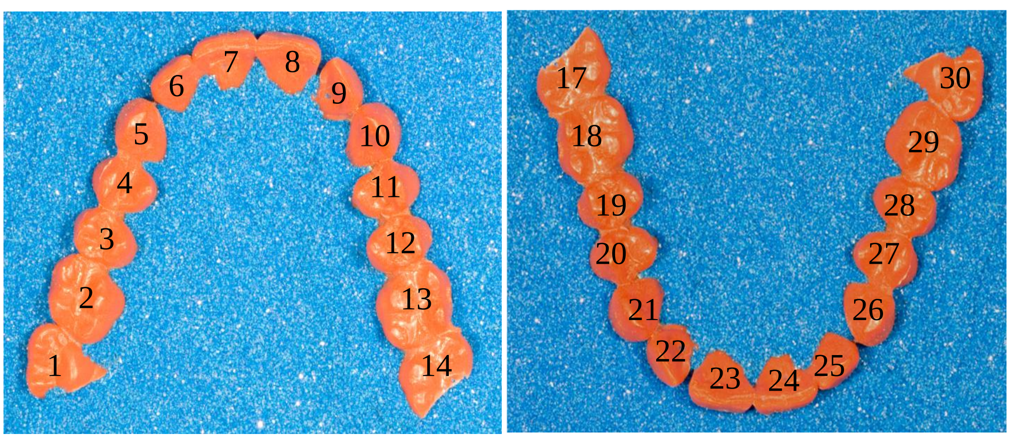

(a) (b)

Figure 3.2. a) The numbering system for maxilla. Since both the third molars are missing, the numbering is from one through 14. b) The numbering system for mandible. Again, since both the third molars are missing, the numbering is from 17 through 30.

In addition to tooth numbers, tooth labels are used in the LHRC studies. Tables 3.2 and 3.3 provide the labels for permanent upper and lower teeth, respectively, and Tables 3.4 and 3.5 provide this information for deciduous teeth.

Table 3.2: Maxilla Notation used at LHRC: Permanent Set.

Tooth Number	***Tooth***	***Tooth Notation (Maxilla)***
1	3rd Molar	RUM3
2	2nd Molar	RUM2
3	1st Molar	RUM1
4	2nd Pre-Molar	RUP4
5	1st Pre-Molar	RUP3
6	Canine	RUC
7	Lateral Incisor	RUI2
8	Central Incisor	RUI1
9	Central Incisor	LUI1
10	Lateral Incisor	LUI2
11	Canine	LUC
12	1st Pre-Molar	LUP3
13	2nd Pre-Molar	LUP4
14	1st Molar	LUM1
15	2nd Molar	LUM2
16	3rd Molar	LUM3

Table 3.3: Mandible Notation used at LHRC: Permanent Set.

Tooth Number	***Tooth***	***Tooth Notation (Mandible)***
17	3rd Molar	RLM3
18	2nd Molar	RLM2
19	1st Molar	RLM1
20	2nd Pre-Molar	RLP4
21	1st Pre-Molar	RLP3
22	Canine	RLC
23	Lateral Incisor	RLI2
24	Central Incisor	RLI1
25	Central Incisor	LLI1
26	Lateral Incisor	LLI2
27	Canine	LLC
28	1st Pre-Molar	LLP3
29	2nd Pre-Molar	LLP4
30	1st Molar	LLM1
31	2nd Molar	LLM2
32	3rd Molar	LLM3

Table 3.4: Maxilla Notation used at LHRC: Deciduous Set.

Tooth Number	***Tooth***	***Tooth Notation (Maxilla)***
1	2^{nd} Molar	DRUM2
2	1^{st} Molar	DRUM1
3	Canine	DRUC
4	2^{nd} Incisor	DRUI2
5	1^{st} Incisor	DRUI1
6	1^{st} Incisor	DLUI1
7	2^{nd} Incisor	DLUI2
8	Canine	DLUC
9	1^{st} Molar	DLUM1
10	2^{nd} Molar	DLUM2

Table 3.5: Mandible Notation used at LHRC: Deciduous Set.

Tooth Number	***Tooth***	***Tooth Notation (Mandible)***
11	2^{nd} Molar	DRLM2
12	1^{st} Molar	DRLM1
13	Canine	DRLC
14	2^{nd} Incisor	DRLI2
15	1^{st} Incisor	DRLI1
16	1^{st} Incisor	DLLI1
17	2^{nd} Incisor	DLLI2
18	Canine	DLLC
19	1^{st} Molar	DLLM1
20	2^{nd} Molar	DLLM2

3.4.3 Order of Manual Coordinate Point Selection

The order of manual point selection for each tooth is: 1) distal, 2) mesial, 3) buccal, and 4) lingual position, starting from the left side of the image and moving to the right for both the maxilla (Figure 3.3) and the mandible (Figure 3.4). Because the maxilla image is oriented as an inverted U-shape and the mandible image as a U-shape, the teeth are addressed sequentially.

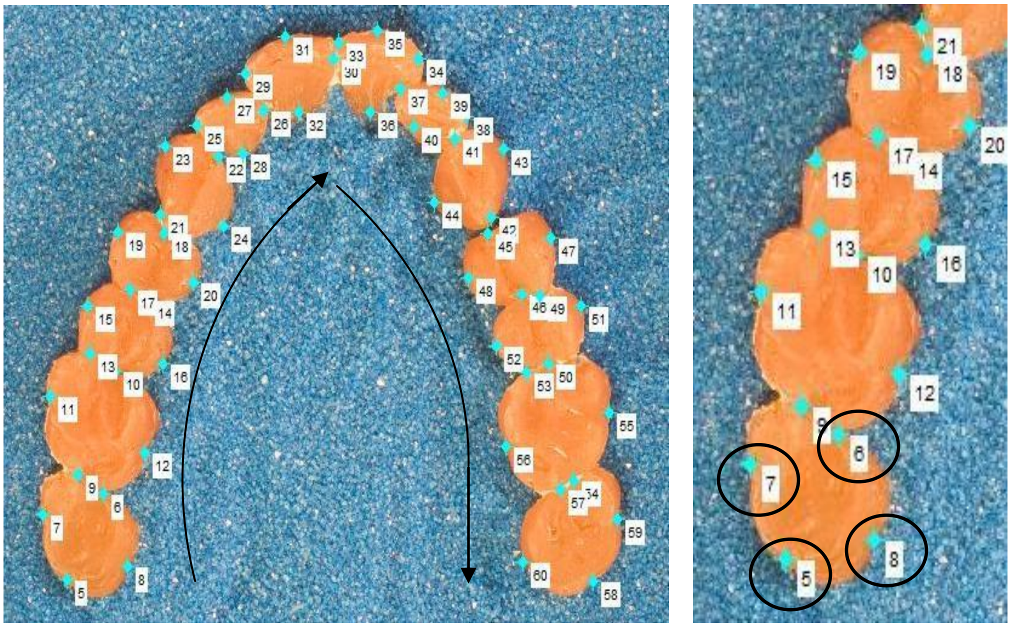

(a) (b)

Figure 3.3. a) The order of manual point selection for the maxilla showing the direction in which the user is to continue clicking. b) A zoomed-in version of a portion of Figure 4a, which more clearly shows the order of point selection for each tooth. The circles highlight point selection for a particular tooth as (5) distal, (6) mesial, (7) buccal and (8) lingual points.

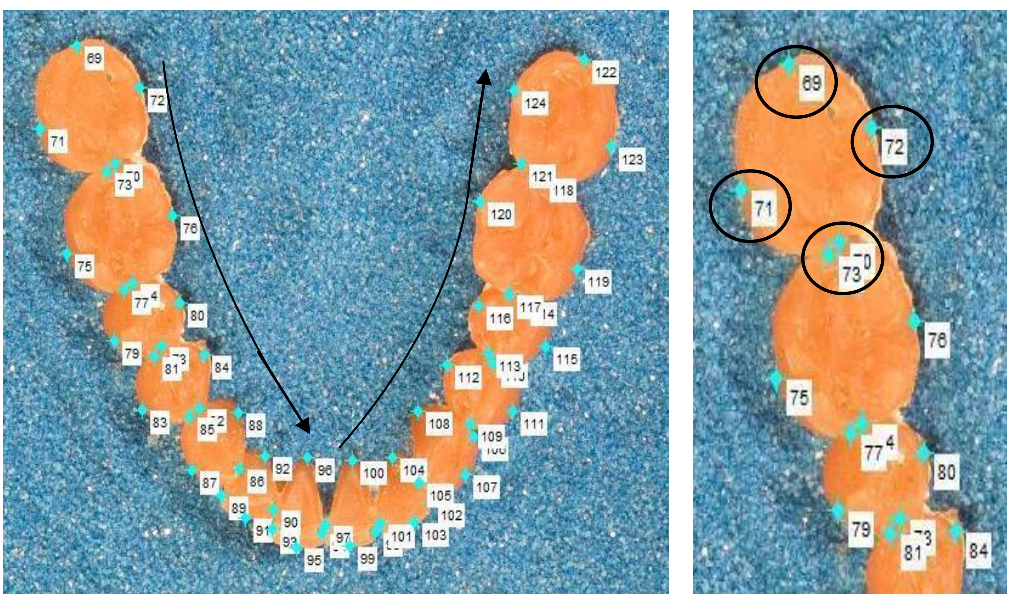

(a) (b)

Figure 3.4. a) The order of manual point selection for the mandible showing the direction in which the user is to continue clicking. b) A zoomed-in version of a portion of Figure 5a which more clearly shows the order of point selection for each tooth. The circles highlight point selection for a particular tooth as (69) distal, (70) mesial, (71) buccal and (72) lingual points.

3.4.4 Boundary Detection

Algorithms, implemented in MATLAB, segment the cast from the image background using the color difference between these two regions. The boundaries are obtained using MATLAB's *watershed* function, which returns an image of labeled segments with each segment ideally corresponding to a single tooth. To deal with the tendency for the watershed method to over-segment, the coordinate points of each tooth are used as quality checks during the process. For each detected boundary, the following checks are performed: 1) Between each set of postero-anterior points, is there only one label or boundary? If not, then relabel according to the order of coordinate-point selection. For example, all objects within the boundary detected along the line joining the third set of postero-anterior points will be re-labeled with a grayscale value of three, and a new boundary will be computed by joining the multiple boundaries. 2) Between each set of bucco-lingual points, is there only one label? Are there multiple labels? If so, relabel and recompute the boundary as above (Figure 3.5 and Figure 3.6).

If, after automatic boundary selection, the user notes errors in boundary placement, two manual fix processes are available: The first enables the user to replace an existing boundary with a hand-drawn boundary, and the second corrective process merges two selected segments into a single segment (as is necessary when one tooth is erroneously split into multiple sections due to tooth defects, odd tooth shapes, etc.). The final boundary image is saved in binary format for later use.

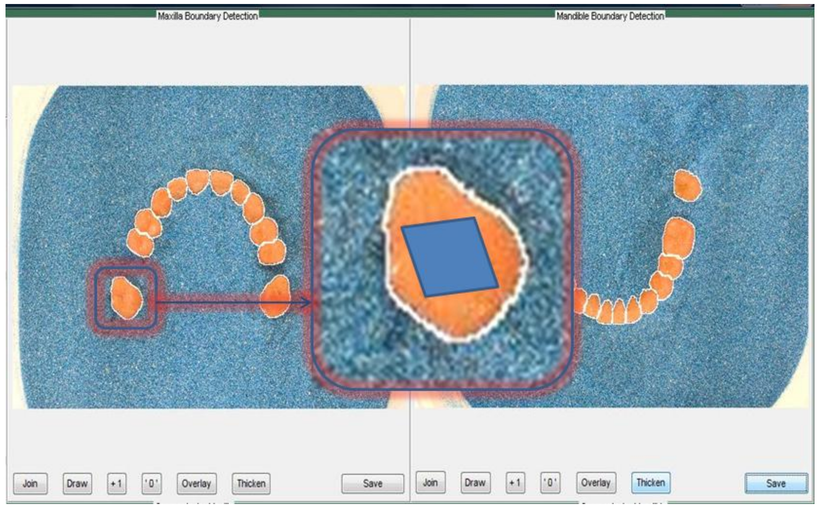

Figure 3.5. Automatic check performed during the boundary detection to ensure only one boundary is detected for each tooth. If multiple boundaries are detected, an automatic correction is performed (Figure 3.6).

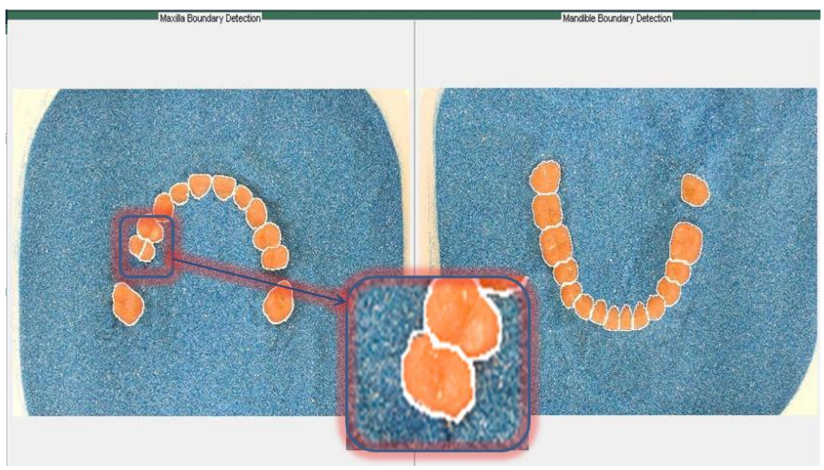

Figure 3.6. Split boundaries are detected during the coordinate point check and automatically corrected into one boundary.

Watershed Method

The watershed method gives a ‘Z’-shaped boundary between regions (each tooth in our case) (Figure 3.7). The true boundaries on the two-dimensional casts are very difficult to determine because of shape inconsistencies and topology of each tooth, especially at the separation between two adjoining teeth. Our attempt at cropping the regions, where the internal boundaries are to be determined, and thresholding this local region still returns edge images with scattered and broken boundaries. The Z-shaped boundary slightly overestimates and underestimates the crown area of each tooth such that the effects probably largely cancel each other out. We confirmed that the Z-shaped boundaries detected using these methods are acceptable for the purposes of this program.

3.4.5 Tooth Measurements

Using the manually-selected tooth coordinates as the limits of each tooth segment, the goal is to automatically derive all teeth and arch measurements.

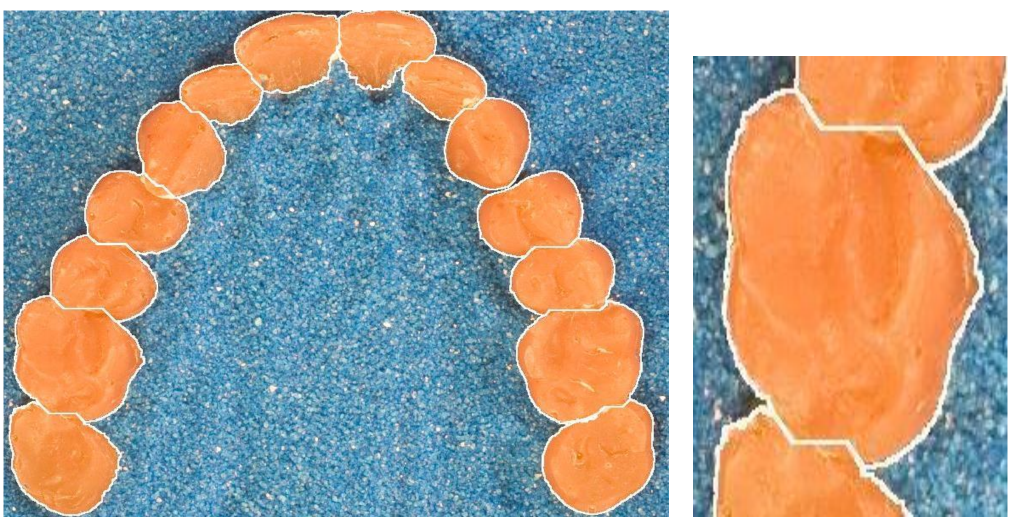

(a) (b)

Figure 3.7. a) Full and b) zoomed-in image of the maxilla showing detected boundaries. Note the Z-shaped inner boundary.

3.4.5.1 Postero-Anterior Distance

The first (distal) and second (mesial) coordinate points for each tooth represent the tooth's posterior and anterior limits, respectively. If the first point is given by (x_1, y_1) and the second point by (x_2, y_2), the mesio-distal distance d (Figure 3.8) is found using the Euclidean distance formula:

$$d = \sqrt{(x_2 - x_1)^2 + (y_2 - y_1)^2} \qquad [3.1]$$

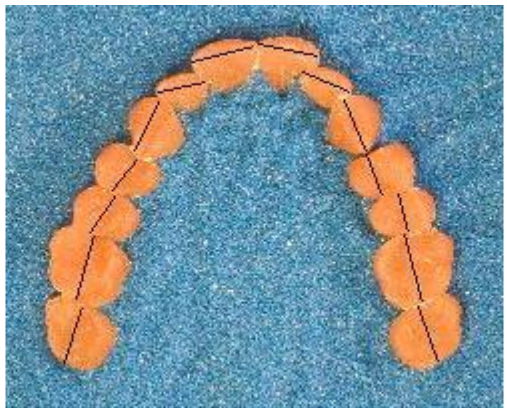

Figure 3.8. Each tooth's postero-anterior distance is marked on the image.

3.4.5.2 Bucco-Lingual Distance

Similarly, bucco-lingual distances are calculated using the third and fourth coordinate points for each tooth (Figure 3.9).

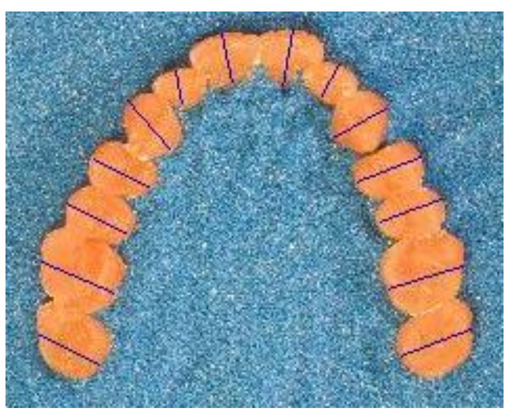

Figure 3.9. Each tooth's bucco-lingual distance is marked on the image.

3.4.5.3 Area of each tooth

Since cusps are ill-defined on most casts, the 'crown area,' or projected surface area, rather than the actual surface area, is found. Once the boundaries are satisfactorily identified, tooth relabeling is necessary. Since MATLAB's *bwlabel* function labels regions based on their location in the image (consecutively, beginning with the first object in the upper left corner and moving down and to the right), these labels are not meaningful. Instead, each tooth is relabeled with the number corresponding to its number in the tooth numbering system. The area of each tooth (in pixels) is then determined using MATLAB's *bwarea* function and is stored in the data structure. Although the crown area is calculated for all teeth, this measurement is only valid for molars and premolars, since the projected area of the canines and incisors does not correspond to their occlusal surface areas.

3.4.5.4 Angle of Rotation

The angle of rotation is defined as the angle between the vertical image axis and the mesio-distal axis of each tooth (Figure 3.10). The image is taken using the camera viewfinder to ensure the correct image orientation is obtained. The sign of the each angle indicates the direction of rotation of that tooth. The left half of the maxilla (Figure 3.3) and the right half of the mandible (Figure 3.4) give positive values for clockwise rotation and negative values for anti-clockwise rotations, whereas the right half of the maxilla and the left half of the mandible give positive values for anti-clockwise rotation and negative values for clockwise rotations.

$$angle = atan2\ (abs(\det(AB, AC)), cross(AB, AC)) \qquad [3.2]$$

where AB is the vertical line for each tooth and AC is the mesio-distal line for each tooth (Figure 3.10).

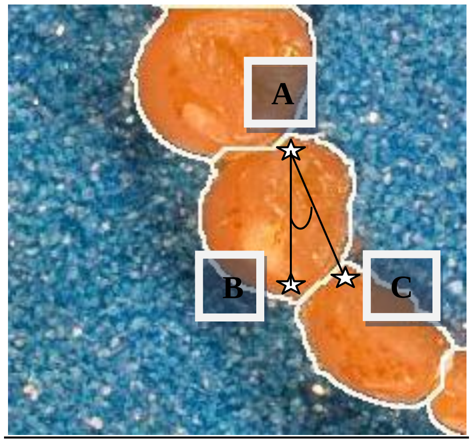

Figure 3.10. The angle is calculated between the lines AC (where A and C are the mesial and distal points of the tooth) and AB (a vertical line extended from the mesial point of the tooth).

3.4.5.5 Arch Measurements

3.4.5.5.1 Selecting the Midline

The initial arch midline estimate, autonomously placed on the image by the software, is the line connecting the point between the central (or first) incisors and the midpoint of the imaginary line connecting the distal coordinate points of the third molars (Figure 3.9). If reference teeth are missing, the next adjacent pair is used as a reference (e.g., midpoint of the line joining the distal points of the lateral incisors or second molars, and so on). Once the midline is displayed, the user can adjust the position of the midline as desired. The coordinates of the endpoints of the final midline are stored in the data structure.

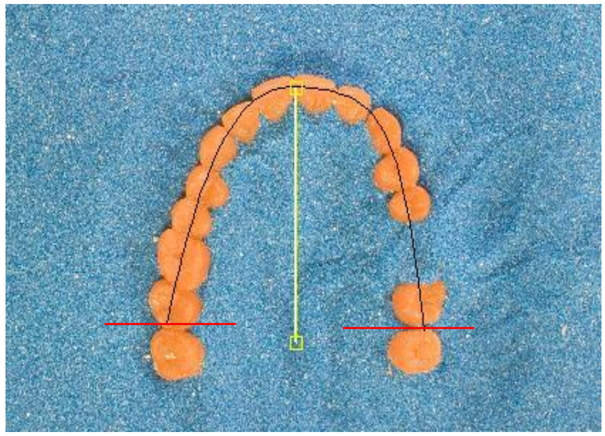

Figure 3.11. The initial midline (yellow line) is automatically placed on the image, but can be manually adjusted by the user as desired. This image also shows the arch fit (black line). The third molars are excluded from the arch fit.

3.4.5.5.2 Arch Fit

The user-selected coordinate points are used to derive all arch measurements. Of interest is the ability to quantitatively describe and compare arch shapes, as well as investigate bilateral symmetry. Several approaches were investigated for fitting a curve to each dental arch. The most successful method first calculates the midpoint of the bucco-lingual distance for each tooth and adds these midpoints to the set of mesial and distal coordinate points. MATLAB's *polyfit* function is then used to define the polynomial coefficients for the best fit n^{th} order curve to the dataset. Trial and error led to the selection of a fourth-order polynomial as the default curve order. If the arch fit appears inaccurate, the user can experiment with different curve orders to improve the fit.

$$p(x) = p_1x^n + p_2x^{n-1} + \ldots + p_nx + p_{n+1} \quad [3.3]$$

Analysis showed that the fourth order polynomial works for the majority of the casts as many previous authors have confirmed, but a user-initiated change in the order of the arch fit curve is sometimes required. Further, any coefficient that leads to an overestimation of the arch length is automatically removed by the program, which makes the fit more accurate.

3.4.5.5.3 Arch Widths

Arch widths are determined separately for both the left and right halves of each dental arch. Widths are calculated at the distal points of the canines and first molars for permanent dentition and at the distal points of canines and second molars for deciduous dentition. The horizontal distance *h* between the reference point (x_{ref}, y_{ref}) (depending on which width is measured) and the corresponding point on the midline ($x_{midline}$, $y_{midline}$) is obtained using the Euclidean distance formula

$$h = \sqrt{\left(x_{\mathrm{ref}} - x_{\mathrm{midline}}\right)^2 + \left(y_{ref} - y_{midline}\right)^2} \quad [3.4]$$

The distance between the mesial end of the midline and the intersection points on the midline (separately for the left and right halves of each measured width) is also determined using Equation [3.4].

Permanent Dentition

The calculated widths are as follows (Figure 3.10):

1) Molar Width: The width between the posterior points of the first molars and the midline is calculated separately for each the left and right sides of the maxilla and the mandible. If a first molar is missing, the anterior point of the second molar is substituted.

2) Canine Width: The width between the posterior points of the canines and the midline (four measurements as above). If a canine is missing, the anterior point of the first premolar is substituted.

3) Lingual Widths: The widths between the left and right lingual points are calculated for the canines, premolars and molars.

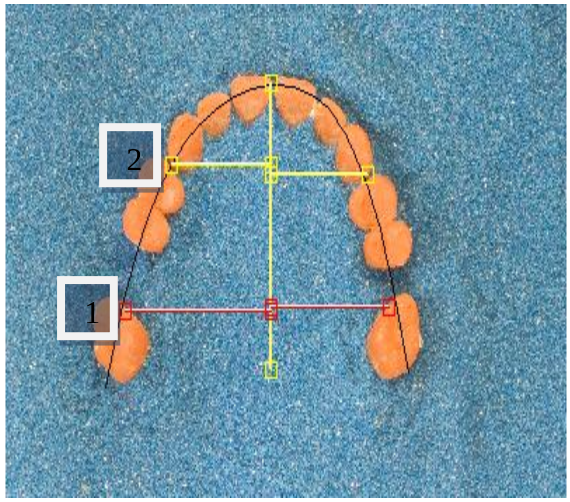

Figure 3.12. Arch width calculations reflect (1) the molar arch width and (2) the canine arch widths.

Deciduous Dentition

Canine Width: The width between the posterior points of the canine and the midline is calculated separately for each the left and right sides of the maxilla and the mandible. If a canine is missing, the anterior point of the first premolar is substituted.

3.4.5.5.4 Arch Lengths

Arch lengths are found using equation [3.1]. In each case, the lengths of the left and right halves of the arch are determined separately.

1) Total arch length: The total dental arch length (the length of the line from the posterior point of the second molar on the left side of the arch to the posterior point of the second molar on the right side of the arch, generally following the mesio-distal points of each tooth) is obtained for the maxilla and the mandible (Figure 3.10).

2) Canine arch length: The length of the arch from the posterior point of the canine on the left side to the posterior point of the canine on the right side is obtained for the maxilla and the mandible. If the canine is not present, the anterior point of the first premolar is substituted (Figure 3.11a).

3) Molar Arch Length: The length of the arch from the posterior point of the second premolar on the left side to the posterior point of the second premolar on the right side of is obtained for the maxilla and mandible. If the second premolar is not present, the anterior point of the first molar is substituted (Figure 3.11b). Deciduous dentition will not have a molar arch length.

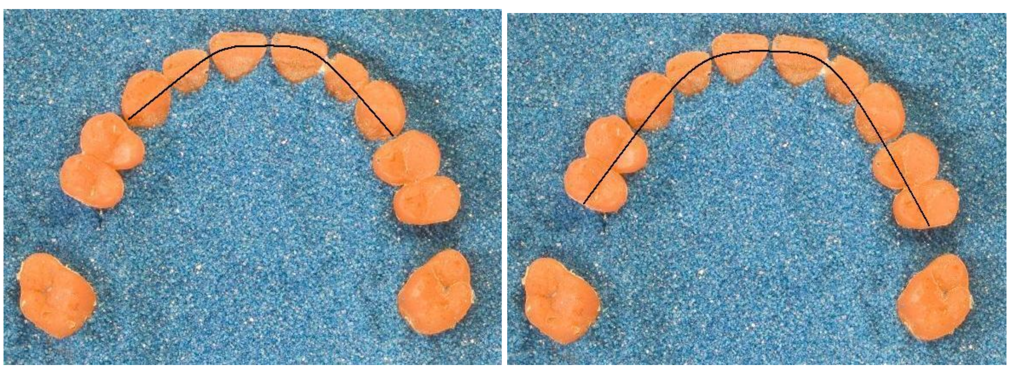

(a) (b)

Figure 3.13. In addition to total arch length, the software calculates a) canine arch lengths and b) molar arch lengths.

3.4.5.6 Midline Lengths

Midline lengths are calculated as follows:

1) Canine Midline Length: The length from the mesial end of the midline to the point on the midline that corresponds to the posterior point of the canine is determined for both the left and right sides. If the canine is not present, the anterior point of the first premolar is substituted (Figure 3.14).

2) Molar Midline Length: The length from the mesial end of the midline to the point on the midline that corresponds to the posterior point of the first molar is determined for both left and right sides. If the first molar is not present, the anterior point of the second mo.lar is substituted (Figure 3.14).

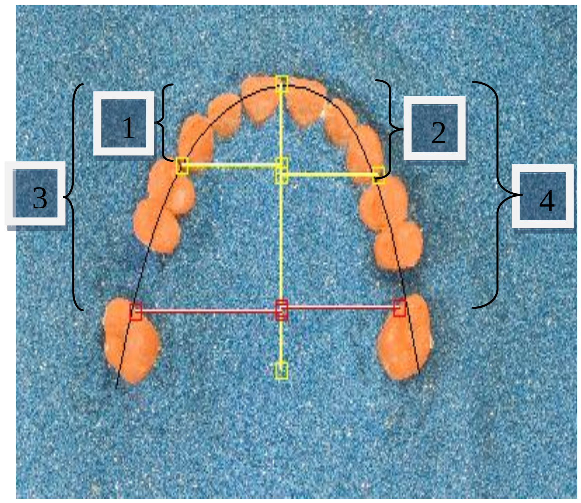

Figure 3.14. Midline length calculations reflect (1) the canine midline length (right-half of maxilla), (2) the canine midline length (left-half of maxilla), (3) the molar midline length (right-half of maxilla) and (4) the molar midline length (left-half of maxilla).

.

4. GRAPHICAL USER INTERFACE

A graphical user interface (GUI) provides the software user with a pictorial view of the algorithm to assist with program interaction. Using MATLAB’s Graphical User Interface Development Environment (GUIDE) (MATLAB R2007b, MathWorks, Inc., Natick, MA, USA), we developed an interface with various user interaction tools, such as display panels, pushbuttons, drop boxes and text boxes.

4.1 Requirements of the GUI

The GUI serves to provide the output (dimensions, boundaries, review) of the automated analysis process and to offer tools for the user to correct the results at various stages of the process in the event that the output of the automatic routines is incorrect. User intervention is possible at the following stages: entering subject information, boundary detection and arch fit.

4.2 Components of the GUI

The main GUI was designed to meet the stated requirements of automatic analysis and manual intervention (Figure 4.1). During the GUI design phase, feedback from the client was incorporated to generate a user-friendly tool to accomplish the analysis. Details of each GUI section are described below.

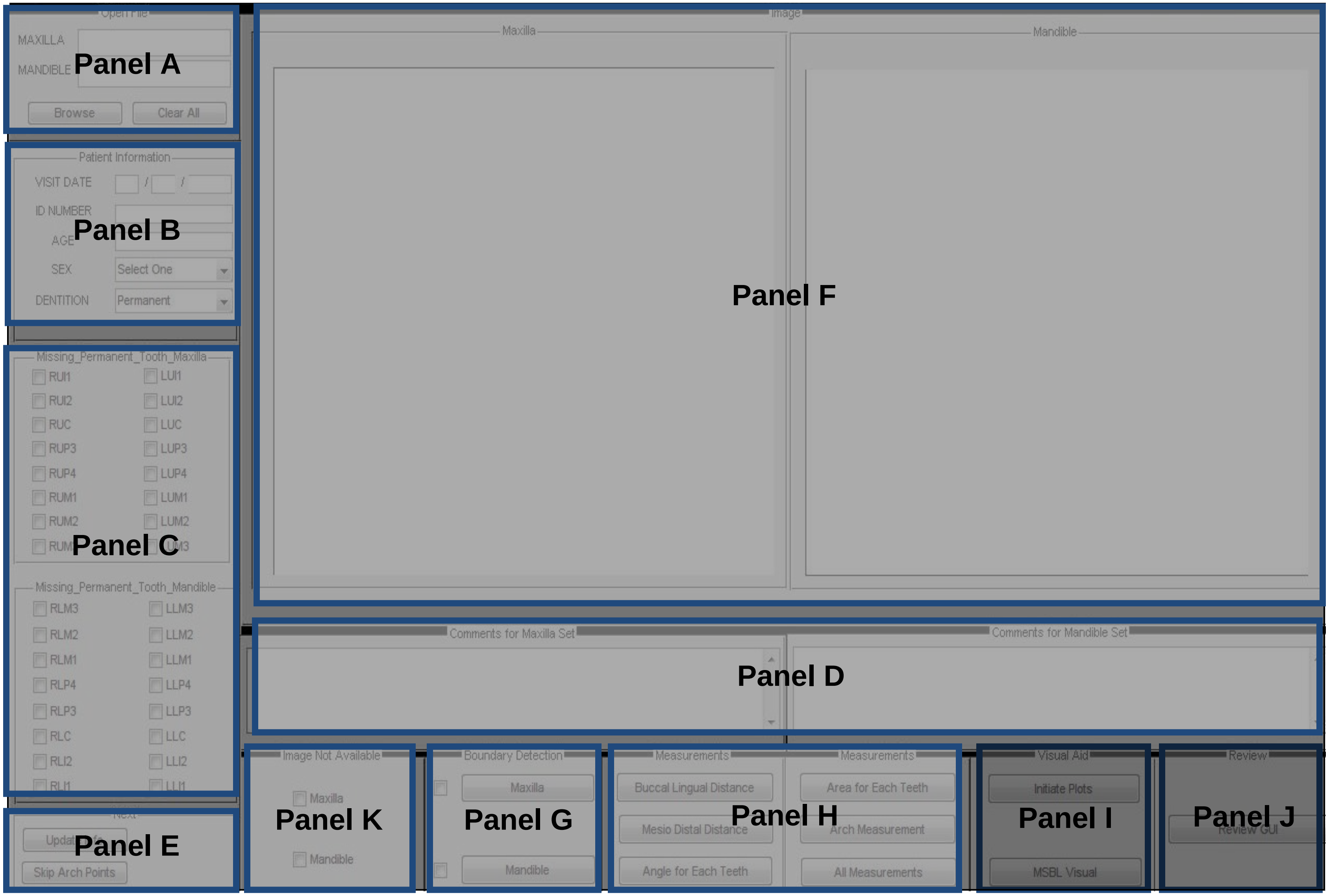

Figure 4.1 Layout of the main GUI. Each panel guides specific tasks as explained in detail in subsequent figures.

4.2.1 Selection of the Individual Directory

The maxillary and mandible images for each individual are saved to particular folder during image acquisition. To initiate a new analysis, the first step is to clear the MATLAB workspace and refresh the GUI by pressing the ‘Clear All’ button. The GUI is then restarted from within MATLAB, and within Panel A (Figure 4.1), using the ‘Browse’ button (Figure 4.2, Item 2), the analyst selects the input directory that contains the participant folders. Selecting the required folder and pressing ‘OK’ will open up the image in Panel F (Figure 4.1), with the maxillary image on the left side and the mandibular image on the right side as shown in Figure 4.3.

Figure 4.2 Layout of Panel A. The user first clears any data in MATLAB and the GUI using the (1) ‘Clear All’ button and then initiates the analysis by selecting the individual folder using the (2) ‘Browse’ button.

4.2.2. Image Not Available / Bad Quality

If either the maxilla or mandible image is not available, the corresponding check-box in Panel K (Figure 4.1) will be automatically marked when the subject folder is selected by the analyst, and a dummy image will be shown instead (Figure 4.4). The Image Not Available check-box can also be enabled if the analyst feels the image in the folder cannot be analyzed or might yield invalid results. In this case, a dummy image is shown in spite of the image being present in the individual’s folder.

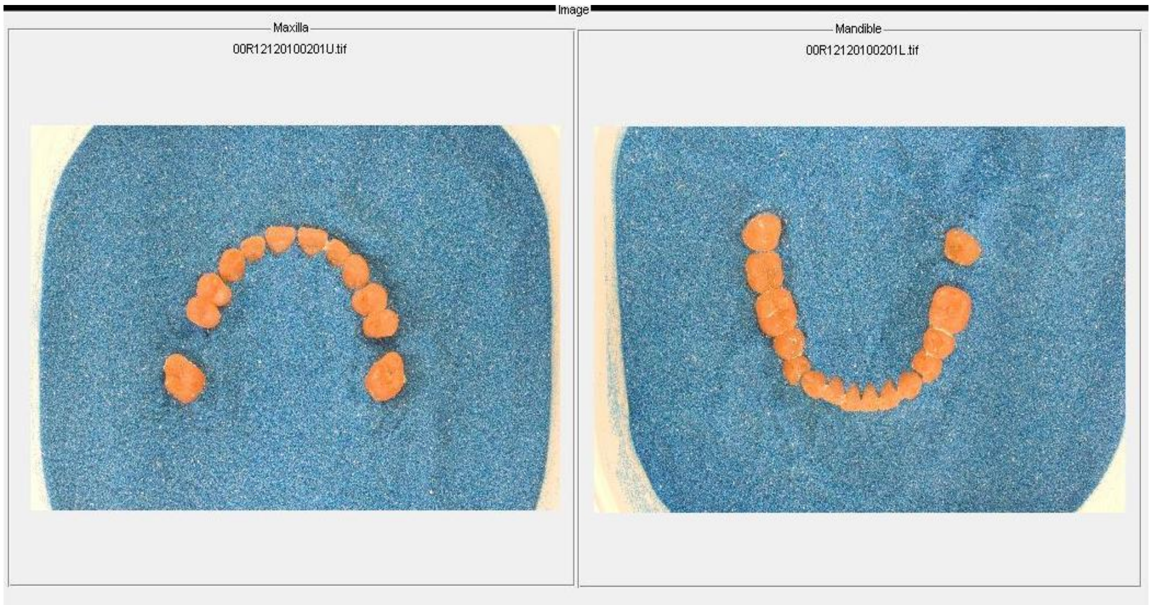

Figure 4.3. The selected participant's maxillary (left) and mandibular (right) images are displayed in Panel F.

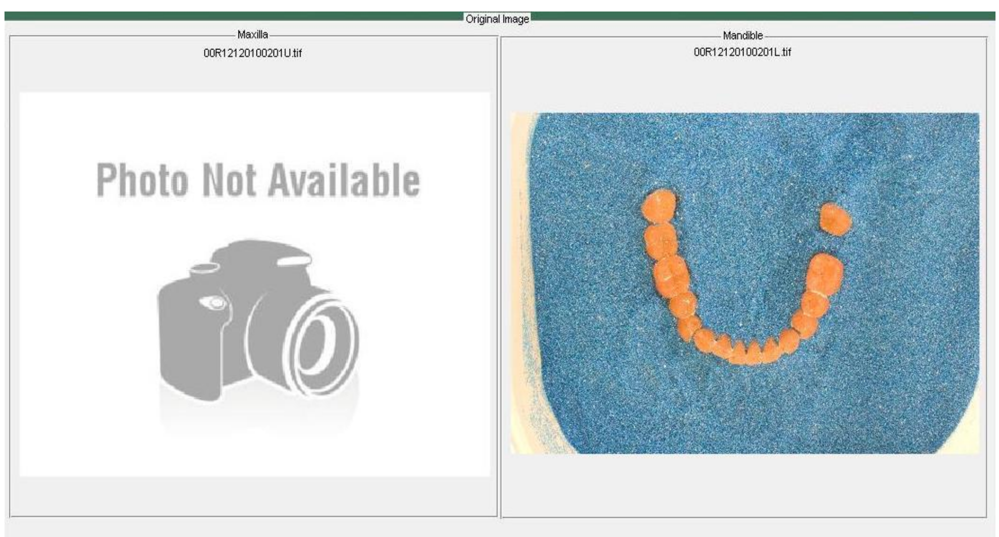

Figure 4.4. This 'dummy image' appears if a maxilla or mandible image is not available or if the user determines that the image will produce invalid results

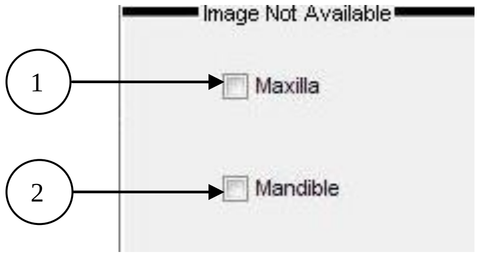

Figure 4.5. Layout of Panel K, showing check-boxes for (1) the maxilla and (2) the mandible. The check boxes are automatically checked if the individual folder contains only the maxilla or only the mandible image. Alternatively, the user can click the check box if the image quality is insufficient to produce desired results.

4.2.3 Entering Subject Information

The 'VISIT DATE' and 'ID NUMBER' for 'Patient Information' (Panel B, Figure 4.1) are directly obtained from the filename for each subject, whereas 'AGE' and 'SEX' must be entered by the analyst. The 'DENTITION' is set to 'Permanent' by default, and the user must change this to 'Deciduous' if required (Figure 4.6).

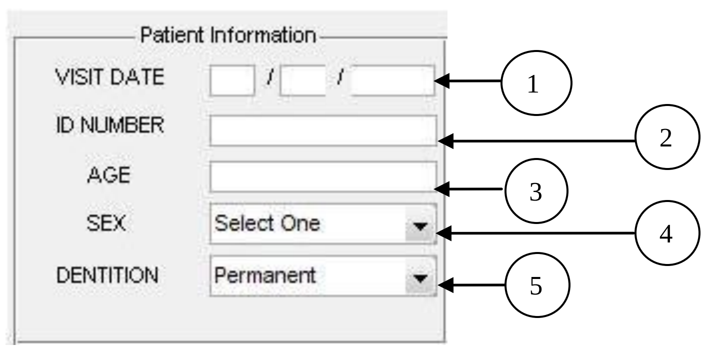

Figure 4.6 Layout of Panel B. (1) is the date the dental impression of the individual was obtained and is recorded from the folder name itself in the order of Month/Day/Year, (2) is the six digit patient identifier, also taken from the filename, (3) is the age of the individual, (4) is the sex of the individual ('male,' 'female' or 'information is not available') and (5) is to declare whether the dental cast is a permanent or deciduous cast; the default setting is 'permanent.'

4.2.4 Account for Missing Teeth

Missing teeth are identified by clicking the required check-boxes in Panel C (Figures 4.1, 4.7 and 4.8). Acronyms for each tooth have been described earlier in Section 3.4.1.

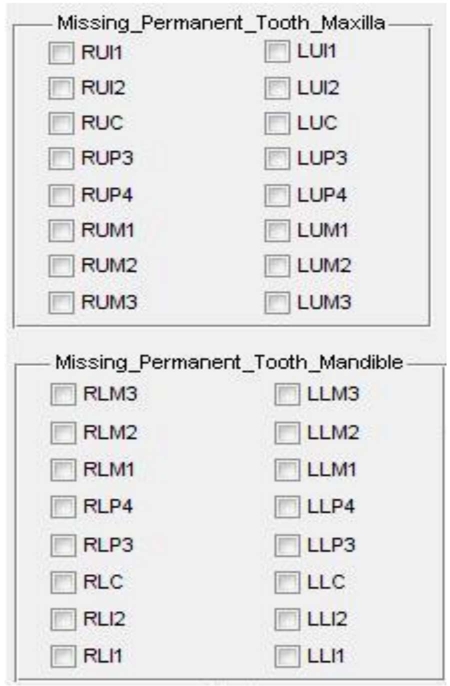

Figure 4.7 The user is to account for any missing permanent teeth by selecting the corresponding check boxes. Within the output file, data fields for missing teeth are populated with a specific value so that the analyst recognizes that these teeth were not available for analysis.

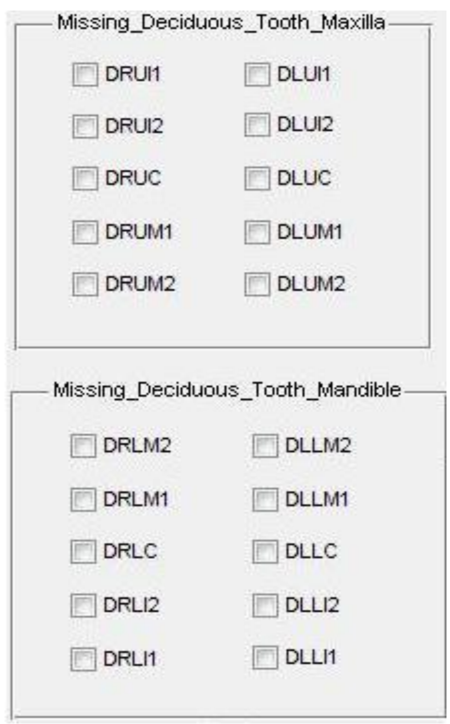

Figure 4.8 As with the permanent teeth, the user identifies missing deciduous teeth via these check boxes.

4.2.5 Eliminate Teeth from Arch Measurements

If the user feels a particular tooth is out of place and will affect the arch fit or arch width measurements, the tooth can be excluded from the arch measurements by clicking ‘Skip Arch Points’ (Figure 4.13, Item 2). This will replace Panels B and C (Figure 4.1) with that shown in Figure 4.9 for permanent dentition and Figure 4.10 for deciduous dentition.

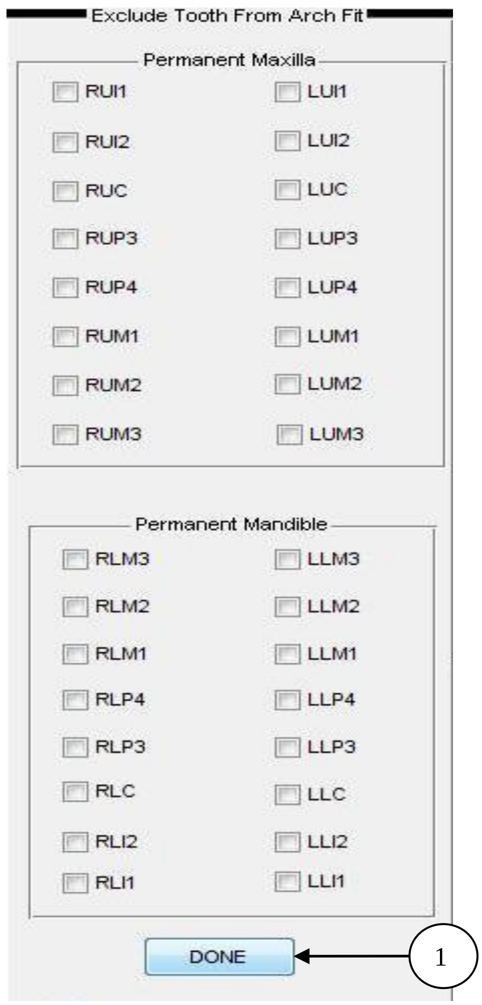

Figure 4.9. To eliminate a permanent tooth/teeth from arch measurements, the user will click the check boxes of the teeth that are to be excluded. (1) is pressed to close the ‘Skip Arch Points’ tab once the data are entered.

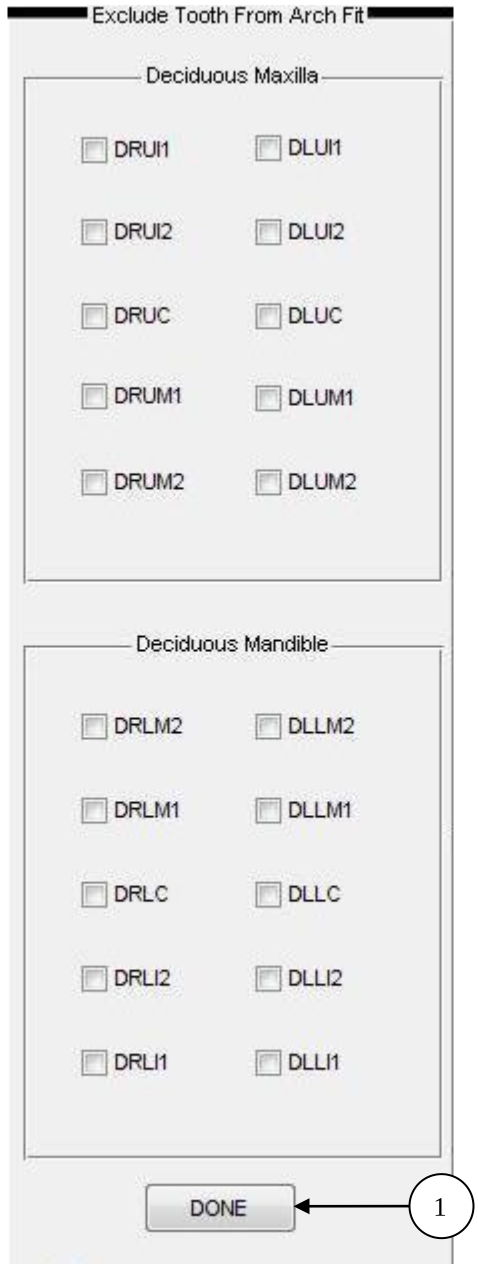

Figure 4.10. As with the permanent dentition, a deciduous tooth/teeth may be excluded from arch measurements by specifying that information here.

4.2.6 Additional User Comments

Any additional narrative comments the analyst wants to record for future reference are to be entered in Panel D (Figure 4.1). There is a separate window for both the maxilla and the mandible, as shown in Figure 4.11 below.

Figure 4.11. Layout of Panel D. Additional comments are to be entered here by the user for the (1) maxilla and (2) mandible.

4.2.7 Updating Subject Information

All subject information entered is saved when the analyst selects the 'Update Info' button in Panel E (Figure 4.1). If any of the fields in Panel A or Panel B are left blank, a warning is shown (Figure 4.12). An Excel spreadsheet is created for each individual for storing the analysis results.

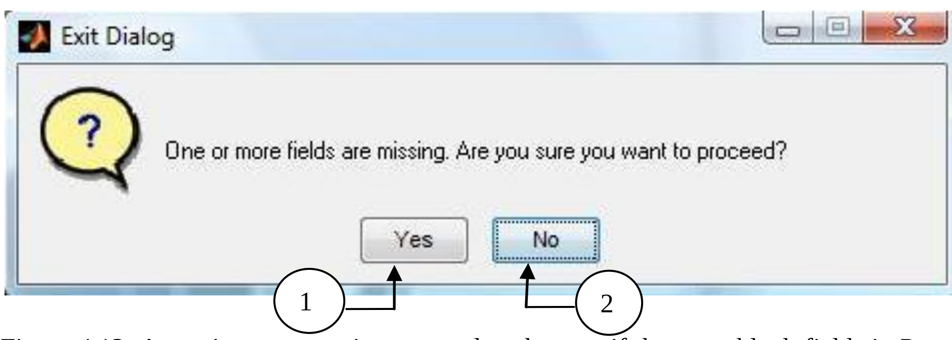

Figure 4.12. Awarning message is presented to the user if there are blank fields in Panel A or Panel B. Pressing (1) Yes ignores the warning and continues the saving process, and pressing (2) No halts the save process and lets the user make the required changes.

4.2.8 Coordinate Point Selection

The 'Point Selection' button (Figure 4.13b, Item 3) will only appear once the 'Update Info' button (Figure 4.13a, Item 1) has been selected (both in Panel E, Figure 4.13). Selecting 'Point Selection' will open a new window, where the user can identify the coordinate points for each tooth.

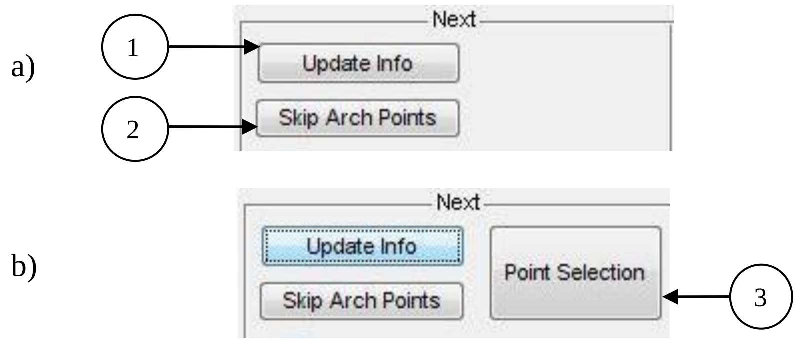

Figure 4.13. a) In Panel E, once the ‘Update Info’ button (1) is pressed, b) the ‘Point Selection’ button (3) is enabled.

4.2.8.1 Selecting the Coordinate Points

During coordinate point selection, each point is labeled with a particular number corresponding to the current tooth. For example, if the third molar on the left side of the maxilla is present, it will be label with points one through four for the first four clicks on that tooth, and the third molar on the right side will receive labels 61 through 64; the automatic labeling will continue through points 125 through 128 for the right mandibular third molar. If a tooth is absent, four labels are automatically skipped. For example, the dental impression in Figure 4.14 has missing left maxillary first and third molars. In this case, the first available tooth (left maxillary second molar) is labeled five through eight and the next available tooth (left maxillary second premolar) gets labels 13 through 16.

Following maxillary, and then mandibular, point selection, dialogue boxes (Figure 4.15) appear to instruct the user to make any necessary changes before proceeding to the next step.

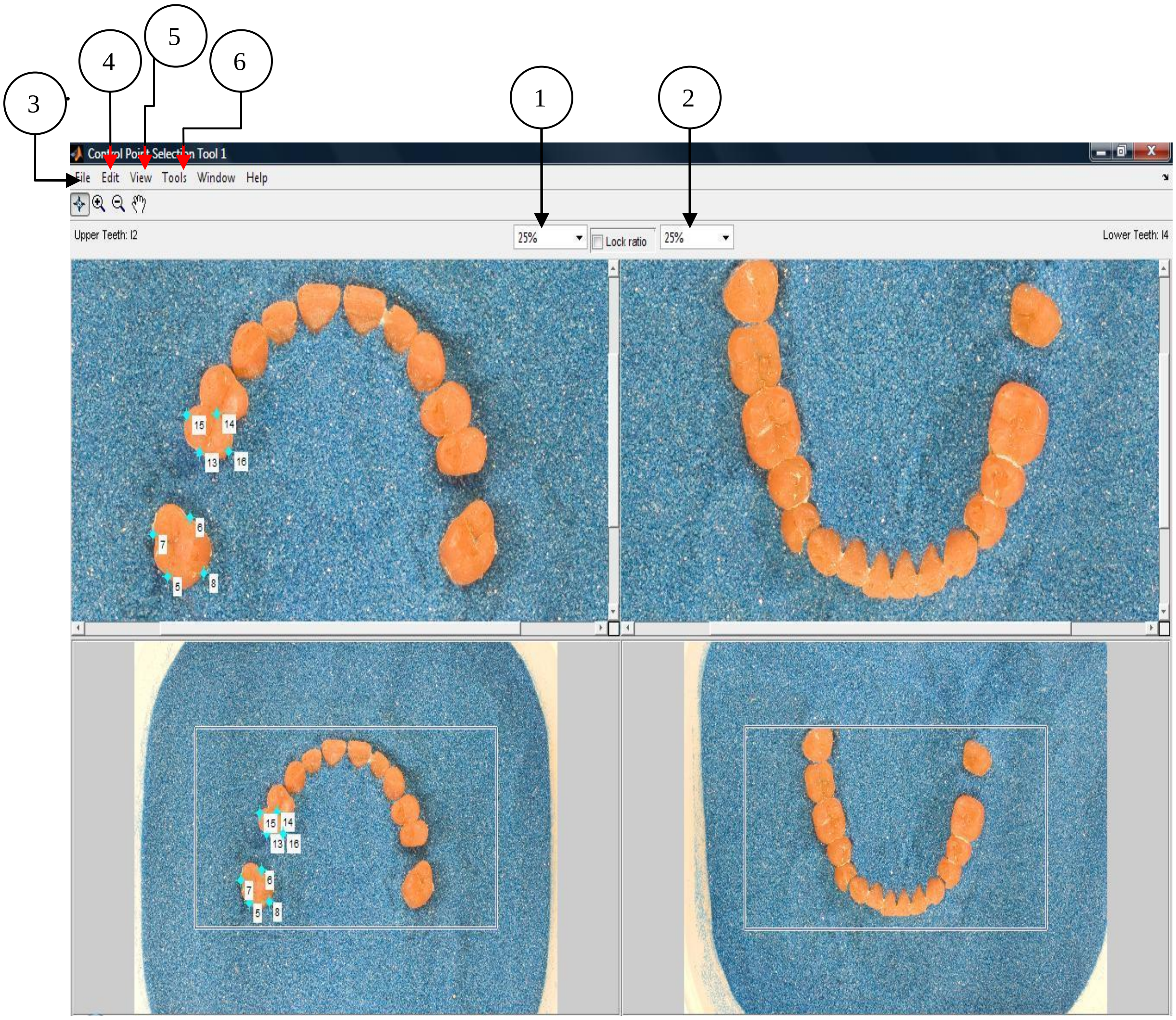

Figure 4.14. Within the coordinate point selection window, the user can (1) zoom into the maxillary image, (2) or mandibular image, (3) select and save all coordinate points or close the coordinate point selection window, (4) delete the active point (to make a point active, that point is clicked upon again) and (5) remove the overview images (bottom half of this window).

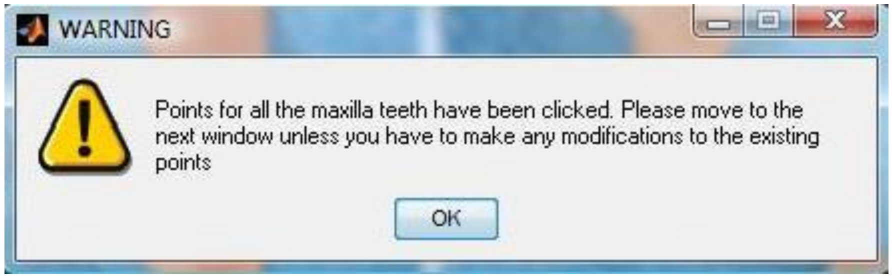

(a)

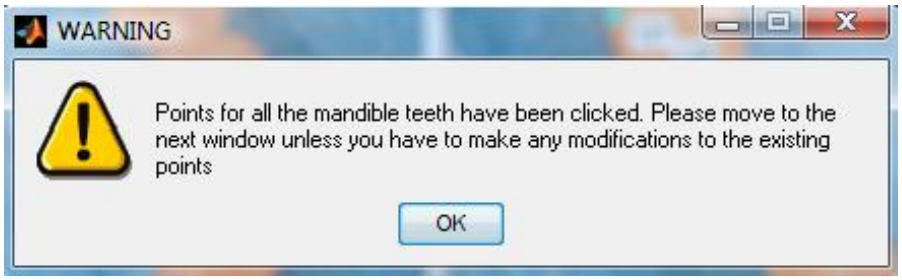

(b)

Figure 4.15. Messages appear when all of the coordinate points on the (a) maxilla and b) mandible have been entered, so that the user can make changes before these points are saved.

4.2.8.2 Features of the Coordinate Point Selection Window

a) Overview Images

By moving the rectangular box, the user can select the appropriate region in the main window to be zoomed in upon (Figure 4.14). The overview images can be removed or made to appear by selecting ‘View’ (Figure 4.1.4, Item 5) and disabling/enabling ‘Show Overview Images,’ respectively. Figure 4.16 shows the window without the overview images.

b) Zoom

The analyst can zoom in up to 800% to better view a tooth of interest. This is particularly useful for locating the mesio-distal coordinate points between adjacent teeth.

c) Coordinate point deletion

Coordinate points can be deleted in two ways: by selecting (clicking on) a particular point and 1) pressing the ‘Delete’ button on the keyboard or 2) choosing ‘Delete Active Upper

Tooth Point' or 'Delete Active Lower Tooth Point' in the 'Edit' tab (Figure 4.14, Item 4) depending on whether the coordinate point is in the maxilla or mandible.

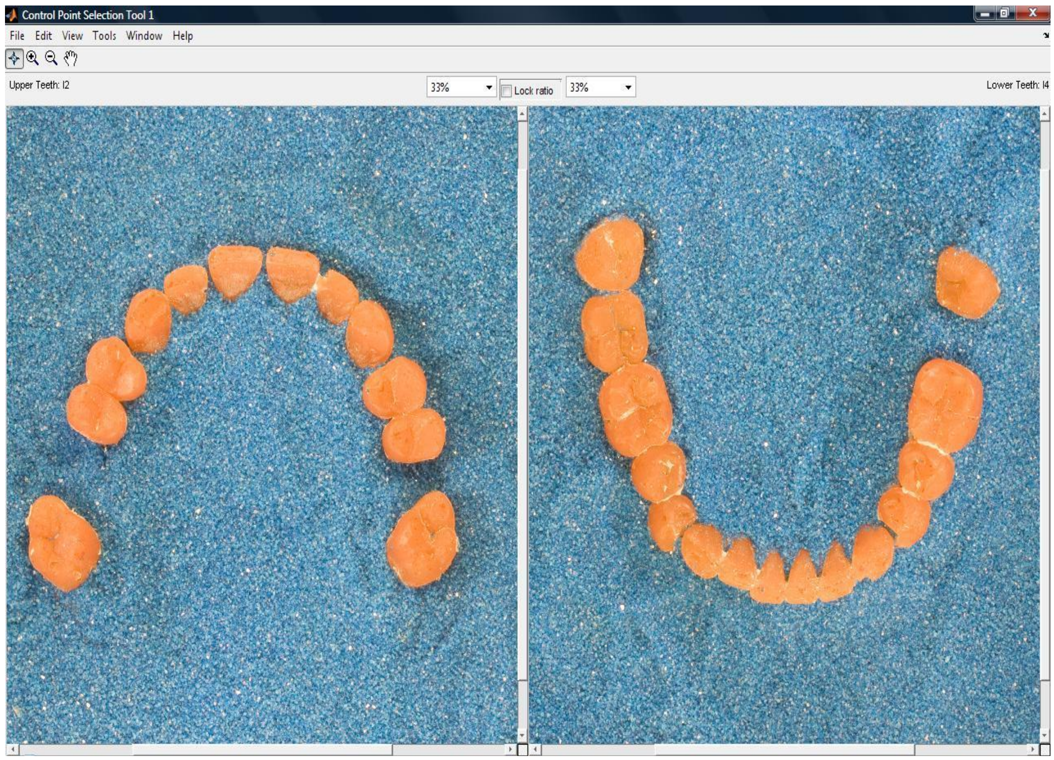

Figure 4.16. Image showing coordinate point selection window without the overview images window. The overview images can be made to reappear by pressing 'View' (Figure 4.1.4, Item 5) and then selecting 'Show Overview Images.'

d) Coordinate point save

After all of the coordinate points have been selected, to save the point set, the user chooses the 'File' tab (Figure 4.14, Item 3) and selects 'Save Teeth Coordinates to Workspace' from the options. This opens a new dialogue box (Figure 4.17) pressing 'OK' (Figure 4.17, Item 1) here saves the coordinate points into the Excel spreadsheet.

e) Closing the control point selection tool

The coordinate selection tool can be closed in two ways: 1) by selecting ‘Close Coordinate Selection Tool’ from the ‘File’ tab (Figure 4.14, Item 3); or 2) by closing the particular control point selection tool figure window.

Figure 4.17. When the user selects ‘Save Teeth Coordinates to Workspace’ pressing (1) will save the coordinate points to an Excel spreadsheet and selecting (2) will cancel the save process. The mandible coordinates are saved as ‘L_Points’, the maxilla coordinates are saved as ‘U_Points’ and the entire data set is saved as ‘cpstruct’. If desired, the user can overwrite the default filenames via the input text boxes.

4.2.9. Boundary detection

The ‘Maxilla’ and ‘Mandible’ buttons in the Boundary Detection Panel (Panel G, Figure 4.1) are selected by the user to obtain the boundaries for the maxillary teeth and mandibular teeth, respectively. The boundary images replace whichever image is in Panel F (Figure 4.1) at that time. Figure 4.18 shows Panel G and Figure 4.19 shows an image with the boundaries detected.

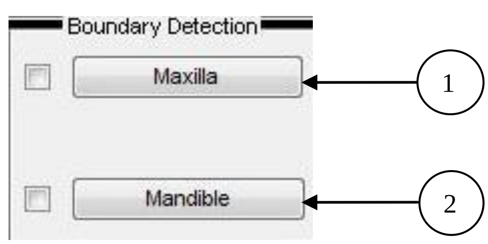

Figure 4.18. Layout of Panel G. Initiation of boundary detection occurs when the (1) Maxilla and (2) Mandible buttons are pressed. When the boundaries are saved (Figure 4.19, Item 7 and Item 14), the appropriate check boxes for the maxilla and mandible will be marked as a visual aid to let the user know the boundary has been saved.

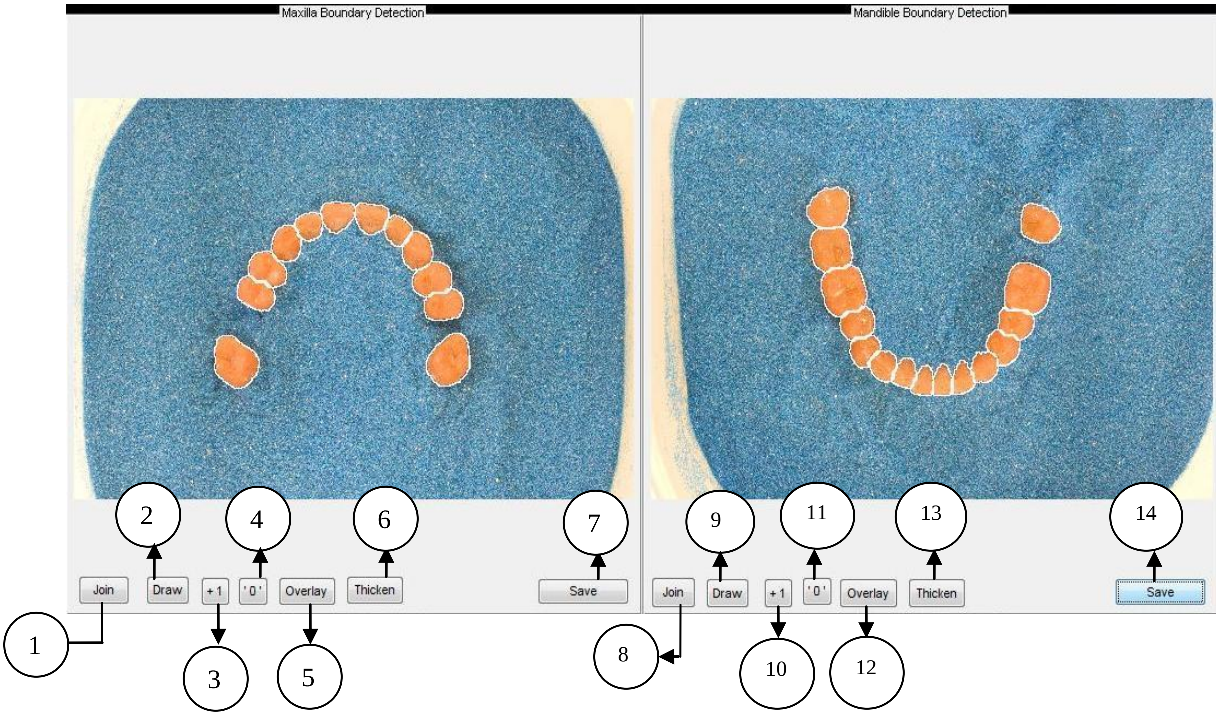

Figure 4.19. The automatically-detected tooth boundaries are shown for both the maxilla and mandible. A number of options are available at this step. (1) joins any split boundaries in the maxilla, (2) lets the user draw one or more maxillary tooth boundaries if the automatic boundaries are not accurate, (3) is used when multiple maxillary teeth are detected as a single region, (3) advances the manual drawing feature to the next available tooth (4) lets the user replace a detected boundary by setting it as background, (5) is used to draw a boundary that totally overlies the detected boundary, (6) lets the user thicken the detected boundary for better visualization, and (7) saves a binary image of the final boundary into the subject's folder, updates any boundary changes made and displays the image in the maxilla region of Panel F. Items (8) through (14) accomplish analogous functions for the mandible.

4.2.9.1 Joining Separately Detected Regions of One Tooth

If the algorithm splits a single tooth into multiple regions, the 'Join' button can be used for correction. Pressing this button will place a 'cross-hair' symbol on the image. The analyst then clicks once inside each of the two regions and presses 'Enter'. This opens up a confirmation dialogue box (Figure 4.20). Pressing 'Yes' (Figure 4.20, Item 1) or 'No' (Figure 4.20, Item 2) accepts or ignores the change, respectively. Pressing 'Save' (Figure

4.19, Item 4 for maxilla and Item 8 for mandible) stores and displays the updated boundary within Panel F. Figure 4.21a and Figure 4.21b show a region joining operation.

Figure 4.20. Confirmation dialogue box gives the following options. (1) proceed with changes or (2) ignore the changes.

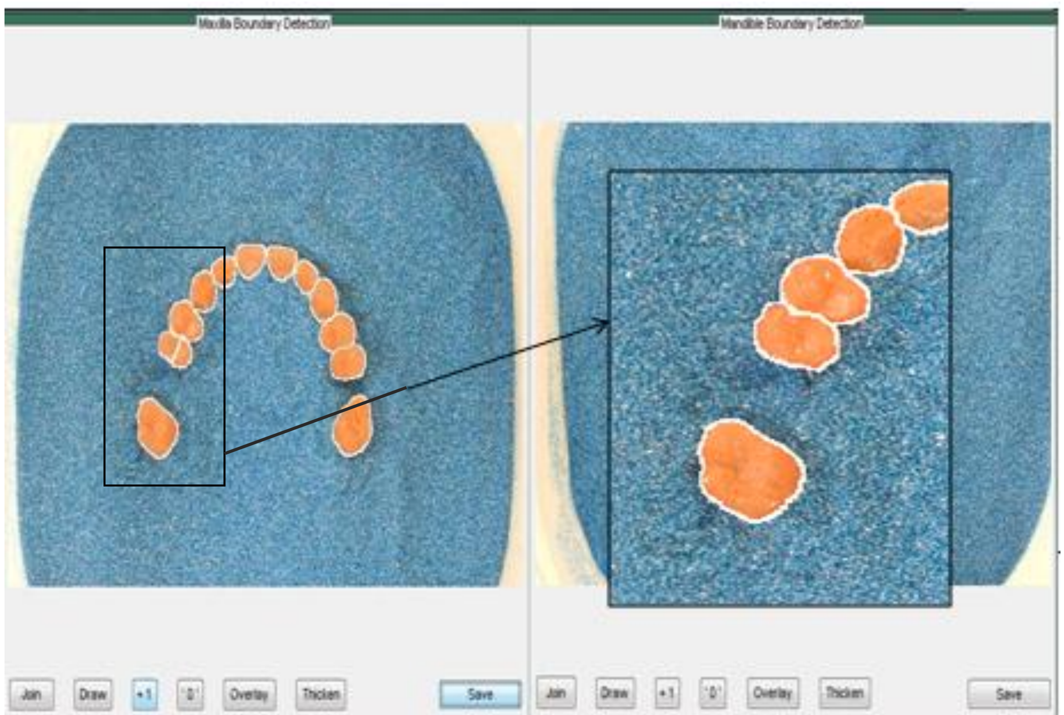

Figure 4.21. In the maxillary image (left), the user has selected two regions that should be merged and the zoomed version shows the maxillary image after the user merged the broken tooth.

4.2.9.2 Drawing boundaries

The ‘Draw’ button (Figure 4.19, Item 2 for the maxilla and Item 9 for the mandible) is used if the analyst is not happy with the automatically-detected boundary. Pressing this button will place a ‘cross-hair’ symbol on the image. The user then clicks anywhere inside the tooth whose boundary is to be replaced with a manually-drawn boundary. Pressing ‘Enter’ on the keyboard will display a confirmation box (Figure 4.20), and pressing ‘Yes’ will open up a new window (Figure 4.22) showing boundaries for all the teeth except the one that is to be redrawn. The computer mouse is used to draw the new boundary; dragging while pressing the left click button and only letting go once the boundary has been drawn. A confirmation box opens when the drawing is complete to allow the user to indicate whether or not the drawn boundary is acceptable (Figure 4.23). The process can be repeated until the user is satisfied with boundary selection. Pressing ‘Save’ button (Figure 4.19, Item 7 for maxilla and Item 14 for mandible) will show the updated boundary in Panel F.

4.2.9.3 Separating teeth that are detected as a single region

The first step in segmenting a single detected region into two or more teeth is to use the ‘Draw’ button to click anywhere inside the boundary of the region to be separated. The user then manually draws the correct boundary for the ‘first’ tooth in that region (‘first’ here refers to the tooth order, i.e., order of coordinate point selection). Once the boundary for the first tooth is saved, the next step is to press the ‘+1’ button (Figure 4.19, Item 3 for the maxilla and Item 10 for the mandible), which opens up a new window, in which the user draws the next tooth’s boundary using the same procedure described in section 4.2.9.1.2. This step may be repeated if additional teeth remain in the original region.

Pressing the ‘Save’ button (Figure 4.19, Item 7 for the maxilla and Item 14 for the mandible) stores and displays the changes in Panel F.

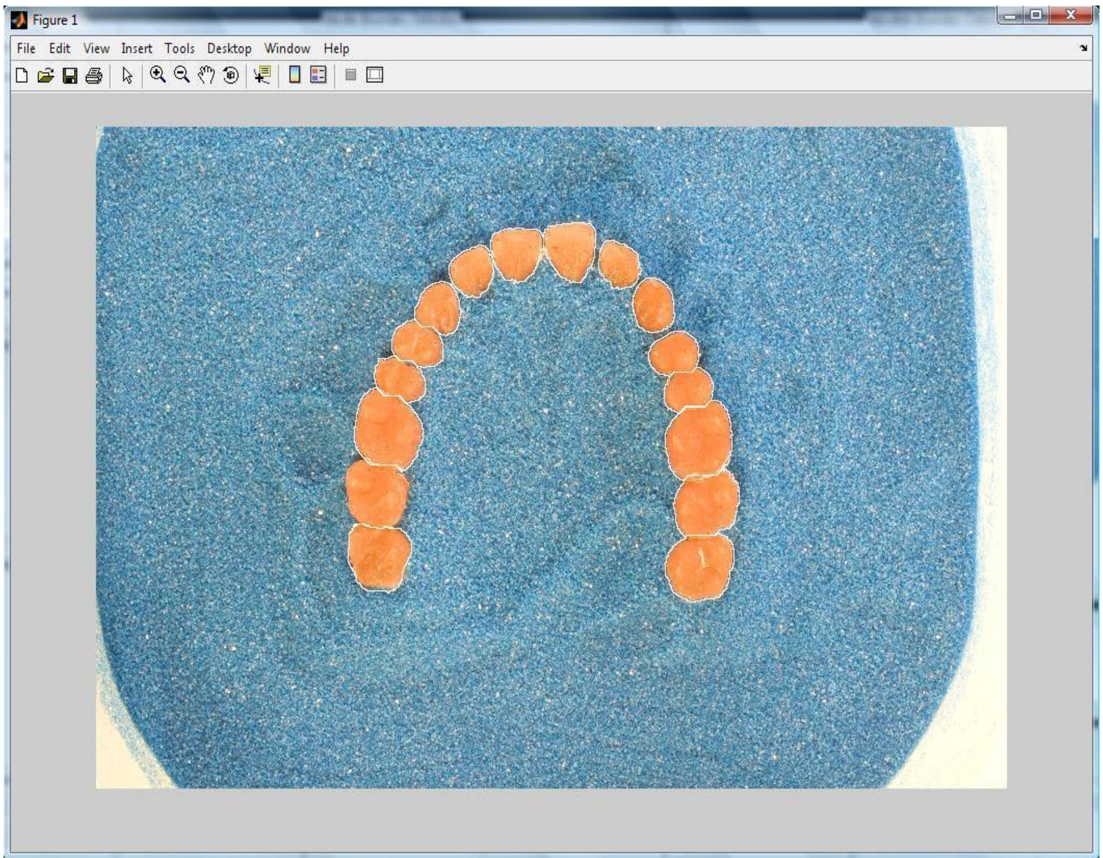

Figure 4.22 When a boundary is to be redrawn manually, the user is presented with an image showing all automatically-detected boundaries except that around the tooth of interest. Using the mouse, the user traces the boundary on the image.

Figure 4.23 Confirmation dialogue box for the new boundary. Selecting (1) accepts the new boundary, whereas selecting (2) rejects the new boundary.

4.2.10 Measurements

A number of measurements may be output (Figure 4.24). The user has the option to perform individual measurements or complete all measurements in a single step by pressing the ‘All Measurements’ button (Figure 4.24, Item 6). The units of measurements are ‘mm’ for bucco-lingual widths, mesio-distal lengths and arch measurements, ‘mm^2’ for area measurements and ‘degrees’ for angles of rotation.

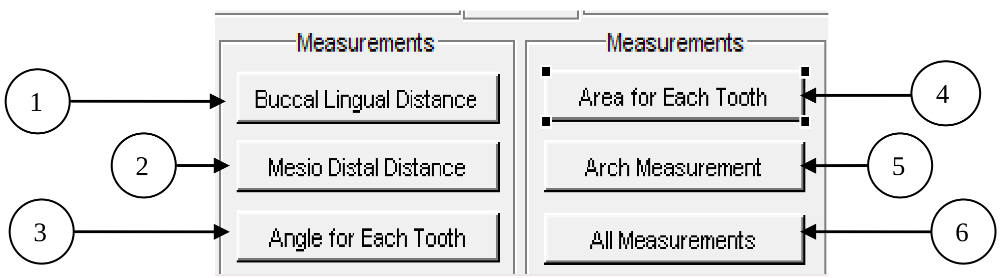

Figure 4.24. Layout of Panel H. (1) calculates the buccal-lingual distance of each maxillary and mandibular tooth, (2) calculates the mesio-distal distance of each tooth, (3) calculates the degree of rotation of each tooth, (4) calculates the area of each tooth, (5) performs all the arch measurements (arch widths and arch lengths) described in section 4.2.10.1 and (6) performs steps (1) through (5) in one click. Since some user input is required for arch measurement, the user is taken to that process when ‘All Measurements’ is selected.

When either the ‘Arch Measurement’ or ‘All Measurements’ button is pressed, Panel F is replaced with an image containing the arch fit interface, and the initial, autonomously-determined maxillary midline is displayed (Figure 4.25). The default arch fit curve order is set to four, but the analyst can easily change this by selecting a new order value from the drop-down box (Figure 4.25, Item 2) after pressing the ‘No’ button (Figure 4.25, Item 5). Once the order for arch fit is decided, the analyst can also manually modify the arch midline by dragging either or both line endpoints to the desired position and pressing the ‘OK’ button (Figure 4.25, Item 6). The user can also extend the arch length to the distal point of the first or last tooth in the arch fit by pressing the ‘L’ (Figure 4.25, Item 4) or ‘R’ (Figure 4.25, Item 7) button(s) for the left and right sides of the image, respectively. Once satisfied with the results, pressing the ‘Save & Next’ button (Figure 4.25, Item 3), will display all of the maxillary arch widths on the image and will initiate the mandibular arch measurement process. The mandibular arch fit and initial midline are displayed (Figure 4.26), and the user continues as with the maxillary arch analysis. Once satisfied with the mandibular arch measurements, pressing ‘Save’ (Figure 4.26, Item 3) enters all arch measurements into the Excel spreadsheet. Figure 4.27 shows the arch analyses results for both the maxilla and the mandible.

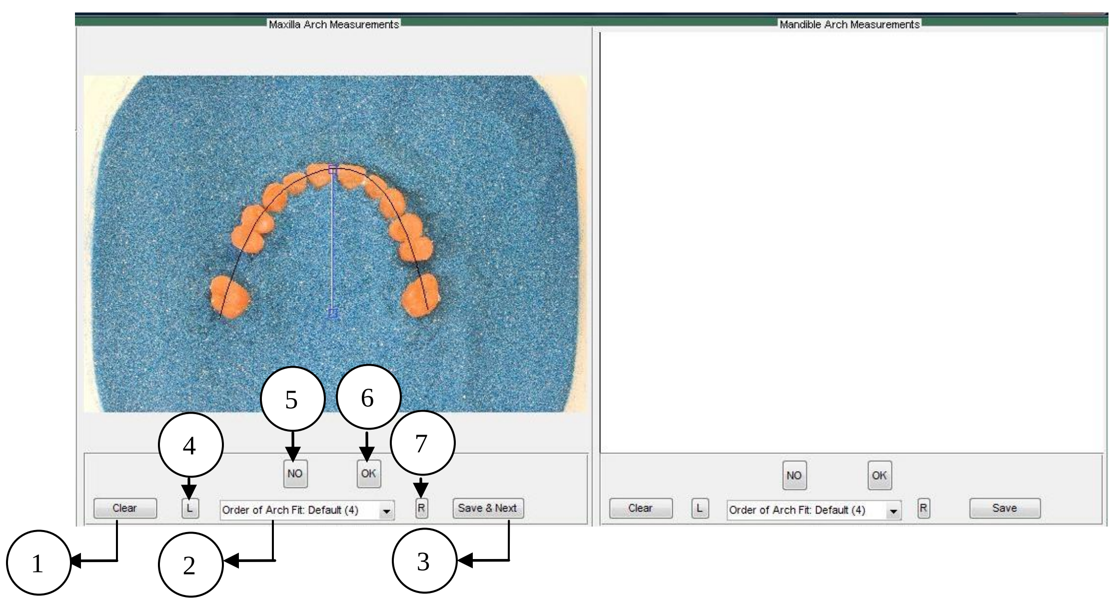

Figure 4.25. Default arch fit and initial midline for the maxillary arch. The analyst can change the order of arch fit by pressing (2) and selecting from the available curve order options. If the user is satisfied with the result, he presses (5); otherwise selecting (6) rejects the fit. Buttons (4) and (7) connect the first and last points of the arch fit to the distal point of the required tooth if the user feels the arch fit is under-estimated. (1) is used to clear the values of (4) and (7). Once the user has selected the proper midline, pressing (3) initiates and displays arch width calculations, saves the results, and initiates mandibular arch measurements.

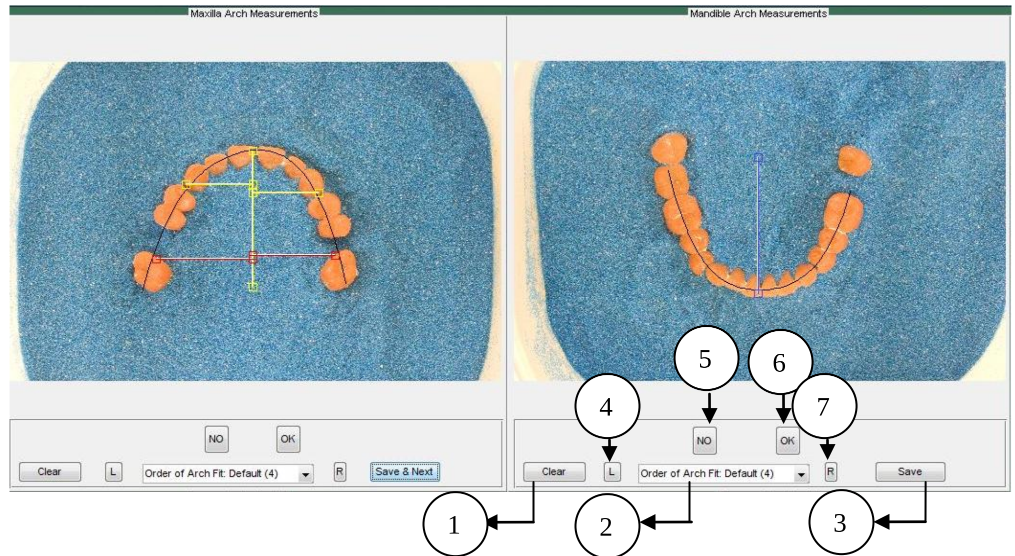

Figure 4.26. Mandibular arch measurement follows maxillary arch measurement using analogous buttons (described in Figure 4.25). Here, the final option is to (3) ‘Save’ the measurements to the Excel output file.

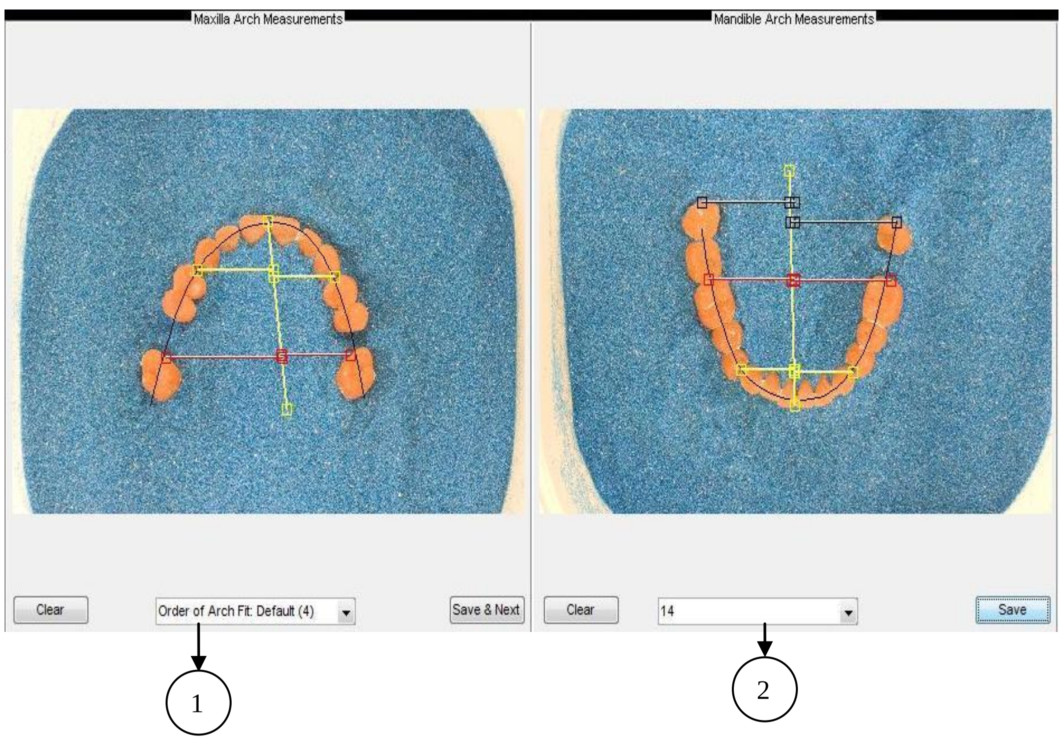

Figure 4.27. Arch fit and widths for the maxilla and mandible. Using drop-down boxes for (1) the maxilla and (2) the mandible, the user can see the results of selecting a different curve order for the arch fit (default is fourth order).

4.2.11 Visual Aids for the User

The user has the option to visualize the measurement results, which is useful for quickly identifying possible errors (Figure 4.28).

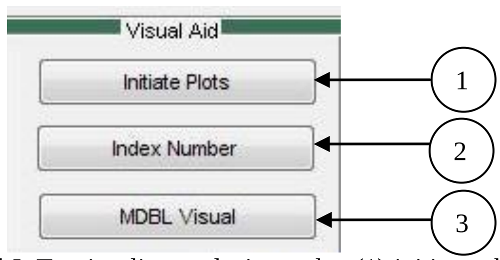

Figure 4.28. Layout of Panel I. To visualize analysis results, (1) initiates the bar plots of mesio-distal distance, bucco-lingual distance and area for each tooth. Pressing (2) shows the order in which the boundary is detected by showing a number on each tooth. Pressing (3) shows the mesio-distal and bucco-lingual distances for each tooth on the cast image (MDBL Visual here refers to Mesio-distal-bucco-lingual Visual).

4.2.11.1 Initiate Plots

Pressing the ‘Initiate Plots’ button (Figure 4.28, Item 1) replaces Panel F in Figure 4.1 with bar graphs showing the area, mesio-distal distance and bucco-lingual distance for each tooth (Figure 4.29). These plots of measurement value, in units of mm for mesio-distal lengths and bucco-lingual widths and mm^2 for area, versus tooth number helps the analyst identify outliers in the measurement set that might require further review. Blank spaces represent one or more missing teeth.

4.2.11.2 MSBL Visual Aid

Pressing the ‘MDBL Visual’ button (Figure 4.28, Item 3) replaces Panel F in Figure 4.1 with images showing the mesio-distal and bucco-lingual measurements for each maxillary and mandibular tooth (Figure 4.30). Looking at these displays, the analyst can determine if any coordinate points have been clicked in the wrong order or at the wrong position.

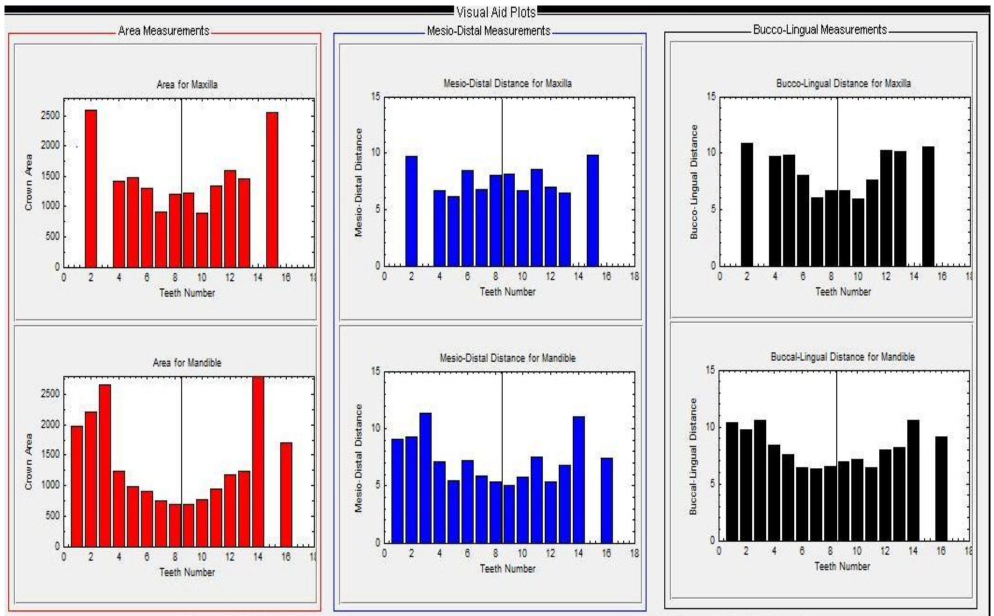

Figure 4.29. Panel I provides plots to visually aid the user in outlier detection and data review. The thin vertical black line in each graph delineates the left and right halves of the maxilla and mandible. Each ‘blank’ bar space represents a missing tooth. The top three panels are maxillary teeth measurements and the bottom three panels depict mandibular teeth measurements. a) Red panels provide tooth area, b) blue panels display mesio-distal distances, and c) black panels show bucco-lingual distances.

Figure 4.30. MSBL Visual Plot. Blue lines represent bucco-lingual distances and black lines represent mesio-distal distances for each maxillary (left) and mandibular (right) tooth.

4.2.11 Review GUI

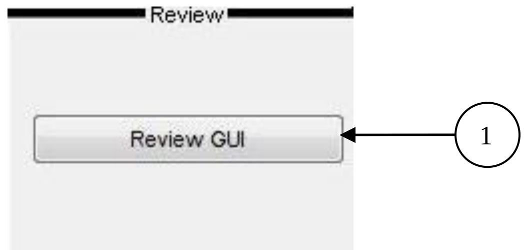

Figure 4.31. Layout of Panel J. This panel is used to review previously analyzed cast images. (1) opens the Review GUI, which enables results to be visualized and changes to be made to previous analyses.

The ‘Review GUI’ button (Figure 4.31, Item 1) allows the user to display and review the results of previously-analyzed cast images. Initiating this step yields six images (top three for maxilla and bottom three for mandible): 1) images showing the arch fit with the user-accepted midline and fit order along with arch width; 2) images displaying the mesio-distal and bucco-lingual distances; and 3) images indicating the final teeth boundaries (Figure 4.32). To initate review, the user simply browses for the individual’s folder and presses the ‘Review GUI’ button.

The images showing the arch measurements, bucco-lingual and mesio-distal widths and boundaries for the maxilla (above) and mandible (below) are presented as soon as the ‘Review GUI’ button in Panel J (Figure 4.7) is pressed; there is no need to press the individual buttons for ‘Arch Measurements’ (Figure 4.32, Item 1), ‘MSBL Visual’ (Figure 4.32, Item 2) and ‘Boundary Detection Visual’ (Figure 4.32, Item 3). Pressing ‘Open Saved Points’ (Figure 4.32, Item 4) opens up a new window with the saved coordinate points marked on the image (Figure 4.33). Within the Review GUI, the user can modify coordinate points (move or delete points), save the updated point locations, and return to the main GUI to compute new values. Pressing the ‘Done’ (Figure 4.32, Item 5) button will close the Review GUI and return the user to the main GUI.

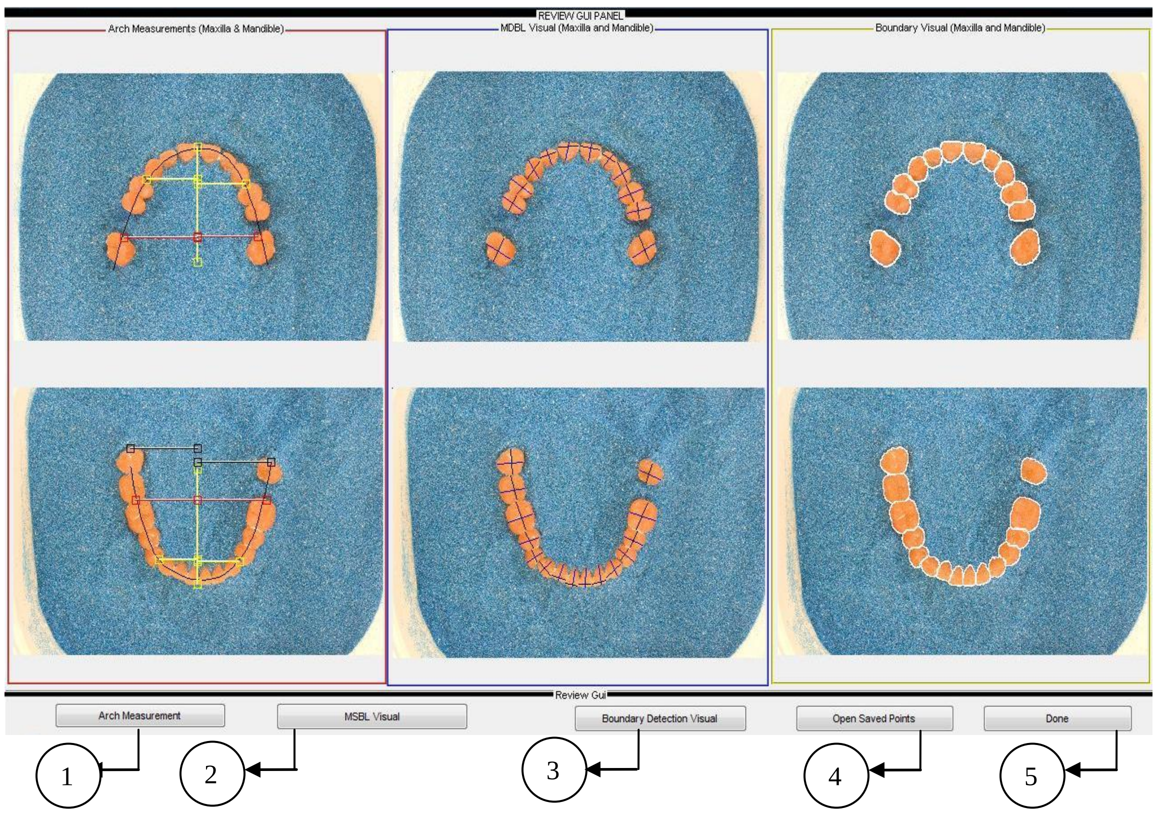

Figure 4.32. The Review GUI Panel. (1) shows all the arch measurements with the user selected midline, (2) shows the mesio-distal and bucco-lingual distances for each tooth on the cast image, (3) shows the boundaries for the maxillary and the mandibular teeth, (4) opens a new window showing the saved coordinate points, and (5) closes the Review GUI and returns the user to the main GUI.

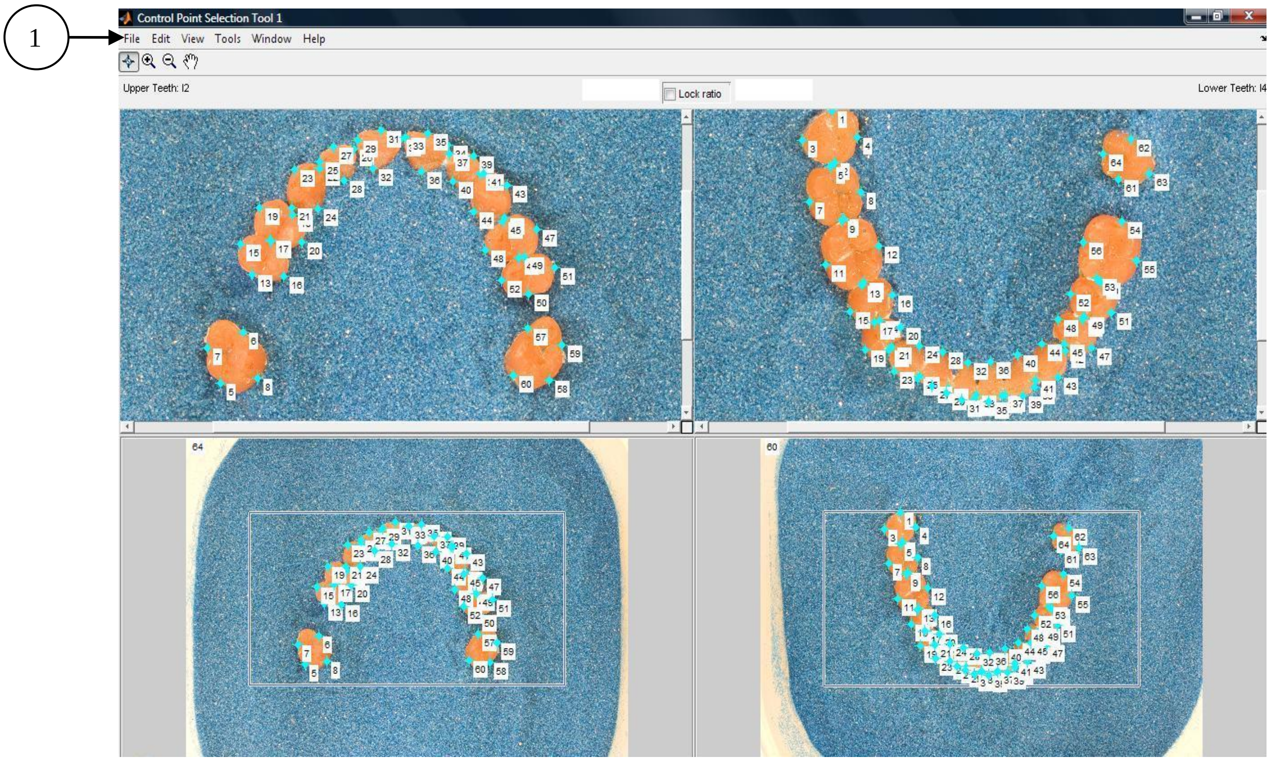

Figure 4.33. The saved coordinate points are marked on the image. The user can either close this window when done or select 'Close Coordinate Selection Tool' from (1).

5. RESULTS

Reproducibility can be defined as the closeness of successive measurements of the same object.[50] Reliability is often used as a synonym for reproducibility. The reproducibility and success rate of quantitative image analysis varies according to the quality of the images, the conditions under which they are measured and the care and skill of the examiner.[50]

Different possibilities may influence the reliability and accuracy of measurements of the individual teeth in the dental arch, including dental spacing condition, the tilting of the teeth, angle of rotations, and interproximal contacts.[1] Replicability of the dental measures is dependent upon the type of measurement (e.g., tooth rotation, tooth width, etc.) and operator training; measurement error can be minimized by careful measurement techniques performed by highly trained analysts.

The possible errors that were considered in this experiment include the slight height variations between the camera and each tooth, the intraoperator and the interoperator errors. Assessment of interoperator error was limited to a few individuals because there is no gold standard for determining the mesial, distal, buccal and lingual points for different shaped teeth. Attempts are being made to resolve this issue because the lack of clear guidelines also affects intraoperator reliability errors.

5.1 Determining the error due to tooth height uncertainty

A source of minor error is the uncertainty in height between the base of the dental cast and the camera. This error arises from 1) variations in the amount of sand into which the cast is placed; and 2) variations in tooth height. To quantify this error, a checkerboard test pattern (square size = 13 mm) (Figure 5.1) was placed at differing heights from the camera (to about 23 mm from the standard position, see Table 5.1) and the number of pixels corresponding to a square side was determined for squares at the image center and sides. There was no difference between the square side length at the center and sides of the image for a particular height, indicating negligible lens distortion errors (e.g., barrel or pincushion effect). The error caused by realistic changes (between 2 and 3 mm) in height was found to be less than 0.2 %, which is considered negligible (Table 5.1).

The maximum absolute error possible due to height issues is for the arch length, since it is the largest value measured. The maximum height from the camera marker to the base of the table is around 470 mm and the Table 5.1 shows the error incorporated into the readings when this height is reduced. The maximum expected height deviation is approximately two mm, and the data confirm that the error associated with this variation will be minimal (0.21 mm for an arch length measurement {less than 0.2%}, for example).

5.2 Example Measurement Set

As an example, one participant's measurements, obtained from his cast images (Figure 5.2), are shown in Tables 5.2, 5.3 and 5.4.

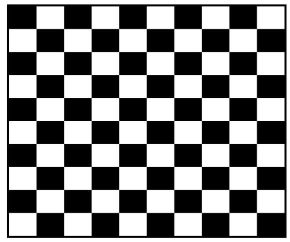

Figure 5.1. The checkerboard test pattern image that was used to determine height-related measurement errors.

Table 5.1. The effect of uncertainty in object-to-camera distance on the dental cast measurements. A checkerboard test pattern was used to assess possible lens distortion errors and to calibrate the measurements (pixel-to-mm conversion). This result allowed assessment of absolute measurement error.

Camera-to-object distance (mm)	***Height Difference from Base Position (mm)***	***Measurement Conversion one pixel equivalent***	***% Increase in Number of Pixels of a Square Side***	***Representative Measurement Differences (Arch Length = 2,500 pixels at Base Level = 116.07 mm)***
470.0 (base height)	0.0	0.0464 mm	0.000	0
467.30	2.7	0.0463 mm	0.178	116.28
462.54	7.46	0.0456 mm	1.785	118.14
459.30	10.7	0.0452 mm	2.500	118.97
446.80	23.2	0.0432 mm	7.321	124.57

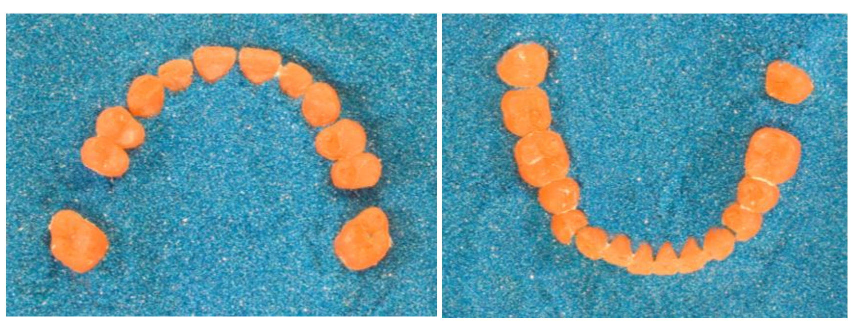

(a) (b)

Figure 5.2. The (a) maxilla and (b) mandible (b) images for the example participant.

Table 5.2. The maxillary parameters of interest (angle of rotation, mesio-distal and bucco-lingual distances and crown area) for the participant whose cast image is shown Figure 5.3a. N/A = not applicable, -9 denotes missing tooth.

Dental Acronym	***Tooth***	***Angle of Rotation [degrees]***	***Mesio-distal Distance [mm]***	***Bucco-lingual Distance [mm]***	***Crown Area [mm^2]***
RUM3	1-Molar	-9	-9	-9	-9
RUM2	2-Molar	33.11	9.27	11.47	105.14
RUM1	3-Molar	-9	-9	-9	-9
RUP4	4-Premolar	36.86	5.06	10.26	57.23
RUP3	5-Premolar	38.65	5.40	8.15	60.62
RUC	6-Canine	43.26	7.88	8.11	N/A
RUI2	7-Incisor	73.85	6.68	5.81	N/A
RUI1	8-Incisor	89.49	7.77	5.66	N/A
LUI1	9-Incisor	68.87	7.96	6.05	N/A
LUI2	10-Incisor	48.81	5.38	5.44	N/A
LUC	11-Canine	50.66	7.86	7.74	N/A
LUP3	12-Premolar	20.73	6.68	8.73	63.63
LUP4	13-Premolar	33.23	5.85	9.63	60.07
LUM1	14-Molar	-9	-9	-9	-9
LUM2	15-Molar	24.78	9.66	11.04	103.58
LUM3	16-Molar	-9	-9	-9	-9

Table 5.3. The mandibular parameters of interest (angle of rotation, mesio-distal and bucco-lingual distances and crown area) for the participant whose cast image is shown Figure 5.3b. N/A = not applicable, -9 denotes missing tooth.

Dental Acronym	***Tooth***	***Angle of Rotation [degrees]***	***Mesio-distal Distance [mm]***	***Buccal-lingual Distance [mm]***	***Crown Area [mm^2]***
RLM3	17-Molar	1.43	6.75	8.61	82.97
RLM2	18-Molar	14.68	7.33	7.12	93.15
RLM1	19-Molar	24.18	9.07	6.57	111.96
RLP4	20-Premolar	38.05	4.93	7.52	52.80
RLP3	21-Premolar	26.05	4.23	6.23	41.31
RLC	22-Canine	34.99	7.21	6.34	N/A
RLI2	23-Incisor	74.29	5.61	5.81	N/A
RLI1	24-Incisor	82.28	5.03	6.28	N/A
LLI1	25-Incisor	88.96	4.64	6.58	N/A
LLI2	26-Incisor	71.26	4.99	6.51	N/A
LLC	27-Canine	55.56	7.16	6.09	N/A
LLP3	28-Premolar	45	3.82	6.63	49.82
LLP4	29-Premolar	26.93	5.96	7.59	52.64
LLM1	30-Molar	22.14	10.75	10.30	117.92
LLM2	31-Molar	-9	-9	-9	-9
LLM3	32-Molar	20.73	6.68	9.29	71.63

Table 5.4. The maxillary and mandibular parameters of interest corresponding to the participant whose images are shown in Figure 5.2. '-9' = missing data.

Description of arch measurement	***Mandible [mm]***	***Maxilla [mm]***
Length of full arch	92.93	127.85
Length of the left half arch	49.45	58.82
Length of the right half arch	42.28	53.86
Distance for canine midline left side	14.94	20.43
Distance for canine midline right side	16.63	20.55
Total canine arch width	31.57	40.98
Total canine arch length	38.42	53.35
Distance for top of midline to left canine side	9.12	11.48
Distance for top of midline to right canine side	7.85	11.86
Distance for molar midline left side	24.44	29.20
Distance for molar midline right side	27.18	24.44
Length of the molar arch	85.98	96.28
Total molar arch width	51.61	53.64
Distance for top of midline to left molar side	29.08	33.60
Distance for top of midline to right molar side	30.30	32.45
Distance for lingual to lingual point for 3rd molar	46.06	-9
Distance for lingual to lingual point for 2nd molar	-9	48.67
Distance for lingual to lingual point for 1st molar	40.30	-9
Distance for lingual to lingual point for 2nd premolar	35.49	41.71
Distance for lingual to lingual point for 1st premolar	31.75	35.77
Distance for lingual to lingual point for canine	23.47	29.80

5.3 Intraoperator Reliability

Intraoperator reliability shows the stability of responses obtained from one operator at separate times.[13] However, the anatomical variations of the teeth make it difficult to test for reliability without first setting specific guidelines on how to identify the mesial, distal, buccal and lingual points for each tooth. A new guideline has been developed, but is yet to be evaluated for accuracy. To examine intraoperator reliability, a test set of maxilla and mandible images from 50 individuals (97 images) were analyzed twice by a trained analyst. The entire set was completed once before repeating the analysis the second time, approximately one month later. Tables 5.5 and 5.6 show the mean, standard deviations, and percentage error for all measurements taken for the maxilla and the mandible. The idea here was to obtain the percentage error for the mean difference of the two trials for each measurement relative to the mean measurement value. Historically, dental cast measurement errors have been shown to be a bit high, especially those associated with tooth rotation. For the percentage error, the average rotation value is not representative of the data because the angles are varied and, hence, there is not a good denominator to normalize to. Within the test set of 50 participants (97 images, approximately 1500 teeth analyzed), only five teeth required manual boundary correction. A fourth-order arch fit (the default setting for both the maxilla and mandible) was successful in 87 images out of the 97 available images.

As expected, the degree of tooth rotation was highly variable, particularly for the molars and premolars. Tooth rotation variability was much lower for the incisors, since the mesial and distal points are easier to identify on these teeth. The percentage error for mesio-distal and bucco-lingual widths, area and arch measurements was under 5% for all subjects, which is considered small. The mean percentage errors for the mesio-distal distances were 3.46% for the maxilla and 3.48% for the mandible and those for the bucco-lingual distances were 3.29% for the maxilla and 2.97% for the mandible.

Table 5.5. Intraoperator differences for cast analysis arch measurements for a set of 50 participants. Measurements were made twice by a trained analyst about one month apart. Reported here are the absolute intraoperator differences (mean, standard deviation (s.d.) and % error

		Absolute Intraoperator Differences			
Arch Measurement Acronyms	***Unit***	***N***	***Mean***	***s.d***	***% Error***
LLFA	mm	47	1.60	2.30	1.62
LLLHA	mm	47	1.18	2.11	2.41
LLRHA	mm	47	0.79	1.08	1.60
LLCW	mm	47	0.32	0.28	2.13
LRCW	mm	47	0.33	0.39	2.18
LTCW	mm	47	0.41	0.40	1.37
LTCAL	mm	47	1.04	1.95	2.78
LLCH	mm	47	0.38	0.37	4.72
LRCH	mm	47	0.42	0.51	5.30
LLMW	mm	45	0.45	0.53	1.91
LRMW	mm	45	0.36	0.52	1.55
LTMAL	mm	47	2.11	2.29	2.46
LTMW	mm	46	0.42	0.38	0.91
LLMH	mm	45	0.31	0.28	1.01
LRMH	mm	45	0.32	0.32	1.04
LRLM3W	mm	15	0.24	0.20	0.52
LRLM2W	mm	37	0.19	0.19	0.47
LRLM1W	mm	41	0.26	0.28	0.75
LRLP4W	mm	46	0.23	0.21	0.73
LRLP3W	mm	47	0.31	0.30	1.14
LRLCW	mm	47	0.29	0.30	1.37
ULFA	mm	47	4.36	15.99	3.97
ULLHA	mm	47	2.76	8.31	5.09
ULRHA	mm	47	1.17	1.60	2.07
ULCW	mm	47	0.26	0.25	1.39
URCW	mm	47	0.34	0.27	1.80
UTCW	mm	47	0.35	0.39	0.95

UTCAL	mm	47	0.82	1.06	1.65
ULCH	mm	46	0.40	0.38	3.37
URCH	mm	46	0.40	0.44	3.17
ULMW	mm	46	0.36	0.40	1.37
URMW	mm	47	0.23	0.21	0.88
UTMAL	mm	46	2.86	4.91	3.10
UTMW	mm	47	0.37	0.36	0.71
ULMH	mm	46	0.33	0.34	0.97
URMH	mm	47	0.26	0.27	0.75
LRUM3W	mm	19	0.39	0.49	0.88
LRUM2W	mm	47	0.27	0.39	0.63
LRUM1W	mm	43	0.49	1.50	1.24
LRUP4W	mm	46	0.26	0.32	0.73
LRUP3W	mm	48	0.41	1.09	1.34
LRUCW	mm	50	0.32	0.38	1.25

Table 5.6. Intraoperator differences for cast analysis measurements for a set of 50 participants. Measurements were made twice by a trained analyst about one month apart. Reported here are the absolute intraoperator differences (mean, standard deviation (s.d.) and % error.

Maxilla		***Absolute Intraoperator Differences***				***Mandible***		***Absolute Intraoperator Differences***			
Tooth measurement acronym	***Unit***	***N***	***Mean***	***s.d.***	***% Error***	***Tooth measurement acronym***	***Unit***	***N***	***Mean***	***s.d***	***% Error***
RUM2RO	degrees	44	2.77	2.81	N/A	RLM2RO	degrees	42	2.57	2.82	N/A
RUM1RO	degrees	44	2.14	2.25	N/A	RLM1RO	degrees	42	2.92	2.68	N/A
RUP4RO	degrees	44	2.70	2.97	N/A	RLP4RO	degrees	47	5.59	6.23	N/A
RUP3RO	degrees	46	3.93	3.62	N/A	RLP3RO	degrees	47	4.83	4.53	N/A
RUCRO	degrees	47	3.44	3.41	N/A	RLCRO	degrees	47	3.84	3.77	N/A
RUI2RO	degrees	46	3.21	2.79	N/A	RLI2RO	degrees	47	3.02	3.12	N/A
RUI1RO	degrees	47	2.11	2.89	N/A	RLI1RO	degrees	47	3.54	5.03	N/A
LUI1RO	degrees	46	3.03	2.97	N/A	LLI1RO	degrees	47	3.70	3.43	N/A
LUI2RO	degrees	46	3.69	3.67	N/A	LLI2RO	degrees	47	3.48	3.76	N/A
LUCRO	degrees	47	3.52	3.74	N/A	LLCRO	degrees	47	4.17	4.88	N/A
LUP3RO	degrees	47	4.00	4.15	N/A	LLP3RO	degrees	47	3.97	3.93	N/A
LUP4RO	degrees	46	4.60	4.83	N/A	LLP4RO	degrees	46	3.07	3.23	N/A
LUM1RO	degrees	42	3.14	3.72	N/A	LLM1RO	degrees	41	2.64	3.93	N/A
LUM2RO	degrees	45	3.14	3.01	N/A	LLM2RO	degrees	40	2.36	2.21	N/A
RUM3MD	mm	21	0.25	0.21	3.22	RLM3MD	mm	17	0.21	0.15	2.38
RUM2MD	mm	44	0.23	0.27	2.78	RLM2MD	mm	42	0.24	0.21	2.53
RUM1MD	mm	44	0.20	0.19	2.09	RLM1MD	mm	43	0.25	0.24	2.37
RUP4MD	mm	44	0.27	0.30	4.41	RLP4MD	mm	47	0.23	0.25	3.53
RUP3MD	mm	46	0.26	0.38	4.10	RLP3MD	mm	47	0.26	0.26	4.09
RUCMD	mm	47	0.25	0.30	3.40	RLCMD	mm	47	0.24	0.21	3.49
RUI2MD	mm	45	0.23	0.20	3.52	RLI2MD	mm	47	0.28	0.32	4.74

RUI1MD	mm	47	0.27	0.31	3.31	RLI1MD	mm	47	0.19	0.18	3.65
LUI1MD	mm	46	0.28	0.31	3.36	LLI1MD	mm	47	0.23	0.20	4.34
LUI2MD	mm	46	0.21	0.21	3.16	LLI2MD	mm	47	0.25	0.23	4.28
LUCMD	mm	47	0.29	0.30	3.81	LLCMD	mm	47	0.27	0.34	4.03
LUP3MD	mm	47	0.33	0.36	5.02	LLP3MD	mm	47	0.30	0.31	4.82
LUP4MD	mm	45	0.24	0.24	3.82	LLP4MD	mm	46	0.24	0.19	3.79
LUM1MD	mm	42	0.21	0.22	2.15	LLM1MD	mm	42	0.25	0.23	2.42
LUM2MD	mm	45	0.28	0.24	3.42	LLM2MD	mm	41	0.27	0.61	2.83
LUM3MD	mm	20	0.29	0.27	3.89	LLM3MD	mm	19	0.21	0.21	2.52
RUM3BL	mm	21	0.36	0.41	3.76	RLM3BL	mm	17	0.28	0.22	3.04
RUM2BL	mm	44	0.37	0.31	3.63	RLM2BL	mm	42	0.23	0.30	2.39
RUM1BL	mm	44	0.31	0.26	2.82	RLM1BL	mm	43	0.21	0.25	2.05
RUP4BL	mm	44	0.28	0.37	3.15	RLP4BL	mm	47	0.17	0.18	2.15
RUP3BL	mm	46	0.25	0.24	2.79	RLP3BL	mm	47	0.21	0.21	2.79
RUCBL	mm	47	0.22	0.27	2.95	RLCBL	mm	47	0.22	0.19	3.24
RUI2BL	mm	46	0.28	0.31	4.55	RLI2BL	mm	47	0.23	0.19	3.62
RUI1BL	mm	47	0.26	0.30	3.68	RLI1BL	mm	46	0.25	0.21	3.81
LUI1BL	mm	46	0.26	0.34	3.64	LLI1BL	mm	47	0.24	0.23	3.67
LUI2BL	mm	46	0.22	0.19	3.66	LLI2BL	mm	47	0.28	0.33	4.56
LUCBL	mm	47	0.28	0.33	3.76	LLCBL	mm	47	0.28	0.33	4.08
LUP3BL	mm	47	0.21	0.19	2.31	LLP3BL	mm	47	0.24	0.27	3.12
LUP4BL	mm	46	0.17	0.16	1.98	LLP4BL	mm	46	0.23	0.27	2.85
LUM1BL	mm	42	0.25	0.23	2.33	LLM1BL	mm	42	0.21	0.23	2.03
LUM2BL	mm	45	0.34	0.37	3.36	LLM2BL	mm	41	0.21	0.21	2.13
LUM3BL	mm	20	0.38	0.29	4.27	LLM3BL	mm	18	0.20	0.17	2.13
RUM3CA	mm^2	21	0.17	0.50	0.12	RLM3CA	mm^2	17	0.00	0.00	0.00
RUM2CA	mm^2	44	0.03	0.16	0.02	RLM2CA	mm^2	42	0.18	1.15	0.13
RUM1CA	mm^2	44	0.00	0.03	0.00	RLM1CA	mm^2	43	0.01	0.07	0.01
RUP4CA	mm^2	44	0.00	0.00	0.00	RLP4CA	mm^2	47	0.08	0.55	0.12

RUP3CA	mm^2	46	0.00	0.00	0.00	RLP3CA	mm^2	47	0.02	0.11	0.03
LUP3CA	mm^2	47	0.00	0.00	0.00	LLP3CA	mm^2	47	0.01	0.07	0.02
LUP4CA	mm^2	46	0.04	0.19	0.05	LLP4CA	mm^2	46	0.18	1.25	0.27
LUM1CA	mm^2	42	0.54	2.96	0.36	LLM1CA	mm^2	42	0.08	0.35	0.05
LUM2CA	mm^2	45	0.41	1.85	0.36	LLM2CA	mm^2	41	0.18	1.12	0.13
LUM3CA	mm^2	20	0.00	0.00	0.00	LLM3CA	mm^2	19	0.13	0.56	0.18

Some example plots are shown below to demonstrate the intraoperator agreement. Figures 5.3, 5.4 and 5.5 show the agreement between Trial One and Trial Two for three measurements. The perfect outcome would a linear line with a slope of one. Figure 5.3 shows that the values obtained for canine rotation were varying non-uniformly, whereas Figures 5.4 and 5.5 show that the tooth width measurements are highly reproducible.

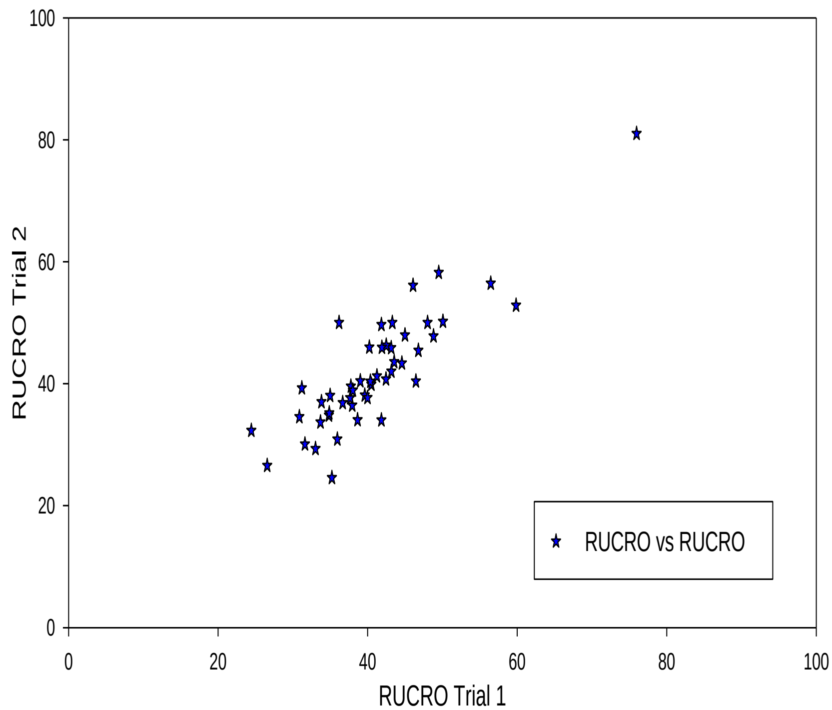

Figure 5.3. Intraoperator error in the measurement of right upper canine (RUCRO) rotation. The plot confirms that the rotation measurements are somewhat variable.

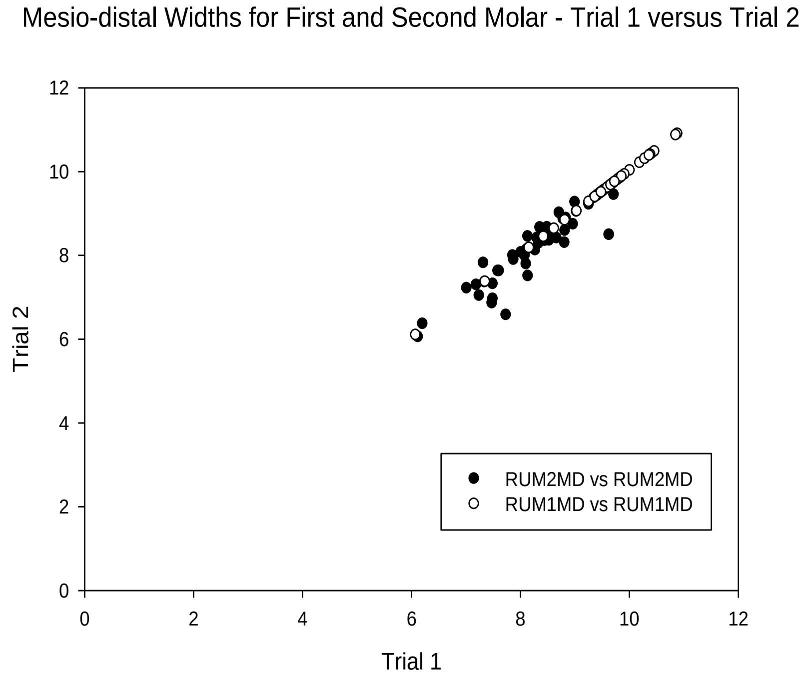

Figure 5.4. Intraoperator error in the measurement of right upper molars (RUM1MD and RUM2MD) mesio-distal widths. The plot confirms that the mesio-distal measurements are reasonably reproducible.

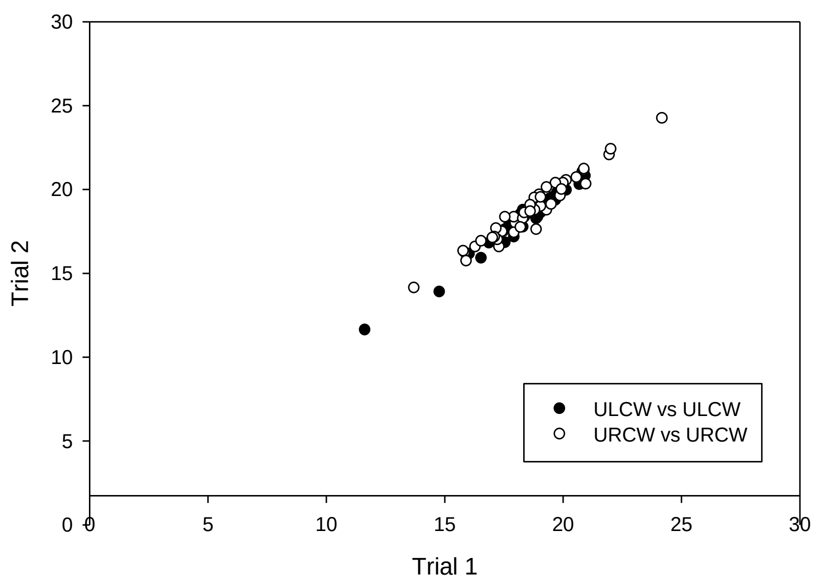

Figure 5.5. Intraoperator error in the measurement of upper canine widths (ULCW and URCW). The plot confirms that the canine width measurements are highly reproducible.

Figure 5.6 compares the molar and canine arch lengths for the maxilla and mandible. The maxillary arch lengths were greater than the mandible arch lengths for the majority of the measured casts, which is consistent with observations in other studies.

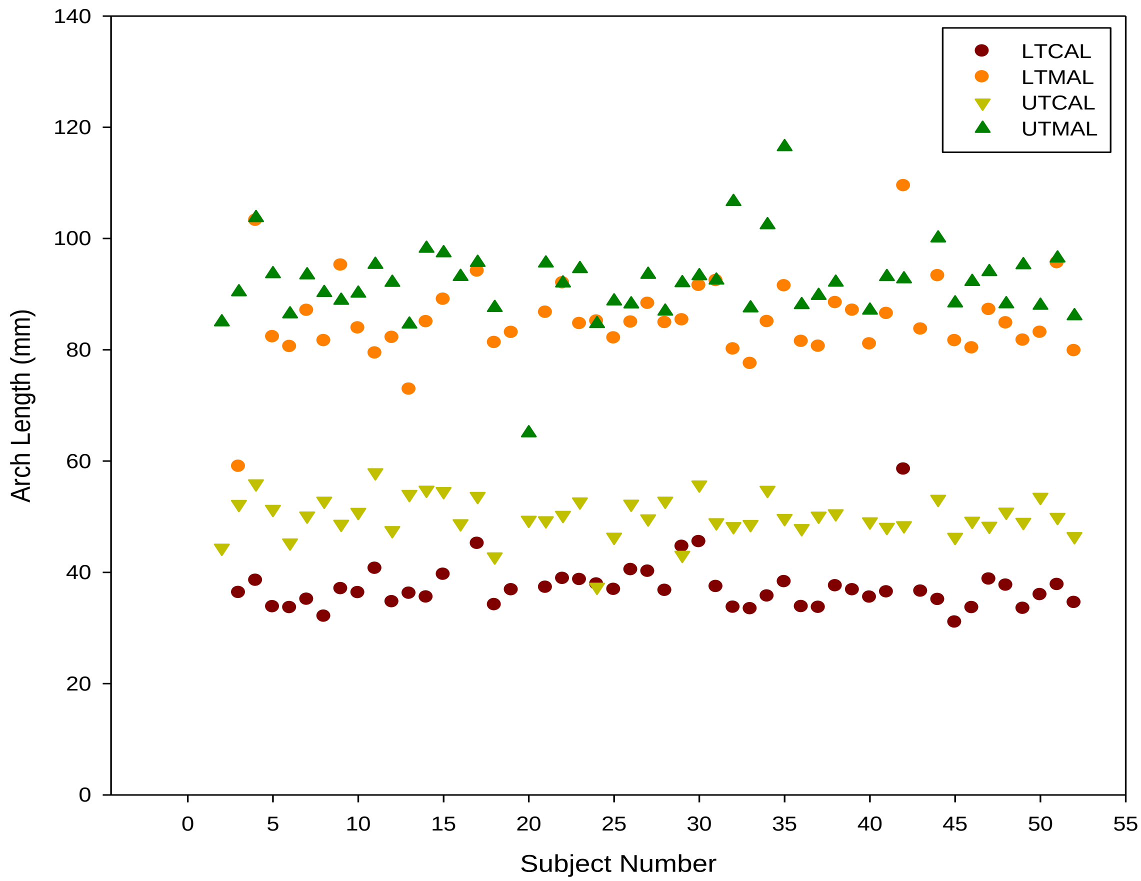

Figure 5.6. Comparison of the molar and canine arch length for the maxilla and mandible for 50 subjects. Here, LTCAL stands for Lower Total Canine Arch Length, LTMAL stands for Lower Total Molar Arch Length, UTCAL stands for Upper Total Canine Arch Length, and UTMAL stands for Upper Total Molar Arch Length.

Figure 5.7 shows the percent error for each measurement; maxillary and mandibular values are arranged next to one another for easy comparison. The percent error is the mean of the absolute differences in the two measurements divided by the average measurement for that variable. The color legend and the x-axis label indicate the values that were measured. Working left to right, the bars showing mesio-distal widths and bucco-lingual widths from the third molars on the right side to the third molars on the left side (for both the maxilla and the mandible). Crown area measurements are obtained for the molars and premolars from right to left (for both the maxilla and the mandible).

Figure 5.8 shows the average differences between the intraoperator measurements for tooth rotation. As expected, there was more variation in the rotational measures, but the intraoberver error (generally less than four degrees and most often less than three degrees) is acceptable because of the possible variations in teeth shape and size and the difficulty in accurately estimating the coordinate points.

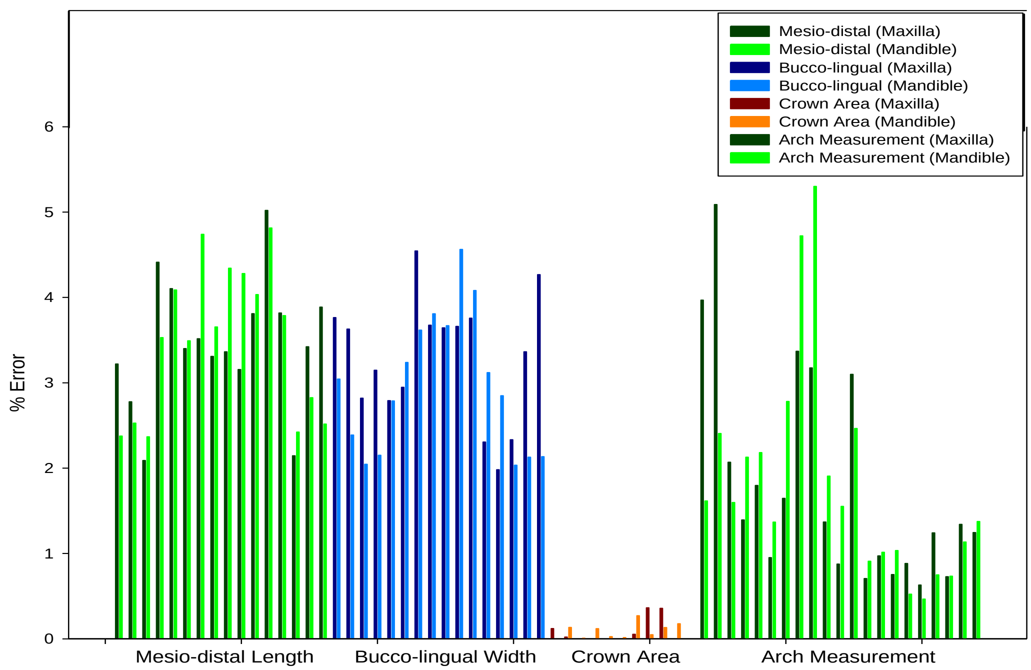

Figure 5.7. The percent error for each measurement with the maxillary and mandibular values adjacent for each measurement.

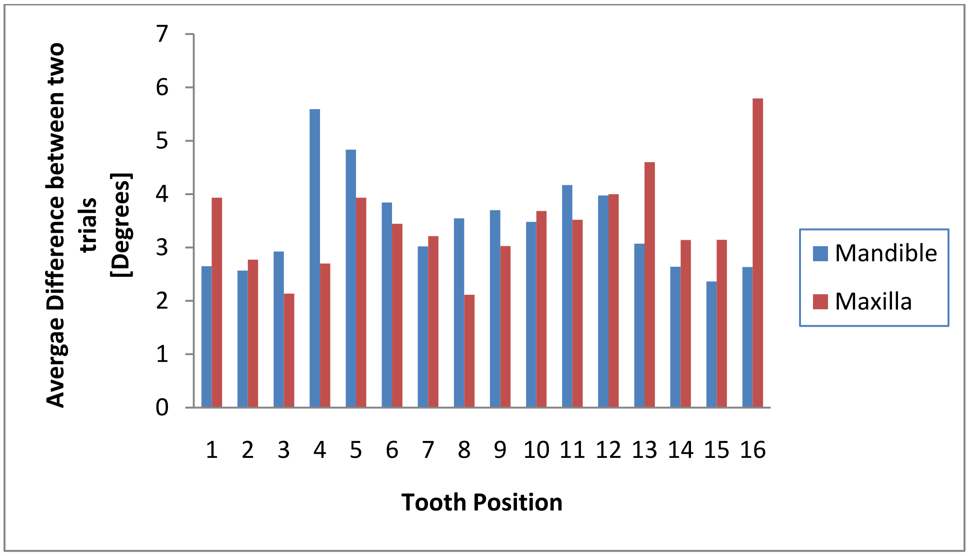

Figure 5.8. The average of the differences of rotation angle measurements in two trials to assess intraoperator error. The tooth numbering here is from the right third molar (Tooth 1) to the left third molar (Tooth 16)

5.4 Interoperator Reliability

Interoperator reliability shows the accuracy of given responses obtained from two different respondents.[13] To assess interoperator reliability, data from eight subjects (a total of 16 images) were analyzed twice by two different trained analysts. Tables 5.7 and 5.8 show the mean, standard deviation, and percent error for all measurements. Again, the idea here was to obtain the percent error for the absolute difference of the two trials for each measurement relative to the average value of that measurement.

As with the intraoperator reliability study, the largest variability was in tooth rotation assessment; the average difference was 4.5 degrees. Mesio-distal and bucco-lingual distance data were more consistent between the two analysts. The mean percentage errors for mesio-distal distances were 5.82% for the maxilla and 4.46% for the mandible, and those for the bucco-lingual distances were 3.32% for the maxilla and 3.81% for the mandible. As expected, the difference between the intraoperator and interoperator error was higher for mesio-distal length measurements by 2.36% for maxilla and 0.98% for mandible because of the variations on teeth shape. The difference between the intraoperator and interoperator error for bucco-lingual measurements were less in comparison with the mesio-distal lengths by 0.03% for maxilla and 0.84% for the mandible.

Table 5.7. Interoperator differences for cast analysis measurements for a set of eight participants. Measurements were made twice by two trained analysts. Reported here are the absolute interoperator differences (mean, standard deviation (s.d.) and % error)

Maxilla		***Absolute Interoperator Differences***				***Mandible***		***Absolute Interoperator Differences***			
Tooth measurement acronym	***Unit***	***N***	***Mean***	***s.d.***	***% Error***	***Tooth measurement acronym***	***Unit***	***N***	***Mean***	***s.d***	***% Error***
RUM2RO	degrees	7	9.30	8.45	N/A	RLM2RO	degrees	6	1.65	1.36	N/A
RUM1RO	degrees	8	4.39	4.37	N/A	RLM1RO	degrees	6	1.44	1.24	N/A
RUP4RO	degrees	7	3.35	4.56	N/A	RLP4RO	degrees	7	5.36	6.09	N/A
RUP3RO	degrees	8	6.28	7.74	N/A	RLP3RO	degrees	7	4.07	5.03	N/A
RUCRO	degrees	8	2.45	1.75	N/A	RLCRO	degrees	7	5.66	5.50	N/A
RUI2RO	degrees	8	3.00	2.23	N/A	RLI2RO	degrees	7	5.00	3.66	N/A
RUI1RO	degrees	8	2.42	2.61	N/A	RLI1RO	degrees	7	6.57	4.10	N/A
LUI1RO	degrees	8	4.33	3.73	N/A	LLI1RO	degrees	7	3.38	4.05	N/A
LUI2RO	degrees	8	5.35	5.19	N/A	LLI2RO	degrees	7	7.88	7.40	N/A
LUCRO	degrees	8	3.62	3.00	N/A	LLCRO	degrees	7	4.41	4.41	N/A
LUP3RO	degrees	8	6.03	6.98	N/A	LLP3RO	degrees	7	5.34	4.25	N/A
LUP4RO	degrees	8	2.63	4.13	N/A	LLP4RO	degrees	7	4.85	3.85	N/A
LUM1RO	degrees	8	5.00	4.55	N/A	LLM1RO	degrees	6	1.94	2.73	N/A
LUM2RO	degrees	7	4.07	4.45	N/A	LLM2RO	degrees	5	6.32	5.23	N/A
RUM3MD	mm	3	0.03	0.05	0.37	RLM3MD	mm	2	0.68	0.27	8.38
RUM2MD	mm	7	0.69	0.41	8.45	RLM2MD	mm	6	0.47	0.27	5.05
RUM1MD	mm	8	0.34	0.31	3.84	RLM1MD	mm	6	0.42	0.23	4.21
RUP4MD	mm	7	0.18	0.17	2.89	RLP4MD	mm	7	0.30	0.23	4.70
RUP3MD	mm	8	0.25	0.30	3.85	RLP3MD	mm	7	0.33	0.36	4.98
RUCMD	mm	8	0.31	0.42	4.49	RLCMD	mm	7	0.35	0.37	5.42
RUI2MD	mm	8	0.33	0.35	5.14	RLI2MD	mm	7	0.21	0.18	3.75
RUI1MD	mm	8	0.29	0.32	3.49	RLI1MD	mm	7	0.34	0.28	6.56
LUI1MD	mm	8	0.38	0.33	4.59	LLI1MD	mm	7	0.24	0.23	4.76
LUI2MD	mm	8	0.36	0.35	5.38	LLI2MD	mm	7	0.30	0.16	5.41
LUCMD	mm	8	0.33	0.32	4.46	LLCMD	mm	7	0.31	0.24	4.89

LUP3MD	mm	8	0.47	0.45	7.26	LLP3MD	mm	7	0.62	0.46	9.86
LUP4MD	mm	8	0.29	0.23	4.70	LLP4MD	mm	7	0.53	0.44	8.40
LUM1MD	mm	8	0.38	0.33	3.94	LLM1MD	mm	6	0.33	0.31	3.29
LUM2MD	mm	7	0.32	0.25	3.83	LLM2MD	mm	5	0.65	0.15	7.54
LUM3MD	mm	3	0.31	0.38	4.74	LLM3MD	mm	2	0.51	0.12	6.04
RUM3BL	mm	3	0.06	0.10	0.62	RLM3BL	mm	2	0.21	0.01	2.16
RUM2BL	mm	7	0.27	0.23	2.68	RLM2BL	mm	6	0.33	0.21	3.43
RUM1BL	mm	8	0.17	0.13	1.60	RLM1BL	mm	6	0.29	0.19	2.96
RUP4BL	mm	7	0.17	0.20	1.92	RLP4BL	mm	7	0.25	0.14	3.23
RUP3BL	mm	8	0.18	0.14	2.07	RLP3BL	mm	7	0.21	0.19	2.80
RUCBL	mm	8	0.32	0.26	4.59	RLCBL	mm	7	0.38	0.34	5.78
RUI2BL	mm	8	0.33	0.40	5.73	RLI2BL	mm	7	0.19	0.17	3.02
RUI1BL	mm	8	0.21	0.21	2.92	RLI1BL	mm	7	0.40	0.28	6.31
LUI1BL	mm	8	0.36	0.34	5.23	LLI1BL	mm	7	0.31	0.36	4.92
LUI2BL	mm	8	0.39	0.39	6.42	LLI2BL	mm	7	0.34	0.29	5.47
LUCBL	mm	8	0.17	0.19	2.30	LLCBL	mm	7	0.24	0.22	3.59
LUP3BL	mm	8	0.25	0.35	2.77	LLP3BL	mm	7	0.18	0.18	2.45
LUP4BL	mm	8	0.15	0.20	1.75	LLP4BL	mm	7	0.22	0.14	2.79
LUM1BL	mm	8	0.33	0.42	3.19	LLM1BL	mm	6	0.31	0.19	3.06
LUM2BL	mm	7	0.59	0.61	5.93	LLM2BL	mm	5	0.71	0.25	7.52
LUM3BL	mm	3	0.31	0.44	3.42	LLM3BL	mm	2	0.15	0.03	1.58
RUM3CA	mm^2	3	0.00	0.00	0.00	RLM3CA	mm^2	2	0.00	0.00	0.00
RUM2CA	mm^2	7	0.00	0.00	0.00	RLM2CA	mm^2	6	0.00	0.00	0.00
RUM1CA	mm^2	8	0.00	0.00	0.00	RLM1CA	mm^2	6	0.00	0.00	0.00
RUP4CA	mm^2	7	0.00	0.00	0.00	RLP4CA	mm^2	7	0.00	0.00	0.00
RUP3CA	mm^2	8	0.00	0.00	0.00	RLP3CA	mm^2	7	0.00	0.00	0.00
LUP3CA	mm^2	8	0.03	0.10	0.06	LLP3CA	mm^2	7	0.00	0.00	0.00
LUP4CA	mm^2	8	1.42	4.01	2.93	LLP4CA	mm^2	7	0.00	0.00	0.00
LUM1CA	mm^2	8	0.03	0.09	0.03	LLM1CA	mm^2	6	0.00	0.00	0.00
LUM2CA	mm^2	7	0.29	0.76	0.37	LLM2CA	mm^2	5	0.00	0.00	0.00
LUM3CA	mm^2	3	0.00	0.00	0.00	LLM3CA	mm^2	2	0.00	0.00	0.00

Table 5.8. Interoperator differences for cast analysis arch measurements for a set of eight participants. Measurements were made twice by two trained analysts. Reported here are the absolute interoperator differences (mean, standard deviation (s.d.) and % error).

		Absolute Intraoperator Differences			
Arch measurement acronyms	***Unit***	***N***	***Mean***	***s.d***	***% Error***
LLFA	mm	7	1.701107	1.772537	1.722702
LLLHA	mm	7	1.367290	1.172081	2.781974
LLRHA	mm	7	1.197184	0.965287	2.421486
LLCW	mm	7	0.335756	0.445678	2.242910
LRCW	mm	7	0.380058	0.483613	2.499946
LTCW	mm	7	0.635505	0.552876	2.106252
LTCAL	mm	7	0.626113	0.633631	1.679031
LLCH	mm	7	0.496553	0.428759	6.233668
LRCH	mm	7	0.536666	0.43781	6.807617
LLMW	mm	6	1.075433	0.806913	4.562456
LRMW	mm	6	0.758182	1.043141	3.230033
LTMAL	mm	7	2.305527	2.277232	2.697558
LTMW	mm	6	0.923852	0.610056	2.007434
LLMH	mm	6	0.533785	0.554334	1.747389
LRMH	mm	6	0.388714	0.303538	1.277589
LRLM3W	mm	2	0.355518	0.017655	0.792942
LRLM2W	mm	5	0.571896	0.568631	1.404604
LRLM1W	mm	6	0.436270	0.39379	1.258471
LRLP4W	mm	7	0.553810	0.308734	1.777294
LRLP3W	mm	7	0.308511	0.224769	1.146368
LRLCW	mm	7	0.333948	0.333554	1.602459
ULFA	mm	8	7.467625	5.162719	6.797711
ULLHA	mm	8	4.717149	7.108327	8.688595
ULRHA	mm	8	3.511526	2.418975	6.232503
ULCW	mm	8	1.432151	2.680832	7.717515
URCW	mm	8	0.260481	0.302464	1.392015
UTCW	mm	8	1.239581	2.698994	3.325982
UTCAL	mm	8	2.581319	2.670678	5.162551
ULCH	mm	8	0.286926	0.238751	2.395972
URCH	mm	8	0.267026	0.229965	2.128637
ULMW	mm	8	0.782844	0.848112	2.980987
URMW	mm	8	0.440242	0.304781	1.685575
UTMAL	mm	8	4.354765	3.764439	4.726230
UTMW	mm	8	0.695019	0.772918	1.341201
ULMH	mm	8	1.369747	3.490768	4.055527

URMH	mm	8	0.353112	0.217114	1.011125
LRUM3W	mm	2	0.013776	0.019482	0.031164
LRUM2W	mm	7	0.471738	0.281201	1.091550
LRUM1W	mm	8	7.339381	15.45428	8.593313
LRUP4W	mm	7	0.439882	0.460870	1.217852
LRUP3W	mm	8	0.510745	0.398171	1.675390
LRUCW	mm	8	0.830134	1.625280	3.187084

Figure 5.9 shows the percentage errors for each measurement; the plots are arranged as for the intraobserver studies. Figure 5.10 shows the average differences between the intraoperator measurements of tooth rotation. As expected, there were more variations (average error is 4.5 degrees) in the interoperator error as a result of the difference in coordinate point selection for all measures, rotation measures being the most affected.

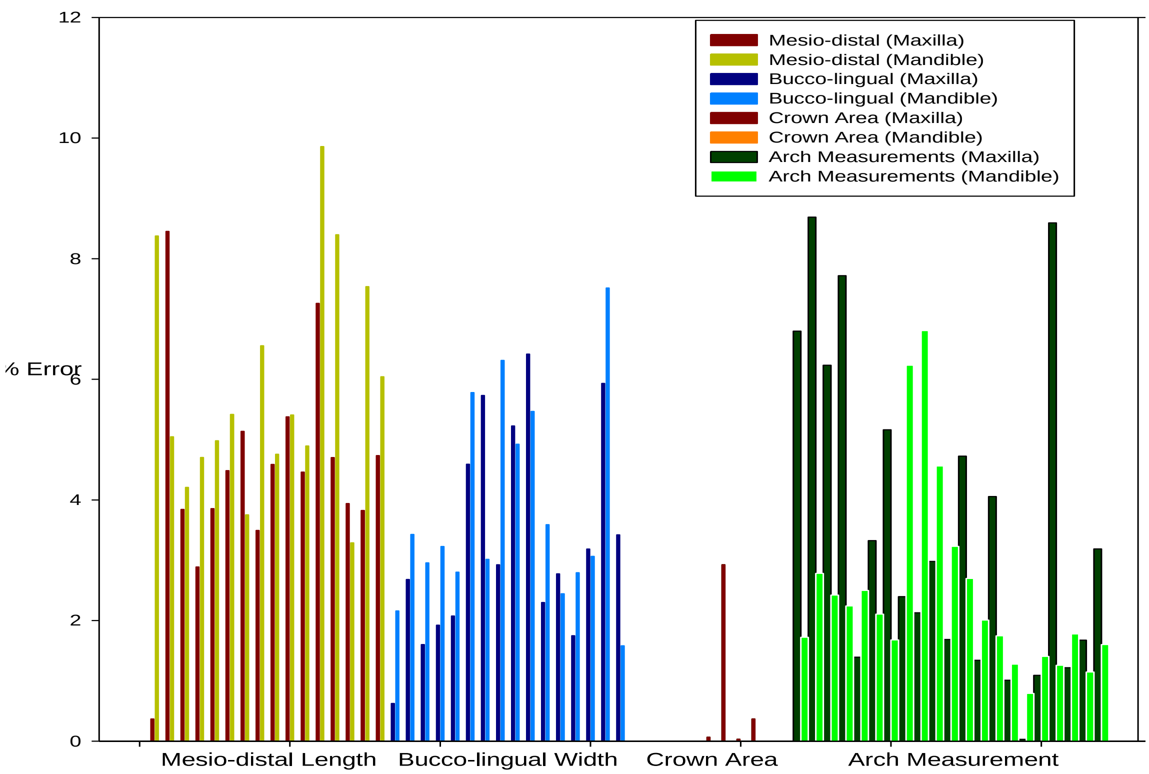

Figure 5.9. The percentage errors for each measurement with the maxillary and mandibular values adjacent for each measurement.

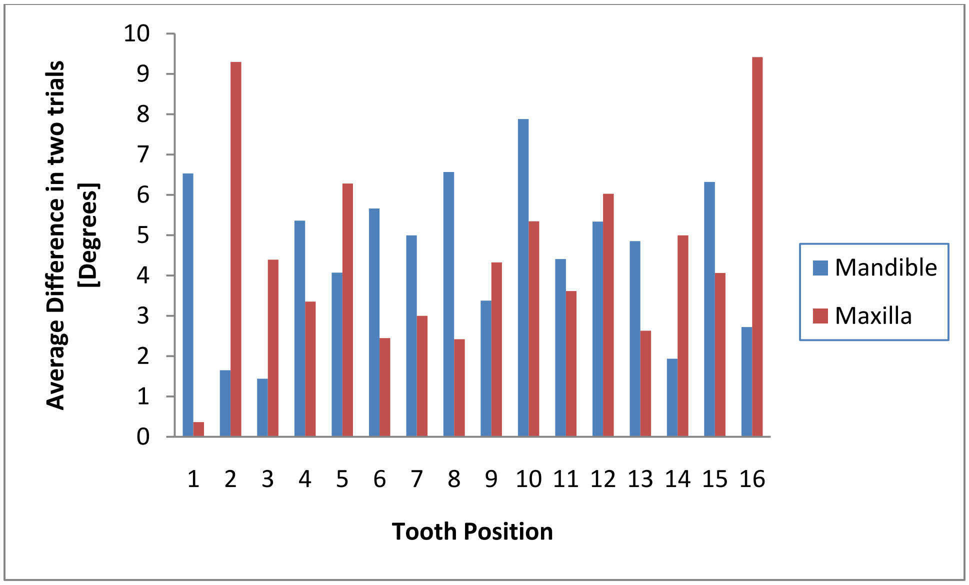

Figure 5.10. The average of the differences of the two trials of tooth rotation measurement to assess interoperator error. The tooth numbering here is from the right third molar (Tooth 1) to the left third molar (Tooth 16).

5.5 Validating Data

The mesio-distal and bucco-lingual widths were compared to readings obtained using a digital caliper for eight sets of maxilla and mandible casts to make sure the results obtained were similar to each other. This was not an accuracy study, but rather a validation of the algorithms' results. The results obtained confirmed the validity of the results obtained using the software for mesio-distal and bucco-lingual widths. The absolute mean difference was 0.24 mm for mesio-distal widths and 0.15 mm for bucco-lingual widths, both giving an error less that 1%.

6. DISCUSSION

We have developed a program for obtaining measurements from dental cast images. We tested the software on a set of 97 images which revealed that the program was successful in analyzing images 100% of the time with no more than very limited manual intervention. The software was suited to the client's requests, incorporating their feedback during the development process. In comparison to commercially developed software, we developed a product that can be changed as needed if new measurement requirements are identified or if changes to the interface layout or results reporting are desired.

Anthropologists are still attempting to clearly define the mesiodistal and buccolingual widths. The varying size and shape of teeth make it difficult to accurately determine the required endpoints. Attempts are also being made to standardize a method to analyze differently-shaped teeth. Once these methods are finalized, properly trained program users should be able to generate highly reproducible results.

When measuring dental casts, as in any investigation, it is obvious that errors and discrepancies will occur.[23] Typically, the more measurements an investigator performs, the more accurately he does so; a training period should be included in any study involving this type of measurement.[23]

Measurement on a two-dimensional representation of a three-dimensional object leads to a number of challenges. For example, crown width and crown area are two variables that become less defined in the two-dimensional space. It is difficult to accurately identify landmarks in tipped and tilted teeth as the image cannot be manipulated or rotated as would be possible with the three-dimensional object.[51] Selecting the maximum mesio-distal crown widths can be difficult and, whereas three-dimensional images can be manipulated to better view landmarks, over-manipulation can occur that leads to subjective errors in identifying points. Accurately determining the mesial and distal points in the 2D image can be limited by the examiner's inability to maneuver the model to reach the most mesial or distal points. Yet another contributing factor to the difference could be the operator's learning curve in order to perform measurements with computer mouse.

With the development of technology, the costs of both taking and storing two-dimensional images have been drastically reduced to an extent that digital imaging is becoming widely used. It has been accepted that there are storage and technical difficulties in using two-dimensional images as an estimate of patients' dentition (which is three-dimensional) and that there are problems with reliability in assessing the images by the examiner.[52] Although measuring two-dimensional images might not be as accurate as measuring three-dimensional casts, experiments have proven that the results are adequate and, considering the cost difference, quite acceptable.[24] The use of three-dimensional digital imaging is starting to replace traditional casts in technologically forward countries. However, the technology is costly and may be prohibitive for several orthodontists. In the present study, none of the required measurements would greatly benefit from a three-dimensional analysis, since they are not dependent on topographic information.

Measuring mesio-distal tooth widths on digital models has been shown to be faster than using digital calipers or other manual methods on a cast, and this was validated in this project. We also found that the same is true for the measurements of rotation, arch length and arch widths. Overall, studies have shown that digital techniques tend to slightly overestimate actual cast measurements.[53] However, since this bias is very small and because a strong correlation exists between the cast measurements and digital measurements, this bias should not restrict clinical use of these techniques.[53] Because of variability in tooth morphology, the magnitude of the measurement error of different teeth varies.

All images of the dental impressions were obtained using the same photographic set up and equipment at one location. All photographs were taken by the same individual and a standardized technique was used to fix the focal lengths, level the camera, and level and position the dental casts. Appropriate lighting was used to decrease the shadowing. Although tooth height varies within and across individuals (between 2 and 4 mm), for the purposes of the dental research being conducted, the impact of these small height differences was shown to have negligible impact on the results.

6.1 Challenges in Automated Image Analysis

Boundary Detection

Although the method and setup for acquiring the dental cast images have been standardized, the quality of the dental casts is highly variable due to the non-ideal conditions under which the impressions were acquired and the process of pouring and subsequently extracting the casts from the molds. This variation in quality, combined with the varying shapes of each tooth, makes tooth boundary detection challenging. Multiple, extraneous marks (surface scratches and indentations) appear all along the edges of the casts, which leads to a number of false edges being detected. Because the cast material is somewhat shiny, light reflections obscure tooth boundaries. Other boundaries are not well delineated on the casts due to smoothing of the edges during the casting process. Also, the fact that a tooth can be rotated, worn (attrition), misplaced etc. makes it impossible to assume that a particular tooth will have any distinctive shape. After trying several methods for boundary detection, watershed segmentation was selected as the best approach. The only drawback of this method is that the contact sides of two teeth do not have a smooth boundary. In this case, watershed segmentation returns not the true boundary, but a Z-shaped edge. This leads to a slight overestimation and a slight underestimation of the crown area value for each tooth, such that it is likely that these errors will cancel each other out. Unfortunately, there is no method to accurately determine the true crown area and validate the accuracy of our results.

In terms of efficiency, the automated software is much faster than manual cast measurements, even though we have included a number of checkpoints to minimize the errors of detecting multiple boundaries or missing boundaries.

Selecting mesial, distal, buccal and lingual points

Since the selection of mesial, distal, buccal and lingual coordinate points affects rotation, width measurements, and arch fit, it is critical that the protocol for point selection be defined prior to analysis. Until dental anthropologists agree on the definitions of mesiodistal and buccolingual diameters, each study will use its own definition. Consistency in point selection is key, and analyst training on the protocol will improve consistency which will, in turn, minimize errors. As part of the follow-on work, we are investigating methods to obtain repeatable coordinate point selection.

6.2 Visual Aid Plots

The bar plots of crown area measurements, bucco-lingual widths, and mesio-distal widths for each tooth potentially help the user identify any major errors in the analysis. If the measurement for any tooth is missing or if there are any abnormal values, it is likely that these plots will convey that information to the user.

6.3 Review GUI

The Review GUI serves several functions. It aids the user in visualizing previously analyzed results and provides error checking. Follow-on work continues here in an effort to enhance the control point selection tool, such that the user can modify the coordinate points within the Review GUI rather than having to re-do point selection.

6.4 Other Approaches Investigated

As with most image processing projects, different methods were tested for each process, and the most efficient and reliable method was used in the final version of the program. This section will describe some techniques that were tried and removed**.**

Skeletonization

Initially, the arch fit is determined using the skeleton of the binary image that is formed after the erosion of the image to an extent where the objects do not break apart. A skeleton is just a pixel wide, and goes through the middle of the object while maintaining the shape of the object. The obtained skeleton can be noisy as it is a dependent of the shape of the object and this different developes branches within its skeleton. Even after minimizing the additional branches, the results appeared to underestimate the arch in most cases. Another incentive to change the method was that it was later decided to take the arch measurements only through the second molars (excluding the third molars), since the third molars are typically not present. Arch fitting was attempted using just the buccal, lingual, mesial and distal points separately. We decided to connect a line between the distal, the median of the bucco-lingual points, and the mesial point for each tooth, which yielded additional points that led to a smoother curve.

Selecting the midline of the arch fit

To ensure the most consistent and accurate midline selection, different approaches were attempted. The first approach was to place the midline vertically along the middle of the two central incisors and let the user move the midline if necessary. The issue with this method was that the user lacks information in the cast image to determine where to place the midline in the program, because the sand obscures landmarks on the palate and tongue regions of the cast. We considered placing a fine thread as the midline over the dental cast before acquiring the image so that it can be seen in the image, or using the dental casts/impressions during arch measurement using the software. These methods were deemed time consuming, and it seemed that consistent use across multiple users would be difficult. Ultimately, we decided to use the camera’s viewfinder to set up the cast such that the viewfinder circle was centered along the four incisors of the cast, since deviations of arch fit generally occur at the posterior end of dentition. This method was tested by four different users, and the outcome was much more accurate than visual estimation.

Edge Selection

Several approaches were investigated for boundary detection. The advantage of the background material (currently, the sand) being a different color than the actual cast meant that most methods gave an accurate estimation of the buccal and lingual boundaries. Initially, different types and colors of sand, small beads, stainless steel powder, coral powder and mustard seeds were tested as background materials. Criteria for the background material were that it had to be very fine so that it could be used to fill small crevices in the casts, non-glossy so that lighting glare was minimized in the images, and non-sticky so that it could be removed from cast in unwanted areas. Colored sand proved the most useful material, and blue sand was chosen because of its contrast with the reddish cast material.

Segmentation of the cast from the background was quite successful. However, automatically finding the mesial and distal tooth boundaries was more difficult. An attempt was made to focus on a smaller section of the contact points between the mesial point of one tooth and the distal point of the next tooth to try and get a cleaner boundary. We also tested an approach of finding each tooth's angle of rotation, rotating the image by that angle and then cropping that particular tooth from the image in order to work locally on the boundary detection problem. Another approach was to theoretically crop out each tooth and detect the boundary for one tooth at a time. In most cases, the several marks at the contact areas between teeth made it hard to determine an accurate boundary for the mesio-distal edges.

6.5 Future Work

Incorporate the same measurements for partial sets

In some cases, it is hard to obtain the impressions for the distal teeth (e.g., molars). This is mainly due to the problems of gagging experienced by participants during the making of the impressions. It would be useful if the same software were able to process partial impressions, where multiple distal teeth are missing. Special arch fit routines may need to be added to accommodate partial cast analysis.

Reducing analysis and processing time

The average time required to analyze an image is approximately five minutes, with time allocations for the maxilla and mandible as follows: point selections require about one minute each, boundary detection varies from 15 sec to over one minute each, depending upon the quality of the cast and dentition, and measurement calculation and plot review requires about one minute. If more manual intervention is required, the analysis could take up to 7 min. It was estimated that the manual analysis of these images, using calipers, would require at least 10 minutes for each the maxilla and mandible; so the automated approach offers a time savings of 65-75%. Additionally, not all measurements that are provided can be obtained using the caliper method.

Although software efficiency was the primary concern at each step in the algorithm, the preference for accurate measurements over speed of execution drove the final approaches of each processes. Of the five minutes required for analysis, only about one minute of processing exists that could be sped up. Options include the incorporation of parallel processing (available in the latest release of MATLAB and, therefore, relatively easy to incorporate) or graphics processing unit (GPU)-based acceleration (requires investment in a higher-end video card and, ideally, interface software), or both.

6.5 Conclusion

Overall, the requirements of the client were full-filled based on their regular inputs and a well-tailored product was developed as a result of this. The software is currently being successfully used at Lifespan Health Research Center (Department of Community Health, Boonshoft School of Medicine, Wright State University) for the analysis of dental casts obtained from the Jiri population in Nepal.

APPENDIX

Table A.1: Measurement Notation used at LHRC: Permanent Set. These are the acronyms used for the program.

Notation	***Measurement***
LLFA	Lower Length Full Arch
LLLHA	Lower Length Left Half Arch
LLRHA	Lower Length Right Half Arch
LLCW	Lower Left Canine Width
LRCW	Lower Right Canine Width
LTCW	Lower total Canine Width
LTCAL	Lower total Canine Arch Length
LLCH	Lower Left Canine Height
LRCH	Lower Right Canine Height
LLMW	Lower Left Molar Width
LRMW	Lower Right Molar Width
LTMAL	Lower total Molar Arch Length
LTMW	Lower total Molar Width
LLMH	Lower Left Molar Height
LRMH	Lower Right Molar Height
ULFA	Upper Length Full Arch
ULLHA	Upper Length Left Half Arch
ULRHA	Upper Length Right Half Arch
ULCW	Upper Left Canine Width
ULCW	Upper Right Canine Width
UTCW	Upper total Canine Width
UTCAL	Upper total Canine Arch Length
ULCH	Upper Left Canine Height
URCH	Upper Right Canine Height
ULMW	Upper Left Molar Width
URMW	Upper Right Molar Width
UTMAL	Upper total Molar Arch Length
UTMW	Upper total Molar Width
ULMH	Upper Left Molar Height

URMH	Upper Right Molar Height
RUM3RO	Right Upper 3rd Molar Rotation
RUM2RO	Right Upper 2nd Molar Rotation
RUM1RO	Right Upper 1st Molar Rotation
RUP4RO	Right Upper 2nd Premolar Rotation
RUP3RO	Right Upper 1st Premolar Rotation
RUCRO	Right Upper Canine Rotation
RUI2RO	Right Upper 2nd Incisor Rotation
RUI1RO	Right Upper 1st Incisor Rotation
LUI1RO	Left Upper 1st Incisor Rotation
LUI2RO	Left Upper 2nd Incisor Rotation
LUCRO	Left Upper Canine Rotation
LUP3RO	Left Upper 1st Premolar Rotation
LUP4RO	Left Upper 2nd Premolar Rotation
LUM1RO	Left Upper 1st Molar Rotation
LUM2RO	Left Upper 2nd Molar Rotation
LUM3RO	Left Upper 3rd Molar Rotation
RUM3MD	Right Upper 3rd Molar Mesio-distal Distance
RUM2MD	Right Upper 2nd Molar Mesio-distal Distance
RUM1MD	Right Upper 1st Molar Mesio-distal Distance
RUP4MD	Right Upper 2nd Premolar Mesio-distal Distance
RUP3MD	Right Upper 1st Premolar Mesio-distal Distance
RUCMD	Right Upper Canine Mesio-distal Distance
RUI2MD	Right Upper 2nd Incisor Mesio-distal Distance
RUI1MD	Right Upper 1st Incisor Mesio-distal Distance
LUI1MD	Left Upper 1st Incisor Mesio-distal Distance
LUI2MD	Left Upper 2nd Incisor Mesio-distal Distance
LUCMD	Left Upper Canine Mesio-distal Distance
LUP3MD	Left Upper 1st Premolar Mesio-distal Distance
LUP4MD	Left Upper 2nd Premolar Mesio-distal Distance
LUM1MD	Left Upper 1st Molar Mesio-distal Distance
LUM2MD	Left Upper 2nd Molar Mesio-distal Distance
LUM3MD	Left Upper 3rd Molar Mesio-distal Distance
RUM3BL	Right Upper 3rd Molar Bucco-lingual Distance
RUM2BL	Right Upper 2nd Molar Bucco-lingual Distance
RUM1BL	Right Upper 1st Molar Bucco-lingual Distance
RUP4BL	Right Upper 2nd Premolar Bucco-lingual Distance
RUP3BL	Right Upper 1st Premolar Bucco-lingual Distance
RUCBL	Right Upper Canine Bucco-lingual Distance
RUI2BL	Right Upper 2nd Incisor Bucco-lingual Distance
RUI1BL	Right Upper 1st Incisor Bucco-lingual Distance

LUI1BL	Left Upper 1st Incisor Bucco-lingual Distance
LUI2BL	Left Upper 2nd Incisor Bucco-lingual Distance
LUCBL	Left Upper Canine Bucco-lingual Distance
LUP3BL	Left Upper 1st Premolar Bucco-lingual Distance
LUP4BL	Left Upper 2nd Premolar Bucco-lingual Distance
LUM1BL	Left Upper 1st Molar Bucco-lingual Distance
LUM2BL	Left Upper 2nd Molar Bucco-lingual Distance
LUM3BL	Left Upper 3rd Molar Bucco-lingual Distance
RUM3CA	Right Upper 3rd Molar Crown Area
RUM2CA	Right Upper 2nd Molar Crown Area
RUM1CA	Right Upper 1st Molar Crown Area
RUP4CA	Right Upper 2nd Premolar Crown Area
RUP3CA	Right Upper 1st Premolar Crown Area
LUP3CA	Left Upper 1st Premolar Crown Area
LUP4CA	Left Upper 2nd Premolar Crown Area
LUM1CA	Left Upper 1st Molar Crown Area
LUM2CA	Left Upper 2nd Molar Crown Area
LUM3CA	Left Upper 3rd Molar Crown Area
LRUCW	Left to Right Upper Canine Width
LRUP3W	Left to Right Upper 1st Premolar Width
LRUP4W	Left to Right Upper 2nd Premolar Width
LRUM1W	Left to Right Upper 1st Molar Width
LRUM2W	Left to Right Upper 2nd Molar Width
LRUM3W	Left to Right Upper 3rd Molar Width
RLM3RO	Right Lower 3rd Molar rotation
RLM2RO	Right Lower 2nd Molar rotation
RLM1RO	Right Lower 1st Molar rotation
RLP4RO	Right Lower 2nd Premolar rotation
RLP3RO	Right Lower 1st Premolar rotation
RLCRO	Right Lower Canine rotation
RLI2RO	Right Lower 2nd Incisor rotation
RLI1RO	Right Lower 1st Incisor rotation
LLI1RO	Left Lower 1st Incisor rotation
LLI2RO	Left Lower 2nd Incisor rotation
LLCRO	Left Lower Canine rotation
LLP3RO	Left Lower 1st Premolar rotation
LLP4RO	Left Lower 2nd Premolar rotation
LLM1RO	Left Lower 1st Molar rotation
LLM2RO	Left Lower 2nd Molar rotation
LLM3RO	Left Lower 3rd Molar rotation
RLM3MD	Right Lower 3rd Molar Mesio-distal Distance

RLM2MD	Right Lower 2nd Molar Mesio-distal Distance
RLM1MD	Right Lower 1st Molar Mesio-distal Distance
RLP4MD	Right Lower 2nd Premolar Mesio-distal Distance
RLP3MD	Right Lower 1st Premolar Mesio-distal Distance
RLCMD	Right Lower Canine Mesio-distal Distance
RLI2MD	Right Lower 2nd Incisor Mesio-distal Distance
RLI1MD	Right Lower 1st Incisor Mesio-distal Distance
LLI1MD	Left Lower 1st Incisor Mesio-distal Distance
LLI2MD	Left Lower 2nd Incisor Mesio-distal Distance
LLCMD	Left Lower Canine Mesio-distal Distance
LLP3MD	Left Lower 1st Premolar Mesio-distal Distance
LLP4MD	Left Lower 2nd Premolar Mesio-distal Distance
LLM1MD	Left Lower 1st Molar Mesio-distal Distance
LLM2MD	Left Lower 2nd Molar Mesio-distal Distance
LLM3MD	Left Lower 3rd Molar Mesio-distal Distance
RLM3BL	Right Lower 3rd Molar Bucco-lingual Distance
RLM2BL	Right Lower 2nd Molar Bucco-lingual Distance
RLM1BL	Right Lower 1st Molar Bucco-lingual Distance
RLP4BL	Right Lower 2nd Premolar Bucco-lingual Distance
RLP3BL	Right Lower 1st Premolar Bucco-lingual Distance
RLCBL	Right Lower Canine Bucco-lingual Distance
RLI2BL	Right Lower 2nd Incisor Bucco-lingual Distance
RLI1BL	Right Lower 1st Incisor Bucco-lingual Distance
LLI1BL	Left Lower 1st Incisor Bucco-lingual Distance
LLI2BL	Left Lower 2nd Incisor Bucco-lingual Distance
LLCBL	Left Lower Canine Bucco-lingual Distance
LLP3BL	Left Lower 1st Premolar Bucco-lingual Distance
LLP4BL	Left Lower 2nd Premolar Bucco-lingual Distance
LLM1BL	Left Lower 1st Molar Bucco-lingual Distance
LLM2BL	Left Lower 2nd Molar Bucco-lingual Distance
LLM3BL	Left Lower 3rd Molar Bucco-lingual Distance
RLM3CA	Right Lower 3rd Molar Crown Area
RLM2CA	Right Lower 2nd Molar Crown Area
RLM1CA	Right Lower 1st Molar Crown Area
RLP4CA	Right Lower 2nd Premolar Crown Area
RLP3CA	Right Lower 1st Premolar Crown Area
LLP3CA	Left Lower 1st Premolar Crown Area
LLP4CA	Left Lower 2nd Premolar Crown Area
LLM1CA	Left Lower 1st Molar Crown Area
LLM2CA	Left Lower 2nd Molar Crown Area
LLM3CA	Left Lower 3rd Molar Crown Area

LRLCW	Left to Right Lower Canine width
LRLP3W	Left to Right Lower 1st Premolar width
LRLP4W	Left to Right Lower 2nd Premolar width
LRLM1W	Left to Right Lower 1st Molar width
LRLM2W	Left to Right Lower 2nd Molar width
LRLM3W	Left to Right Lower 3rd Molar width

Table A.2: Measurement Notation used at LHRC: Deciduous Set. These are the acronyms used for the program.

Notation	***Measurement***
DLLFA	Deciduous Lower Length Full Arch
DLLLHA	Deciduous Lower Length Left half Arch
DLLRHA	Deciduous Lower Length Right half Arch
DLLMW	Deciduous Lower Left Molar Width
DLRMW	Deciduous Lower Right Molar Width
DLTMAL	Deciduous Lower Total Molar Arch Length
DLTMW	Deciduous Lower Total Molar Width
DLLMH	Deciduous Lower Left Molar Height
DLRMH	Deciduous Lower Right Molar Height
DULFA	Deciduous Upper Length Full Arch
DULLHA	Deciduous Upper Length Left half Arch
DULRHA	Deciduous Upper Length Right half Arch
DULMW	Deciduous Upper Left Molar Width
DURMW	Deciduous Upper Right Molar Width
DUTMAL	Deciduous Upper Total Molar Arch Length
DUTMW	Deciduous Upper Total Molar Width
DULMH	Deciduous Upper Left Molar Height
DURMH	Deciduous Upper Right Molar Height
DRUM2RO	Deciduous Right Upper 2nd Molar Rotation
DRUM1RO	Deciduous Right Upper 1st Molar Rotation
DRUCRO	Deciduous Right Upper Canine Rotation
DRUI2RO	Deciduous Right Upper 2nd Incisor Rotation
DRUI1RO	Deciduous Right Upper 1st Incisor Rotation
DLUI1RO	Deciduous Left Upper 1st Incisor Rotation
DLUI2RO	Deciduous Left Upper 2nd Incisor Rotation
DLUCRO	Deciduous Left Upper Canine Rotation
DLUM1RO	Deciduous Left Upper 1st Molar Rotation
DLUM2RO	Deciduous Left Upper 2nd Molar Rotation
DRUM2MD	Deciduous Right Upper 2nd Molar Mesio-distal Distance
DRUM1MD	Deciduous Right Upper 1st Molar Mesio-distal Distance

DRUCMD	Deciduous Right Upper Canine Mesio-distal Distance
DRUI2MD	Deciduous Right Upper 2nd Incisor Mesio-distal Distance
DRUI1MD	Deciduous Right Upper 1st Incisor Mesio-distal Distance
DLUI1MD	Deciduous Left Upper 1st Incisor Mesio-distal Distance
DLUI2MD	Deciduous Left Upper 2nd Incisor Mesio-distal Distance
DLUCMD	Deciduous Left Upper Canine Mesio-distal Distance
DLUM1MD	Deciduous Left Upper 1st Molar Mesio-distal Distance
DLUM2MD	Deciduous Left Upper 2nd Molar Mesio-distal Distance
DRUM2BL	Deciduous Right Upper 2nd Molar Bucco-lingual Distance
DRUM1BL	Deciduous Right Upper 1st Molar Bucco-lingual Distance
DRUCBL	Deciduous Right Upper Canine Bucco-lingual Distance
DRUI2BL	Deciduous Right Upper 2nd Incisor Bucco-lingual Distance
DRUI1BL	Deciduous Right Upper 1st Incisor Bucco-lingual Distance
DLUI1BL	Deciduous Left Upper 1st Incisor Bucco-lingual Distance
DLUI2BL	Deciduous Left Upper 2nd Incisor Bucco-lingual Distance
DLUCBL	Deciduous Left Upper Canine Bucco-lingual Distance
DLUM1BL	Deciduous Left Upper 1st Molar Bucco-lingual Distance
DLUM2BL	Deciduous Left Upper 2nd Molar Bucco-lingual Distance
DRUM2CA	Deciduous Right Upper 2nd Molar Crown Area
DRUM1CA	Deciduous Right Upper 1st Molar Crown Area
DLUM1CA	Deciduous Left Upper 1st Molar Crown Area
DLUM2CA	Deciduous Left Upper 2nd Molar Crown Area
DLRUCW	Deciduous Left to Deciduous Right Upper Canine Width
DLRUM1W	Deciduous Left to Deciduous Right Upper 1st Molar Width
DLRUM2W	Deciduous Left to Deciduous Right Upper 2nd Molar Width
DRLM2RO	Deciduous Right Lower 2nd Molar Rotation
DRLM1RO	Deciduous Right Lower 1st Molar Rotation
DRLCRO	Deciduous Right Lower Canine Rotation
DRLI2RO	Deciduous Right Lower 2nd Incisor Rotation
DRLI1RO	Deciduous Right Lower 1st Incisor Rotation
DLLI1RO	Deciduous Left Lower 1st Incisor Rotation
DLLI2RO	Deciduous Left Lower 2nd Incisor Rotation
DLLCRO	Deciduous Left Lower Canine Rotation
DLLM1RO	Deciduous Left Lower 1st Molar Rotation
DLLM2RO	Deciduous Left Lower 2nd Molar Rotation
DRLM2MD	Deciduous Right Lower 2nd Molar Mesio-distal Distance
DRLM1MD	Deciduous Right Lower 1st Molar Mesio-distal Distance
DRLCMD	Deciduous Right Lower Canine Mesio-distal Distance
DRLI2MD	Deciduous Right Lower 2nd Incisor Mesio-distal Distance
DRLI1MD	Deciduous Right Lower 1st Incisor Mesio-distal Distance
DLLI1MD	Deciduous Left Lower 1st Incisor Mesio-distal Distance

DLLI2MD	Deciduous Left Lower 2nd Incisor Mesio-distal Distance
DLLCMD	Deciduous Left Lower Canine Mesio-distal Distance
DLLM1MD	Deciduous Left Lower 1st Molar Mesio-distal Distance
DLLM2MD	Deciduous Left Lower 2nd Molar Mesio-distal Distance
DRLM2BL	Deciduous Right Lower 2nd Molar Bucco-lingual Distance
DRLM1BL	Deciduous Right Lower 1st Molar Bucco-lingual Distance
DRLCBL	Deciduous Right Lower Canine Bucco-lingual Distance
DRLI2BL	Deciduous Right Lower 2nd Incisor Bucco-lingual Distance
DRLI1BL	Deciduous Right Lower 1st Incisor Bucco-lingual Distance
DLLI1BL	Deciduous Left Lower 1st Incisor Bucco-lingual Distance
DLLI2BL	Deciduous Left Lower 2nd Incisor Bucco-lingual Distance
DLLCBL	Deciduous Left Lower Canine Bucco-lingual Distance
DLLM1BL	Deciduous Left Lower 1st Molar Bucco-lingual Distance
DLLM2BL	Deciduous Left Lower 2nd Molar Bucco-lingual Distance
DRLM2CA	Deciduous Right Lower 2nd Molar Crown Area
DRLM1CA	Deciduous Right Lower 1st Molar Crown Area
DLLM1CA	Deciduous Left Lower 1st Molar Crown Area
DLLM2CA	Deciduous Left Lower 2nd Molar Crown Area
DLRLCW	Deciduous Left to Deciduous Right Lower Canine Width
DLRLM1W	Deciduous Left to Deciduous Right Lower 1st Molar Width
DLRLM2W	Deciduous Left to Deciduous Right Lower 2nd Molar Width

REFERENCES

1) Bishara, S. E., Jakobsen, J. R., Abdallah, E. M., & Fernandez Garcia, A. (1989). Comparisons of mesiodistal and buccolingual crown dimensions of the permanent teeth in three populations from egypt, mexico, and the united states. *American Journal of Orthodontics and Dentofacial Orthopedics : Official Publication of the American Association of Orthodontists, its Constituent Societies, and the American Board of Orthodontics, 96*(5), 416-422.
2) Barrett, M. J., Brown, T., & Luke, J. I. (1963). Dental observations on australian aborigines: Mesiodistal crown diameters of deciduous teeth. *Australian Dental Journal., 8*(4), 299-302.
3) Barrett, M. J., Brown, T., Arato, G., & Ozols, I. V. (1964). Dental observations on australian aborgines: Buccolingual crown diameters of deciduous and permanent dentition. *Australian Dental Journal., 9*(4), 280-285.
4) Sherwood, R. J. (2009). Research project: Genetics of orofacial cleft endophenotypes and the midface (Research Plan).
5) Hashim, H. A., & Murshid, Z. A. (1993). Mesiodistal tooth width in a saudi population sample comparing right and left sides. part 2. *Egyptian Dental Journal, 39*(1), 347-350.

6) Hayashi, K., Uechi, J., & Mizoguchi, I. (2003). Three-dimensional analysis of dental casts based on a newly defined palatal reference plane. *The Angle Orthodontist, 73*(5), 539-544.

7) Hillson, S., Fitzgerald, C., & Flinn, H. (2005). Alternative dental measurements: Proposals and relationships with other measurements. *American Journal of Physical Anthropology, 126*(4), 413-426. doi:10.1002/ajpa.10430

8) Brodie, A. G. (1969). The three arcs of mandibular movement as they affect the wear of teeth. *The Angle Orthodontist, 39*(4), 217-229.

9) F.P.G.M, Van der Linden, Boersma, H., Zelders, T., Peters, K.A., & Raaben, J.H. (1972). Three-Dimensional Analysis of Dental Casts by Means of the Optocom. *Journal of Dental Research, 51,* 1100.

10) Martensson, B., & Ryden, H. (1992). The holodent system, a new technique for measurement and storage of dental casts. *American Journal of Orthodontics and Dentofacial Orthopedics : Official Publication of the American Association of Orthodontists, its Constituent Societies, and the American Board of Orthodontics, 102*(2), 113-119.

11) Yergin, E., Ozturk, C., & Sermet, B. (2001). Image processing techniques for assessment of dental trays. *Engineering in Medicine and Biology Society, 3*, 2571-2573.

12) Lestrel, P. E., Takahashi, O., & Kanazawa, E. (2004). A quantitative approach for measuring crowding in the dental arch: Fourier descriptors. *American Journal of Orthodontics and Dentofacial Orthopedics : Official Publication of the American*

Association of Orthodontists, its Constituent Societies, and the American Board of Orthodontics, 125(6), 716-725. doi:10.1016/S0889540603010825

13) Lindsten, R., Ogaard, B., & Larsson, E. (2002). Dental arch space and permanent tooth size in the mixed dentition of a skeletal sample from the 14th to the 19th centuries and 3 contemporary samples. *American Journal of Orthodontics and Dentofacial Orthopedics : Official Publication of the American Association of Orthodontists, its Constituent Societies, and the American Board of Orthodontics, 122*(1), 48-58.

14) Keating, P. J., Parker, R. A., Keane, D., & Wright, L. (1984). The holographic storage of study models. *British Journal of Orthodontics, 11*(3), 119-125.

15) Kaifu, Y., Kasai, K., Townsend, G. C., & Richards, L. C. (2003). Tooth wear and the "design" of the human dentition: A perspective from evolutionary medicine. *American Journal of Physical Anthropology, Suppl 37*, 47-61. doi:10.1002/ajpa.10329

16) Doris, J. M., Bernard, B. W., Kuftinec, M. M., & Stom, D. (1981). A biometric study of tooth size and dental crowding. *American Journal of Orthodontics, 79*(3), 326-336.

17) Garn, S. M., Lewis, A. B., & Kerewsky, R. S. (1965). Size interrelationships of the mesial and distal teeth. *Journal of Dental Research, 44*, 350-354.

18) Garn, S. M., Lewis, A. B., & Kerewsky, R. S. (1963). Third molar agenesis and size reduction of the remaining teeth. *Nature*, *200*, 488-489.

19) Brehnan, K., Boyd, R. L., Laskin, J., Gibbs, C. H., & Mahan, P. (1981). Direct measurement of loads at the temporomandibular joint in macaca arctoides. *Journal of Dental Research*, *60*(10), 1820-1824.

20) Braun, S., Hnat, W. P., Fender, D. E., & Legan, H. L. (1998). The form of the human dental arch. *Angle Orthod., 68*(1), 29-36.

21) Seipel, C. M. (1948). Variations of tooth position, a metric study of variation and adaptation in the deciduous and permanent dentitions. *American Journal of Orthodontics., 34*(4), 369-372.

22) Fujita, K., Takada, K., QianRong, G., & Shibata, T. (2002). Patterning of human dental arch wire blanks using a vector quantization algorithm. *The Angle Orthodontist, 72*(4), 285-294.

23) Mehta, J. D., & Evans, C. C. (1966). A study of attrition of teeth in the arkansas indian skulls. *The Angle Orthodontist, 36*(3), 248-257.

24) Hunter, W.S., & Priest, W.R. (1960). Errors and Discrepancies in Measurement of Tooth Size. *Journal of Dental Research., 39,* 405-414.

25) Sohmura, T., Kojima, T., Wakabayashi, K., & Takahashi, J. (2000). Use of an ultrahigh-speed laser scanner for constructing three-dimensional shapes of dentition and occlusion. *The Journal of Prosthetic Dentistry, 84*(3), 345-352. doi:10.1067/mpr.2000.109786

26) Lundstrom, A., & Lysell, L. (1953). An anthropological examination of a group of medieval danish skulls, with particular regard to the jaws and occlusal conditions. *Acta Odontologica Scandinavica, 11*(2), 111-128.

27) Schirmer, U. R., & Wiltshire, W. A. (1997). Manual and computer-aided space analysis: A comparative study. *American Journal of Orthodontics and Dentofacial Orthopedics : Official Publication of the American Association of Orthodontists, its Constituent Societies, and the American Board of Orthodontics, 112*(6), 676-680.

28) Khalaf, K., Robinson, D. L., Elcock, C., Smith, R. N., & Brook, A. H. (2005). Tooth size in patients with supernumerary teeth and a control group measured by image analysis system. *Archives of Oral Biology, 50*(2), 243-248. doi:10.1016/j.archoralbio.2004.09.013

29) Bhatia, S. N., & Harrison, V. E. (1987). Operational performance of the travelling microscope in the measurement of dental casts. *British Journal of Orthodontics, 14*(3), 147-153.

30) Agha, N. F., & Al–Saleem, N. R. (2006). Different methods to measure canine rotation. *Al–Rafidain Dent J., 6*(2), 122-129.

31) Rougier, H., Crevecoeur, I., & Wolpoff, M. H. (2006). Lower third premolar in the krapina dental sample. *Periodicum Biologorum., 108*(3), 269-278.

32) Potter, R. H., Nance, W. E., & Yu, P. L. (1978). Genetic determinants of dental dimension: A twin study. *Progress in Clinical and Biological Research, 24 Pt C*, 235-240.

33) BeGole, E.A. (1980). Application of cubic spline function in the description of dental arch form. *Journal of Dental Research., 59*, 1542-1556.

34) Lu, K.H. (1964). Analysis of dental arch symmetry. *Journal of Dental Research., 43*, 885.

35) Woodworth, D. A., Sinclair, P. M., & Alexander, R. G. (1985). Bilateral congenital absence of maxillary lateral incisors: A craniofacial and dental cast analysis. *American Journal of Orthodontics, 87*(4), 280-293.

36) Rudge, S. J. (1982). A computer program for the analysis of study models. *European Journal of Orthodontics., 4*(4), 269-273.

37) Berkowitz, S. (1971). Stereophotogrammetric analysis of casts of normal and abnormal palates. *American Journal of Orthodontics., 60(1)*.

38) Richmond, S. (1987). Recording the dental cast in three dimensions. *American Journal of Orthodontics Dentofacial Orthop., 92*, 199-206.

39) Rudge, S. (1981). Dental Arch Analysis: A literature review. *European Journal of Orthodontics.*, *3(4)*, 279-284.

40) Trivino, T., Siqueira, D. F., Scanavini, M. A. (2007). The lower dental arch form in the literature viewpoint. *Dent. Press Orthop, 12*, 61-72.

41) Duguid, R., & McKay, G. S. (1981). Bite length measurements and tooth-to-arch relationships obtained from dental casts using an X, Y-digitiser and computer. *Journal - Forensic Science Society*, *21*(3), 211-223.

42) Mok, K. H., & Cooke, M. S. (1998). Space analysis: A comparison between sonic digitization (DigiGraph workstation) and the digital caliper. *European Journal of Orthodontics, 20*(6), 653-661.

43) Redlich, M., Weinstock, T., Abed, Y., Schneor, R., Holdstein, Y., & Fischer, A. (2008). A new system for scanning, measuring and analyzing dental casts based on a 3D holographic sensor. *Orthodontics & Craniofacial Research, 11*(2), 90-95. doi:10.1111/j.1601-6343.2007.00417.x

44) Lavelle, C. L. (1975). The shape of the dental arch. *American Journal of Orthodontics*, *67*(2), 176-84.

45) Neiburger, E. J. (2002). The evolution of human occlusion--ancient clinical tips for modern dentists. *General Dentistry, 50*(1), 44-9; quiz 50-1.

46) White, L. W. (1977). Accurate arch-discrepancy measurements. *American Journal of Orthodontics, 72*(3), 303-308.

47) Quimby, M. L., Vig, K. W., Rashid, R. G., & Firestone, A. R. (2004). The accuracy and reliability of measurements made on computer-based digital models. *The Angle Orthodontist, 74*(3), 298-303.

48) Tomassetti, J. J., Taloumis, L. J., Denny, J. M., & Fischer, J. R.,Jr. (2001). A comparison of 3 computerized bolton tooth-size analyses with a commonly used method. *The Angle Orthodontist, 71*(5), 351-357.

49) Bishara, S. E., Jakobsen, J. R., Treder, J., & Nowak, A. (1998). Arch length changes from 6 weeks to 45 years. *The Angle Orthodontist, 68*(1), 69-74.

50) Kageyama, T., Dominguez-Rodriguez, G. C., Vigorito, J. W., & Deguchi, T. (2006). A morphological study of the relationship between arch dimensions and craniofacial structures in adolescents with class II division 1 malocclusions and various facial types. *American Journal of Orthodontics and Dentofacial Orthopedics : Official Publication of the American Association of Orthodontists, its Constituent Societies, and the American Board of Orthodontics, 129*(3), 368-375. doi:10.1016/j.ajodo.2005.12.005

51) Singh, I. J., & Savara, B. S. (1964). A method for making tooth and dental arch measurements. *Journal of the American Dental Association (1939), 69*, 719-721.

52) Dempsey, P. J., Townsend, G. C., Martin, N. G., & Neale, M. C. (1995). Genetic covariance structure of incisor crown size in twins. *Journal of Dental Research, 74*(7), 1389-1398.

53) Garn, S. M., Lewis, A. B., & Shoemaker, D. W. (1956). The sequence of calcification of the mandibular molar and premolar teeth. *Journal of Dental Research, 35*(4), 555-561.